IMPLICATIONS OF ADVANCED GLYCATION ENDPRODUCTS IN OXIDATIVE STRESS AND NEURODEGENERATIVE DISORDERS

Dissertation zur Erlangung des

naturwissenschaftlichen Doktorgrades

der Bayerischen Julius-Maximilians-Universität Würzburg

vorgelegt von
Amanda Wong

aus
Sydney, Australien

Würzburg, Februar 2001

Summary

The reactions of reducing sugars with primary amino groups are the most common nonenzymatic modifications of proteins. Subsequent rearrangements, oxidations, and dehydrations yield a heterogeneous group of mostly colored and fluorescent compounds, termed "Maillard products" or advanced glycation end products (AGEs). AGE formation has been observed on long-lived proteins such as collagen, eye lens crystalline, and in pathological protein deposits in Alzheimer's (AD) and Parkinson's disease (PD) and dialysis-related amyloidosis. AGE-modified proteins are also involved in the complications of diabetes.

AGEs accumulate in the the β-amyloid plaques and neurofibrillary tangles (NFT) associated with AD and in the Lewy bodies characteristic of PD. Increasing evidence supports a role for oxidative stress in neurodegenerative disorders such as AD and PD. AGEs have been shown to contribute towards oxidative damage and chronic inflammation, whereby activated microglia secrete cytokines and free radicals, including nitric oxide (NO). Roles proposed for NO in the pathophysiology of the central nervous system are increasingly diverse and range from intercellular signaling, through necrosis of cells and invading pathogens, to the involvement of NO in apoptosis.

Using *in vitro* experiments, it was shown that AGE-modified bovine serum albumin (BSA-AGE) and AGE-modified β-amyloid, but not their unmodified proteins, induce NO production in N-11 murine microglia cells. This was mediated by the receptor for AGEs (RAGE) and upregulation of the inducible nitric oxide synthase (iNOS). AGE-induced enzyme activation and NO production could be blocked by intracellular-acting antioxidants: *Ginkgo biloba* special extract EGb 761, the estrogen derivative, 17β-estradiol, R-(+)-thioctic acid, and a nitrone-based free radical trap, N-tert.-butyl-α-phenylnitrone (PBN). Methylglyoxal (MG) and 3-deoxyglucosone (3-DG), common precursors in the Maillard reaction, were also tested for their ability to induce the production of NO in N-11 microglia. However, no significant changes in nitrite levels were detected in the cell culture medium.

The significance of these findings was supported by *in vivo* immunostaining of AD brains. Single and double immunostaining of cryostat sections of normal aged and AD brains was performed with polyclonal antibodies to AGEs and iNOS and monoclonal antibodies to Aβ and PHF-1 (marker for NFT) and reactive microglia. In aged normal individuals as well as early stage AD brains (i.e. no pathological findings in isocortical areas), a few astrocytes showed co-localisation of AGE and iNOS in the upper neuronal layers of the temporal (Area

22) and entorhinal (Area 28, 34) cortices compared with no astrocytes detected in young controls. In late AD brains, there was a much denser accumulation of astrocytes co-localised with AGE and iNOS in the deeper and particularly upper neuronal layers. Also, numerous neurons with diffuse AGE but not iNOS reactivity and some AGE and iNOS-positive microglia were demonstrated, compared with only a few AGE-reactive neurons and no microglia in controls. Finally, astrocytes co-localised with AGE and iNOS as well as AGE and β-amyloid were found surrounding mature but not diffuse β-amyloid plaques in the AD brain. Parts of NFT were AGE-immunoreactive.

Immunohistochemical staining of cryostat sections of normal aged and PD brains was performed with polyclonal antibodies to AGEs. The sections were counterstained with monoclonal antibodies to neurofilament components and α-synuclein. AGEs and α-synuclein were colocalized in very early Lewy bodies in the substantia nigra of cases with incidental Lewy body disease.

In order to systematically assay the relative reactivities of amino acid side chains to sugars was, libraries of tripeptides on cellulose membranes (SPOT library) were produced. The sugars reacted preferentially with lysine, arginine, and cysteine. Four different polyclonal and monoclonal anti-AGE antibodies were characterised in respect to their recognition of defined modified tripeptides. The antibodies predominantly recognised lysine and arginine amino acid residues. Hence, peptide SPOT libraries are excellent tools for comparing individual reactivities of amino acids for nonenzymatic modifications and identifying the specific epitopes of anti-AGE antibodies.

These results support an AGE-induced oxidative damage due to the action of free radicals, such as NO, occurring in the AD and PD brains. Furthermore, the involvement of astrocytes and microglia in this pathological process was confirmed immunohistochemically in the AD brain. It is suggested that oxidative stress and AGEs participate in the very early steps of Lewy body formation and resulting cell death in PD. Since the iNOS gene can be regulated by redox-sensitive transcription factors, the use of membrane permeable antioxidants could be a promising strategy for the treatment and prevention of chronic inflammation in neurodegenerative disorders.

Zusammenfassung

Die Glykierung oder Maillard-Reaktion ist neben der oxidativen Modifikation die bekannteste nicht-enzymatische posttranslationale Modifikation von Proteinen. Glykierung startet mit der Reaktion von reduzierenden Zuckern mit primären Aminogruppen. Nachfolgenden Umlagerungen, Oxidationen und Dehydrationen führen zu einer heterogenen Gruppe von farbigen und fluoreszierenden Verbindungen, den sogenannten "Maillard products" oder "advanced glycation end products" (AGEs). Diese Vorgänge werden besonders an langlebigen Proteinen wie Kollagen und Kristallin der Augenlinsen sowie in pathologischen Proteinablagerungen bei der Alzheimer-Demenz (AD), der Parkinson-Krankheit (PD) und bei Hämodialyse beobachtet. AGE-modifizierte Proteine sind auch aktiv beteiligt an den Spätkomplikationen des Diabetes mellitus.

AGEs reichern sich im Alzheimer Gehirn in den β-Amyloid-Plaques und den neurofibrillären Bündeln (tangles, NFT), sowie in den für PD charakteristischen Lewi-Körpern an. Immer mehr Befunde belegen die Rolle von oxidativem Stress in neurodegenerativen Erkrankungen wie AD und PD. Es konnte gezeigt werden, dass AGEs an oxidativer Schädigung und chronischer Entzündung Anteil haben, wobei aktivierte Mikroglia Cytokine und freie Radikale, inklusive Stickstoffmonoxid (NO) sezernieren. Vermutungen über die Rolle von NO in der Pathophysiologie des Zentralnervensystems gehen weit auseinander und reichen von interzellulärer Signalübertragung über nekrotischen Zelltod und eindringende pathogene Substanzen bis zur Beteiligung von NO an der Apoptose.

In einem Zellkultur Modell konnte *in vitro* gezeigt werden, dass AGE- modifiziertes Albumin (BSA-AGE) und AGE-modifiziertes β–Amyloid, aber nicht die unmodifizierten Proteine, die Synthese von NO in N-11 Maus-Mikrogliazellen induzieren. Diese wird möglicherweise vom Rezeptor für AGE (RAGE) und durch eine Steigerung der Expression der induzierbaren Stickstoffmonoxid-Synthase (iNOS) vermittelt. AGE-induzierte Enzymexpression und NO-Produktion konnten durch folgende intrazellulär wirkende Antioxidantien blockiert werden: *Ginkgo biloba* Spezialextrakt EGb 761, das Östrogenderivat 17β-Estradiol, alpha-Liponsäure, und ein Radikalfänger, N-tert.-butyl-α-phenylnitrone (PBN).

Neben AGEs wurden auch reaktive Dicarbonyle wie Methylglyoxal (MG) und 3-Deoxyglucosone (3-DG), Vorläufer der Maillard-Reaktion, auf ihre Fähigkeit untersucht, die Synthese von NO in N-11 Mikroglia zu induzieren. Es konnten jedoch keine Induktion der NO-Produktion festgestellt werden.

Die Bedeutung dieser *in vitro*-Ergebnisse wurden durch *in vivo* Immunohistochemischen Untersuchungen an AD Gehirnen bestätigt. Einfache und doppelte Immunfärbungen wurden an Gefrierschnitten von normal gealterten Gehirnen und AD-Gehirnen mit polyklonalen Antikörpern gegen AGEs und iNOS und monoklonalen Antikörpern gegen Aβ, PHF-1 (zur spezifischen Markierung der NFT) und reaktive Mikroglia angefertigt. Bei normal gealterten Personen sowie bei AD Erkrankten im Frühstadium (d.h. keine pathologischen Veränderungen in isokortikalen Gebieten) wiesen wenige Astrozyten eine Kolokalisation von AGE und iNOS in den oberen Neuronenschichten des temporalen (Area 22) und entorhinalen (Area 28, 34) Kortex auf. Im Vergleich dazu wurden keine Astrozyten in jungen Kontrollgehirnen gefunden. In fortgeschrittenen Alzheimergehirnen wurde eine viel dichtere Anreicherung von Astrozyten, kolokalisiert mit AGE und iNOS in den tieferen, und insbesondere in den oberen Neuronenschichten gefunden. Weiterhin konnten zahlreiche Neurone mit diffuser AGE-Reaktivität, aber ohne iNOS-Reaktivität, sowie einige AGE- und iNOS-positive Mikroglia gezeigt werden, im Vergleich zu nur wenigen AGE-reaktiven Neuronen und keinen Mikroglia in den Kontrollen. Schliesslich wurden in Astrozyten, die reife, aber nicht diffuse β-Amyloid-Plaques im AD-Gehirn umlagern, AGE mit iNOS sowie mit β-Amyloid kolokalisiert gefunden. Teile der NFT waren AGE-immunoreaktiv.

Immunhistochemische Färbung an Gefrierschnitten von normal gealterten und PD-Gehirnen wurden mit polyklonalen Antikörpern gegen AGEs durchgeführt. Die Schnitte wurden mit monoklonalen Antikörpern gegen Neurofilamentkomponenten und α-Synuclein gegengefärbt. AGEs und α-Synuclein waren kolokalisiert in sehr frühen Lewi-Körpern der Substantia nigra in Gehirnen mit vorhandener Lewi-Körper-Demenz.

Um die relative Reaktivität von Aminosäureseitenketten mit Zuckern zu bewerten, wurde systematisch mit Bibliotheken von Tripeptiden auf Zellulose-Membranen (SPOT Bibliothek) durchgeführt. Die Zucker reagierten bevorzugt mit Lysin, Arginin und Cystein. Vier verschiedene polyklonale und monoklonale Anti-AGE-Antikörper wurden bezüglich ihrer Erkennung bestimmter veränderter Tripeptide charakterisiert. Die Antikörper erkannten vorwiegend Lysin- und Arginin-Reste. SPOT-libraries von Peptiden sind also ausgezeichnete Hilfsmittel für den Vergleich einzelner Aminosäuren bezüglich nicht-enzymatischer Veränderungen sowie für die Identifizierung spezifischer Epitope von Anti-AGE-Antikörpern.

Diese Ergebnisse unterstützen die These AGE-induzierter oxidativer Schädigung mittels freier Radikale wie z.B. NO in AD- und PD- Gehirnen. Ausserdem wurde die

Beteiligung von Astrozyten und Mikroglia an diesem pathologischen Prozess immunhistochemisch im Alzheimergehirn bestätigt. Es liegt nahe, dass oxidativer Stress und AGEs an den sehr frühen Stufen der Lewi-Körper-Bildung und dem daraus resultierenden Zelltod in PD beteiligt sind. Da das iNOS-Gen durch redoxsensitive Transkriptionsfaktoren reguliert werden kann, könnte die Verwendung membranpermeabler Antioxidantien eine erfolgversprechende Strategie für die Behandlung und Prävention chronischer Entzündungen bei neurodegenerativen Erkrankungen darstellen.

CONTENTS

1. INTRODUCTION

1.1 Advanced Glycation Endproducts (AGEs): Chemistry

The amino groups of proteins, particularly the side chains of lysine, arginine and histidine, react non-enzymatically with reducing sugars, including glucose, fructose, hexose-phosphates, trioses and triose-phosphates. This posttranslational modification, termed "non-enzymatic glycosylation", "glycation" or "Maillard reaction", leads via reversible Schiff-base adducts to protein bound Amadori products. Through subsequent oxidations and dehydrations, a broad range of heterogeneous fluorescent and brown products with nitrogen- and oxygen- containing heterocycles is formed, the so-called "Advanced Glycation Endproducts" (AGEs) (Brownlee, 1995). These latter reactions are accelerated by transition metals, such as copper and iron, which oxidize the protein-bound Amadori-products. AGE formation is irreversible and causes protease-resistant cross-linking of peptides and proteins, leading to protein deposition and amyloidosis (Smith *et al*., 1996; Münch *et al*., 1998) (Fig. 1.1). Accumulation of AGEs with normal ageing occurs in long-lived proteins such as crystalline lens (Dyer *et al*., 1991) and tissue collagens (Dunn *et al*., 1991; Sell *et al*., 1992; Dyer *et al*., 1993). AGEs are also known to cause modification of pathological proteins such as beta-2-microglobulin (in dialysis related amyloidosis*)* (Miyata *et al*., 1994; Ehlerding *et al*., 1998), islet amyloid polypeptide (in Type II diabetes mellitius) (Ma *et al*., 2000) and ß-amyloid plaques (in Alzheimer's disease, AD). (Smith *et al*., 1997; Hensley *et al*., 1998).
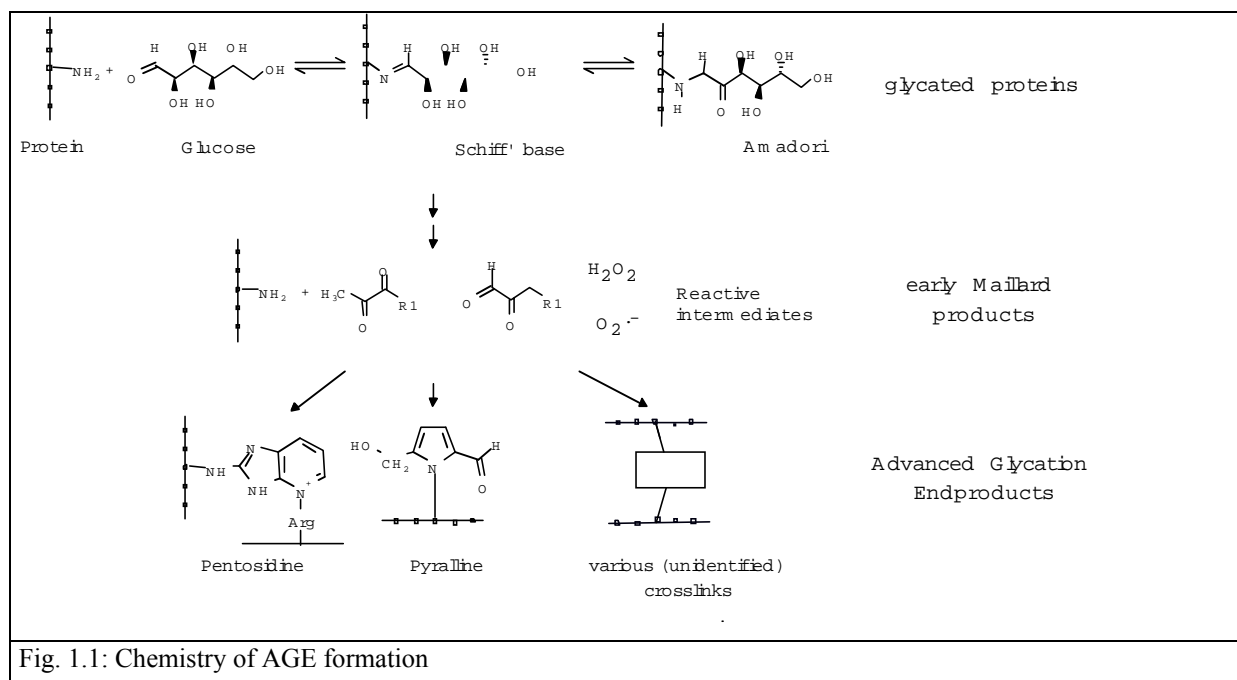
Fig. 1.1: Chemistry of AGE formation

1.2 Glycation precursors

AGEs are also formed by alternative glycolytic pathways with methylglyoxal (MG), glyoxal and 3-deoxyglucosone (3-DG) as precursors of the Maillard reaction. These compounds are also referred to as α-oxoaldehydes and are formed by lipid peroxidation, glycation and degradation of glycolytic intermediates. The reaction of α-oxoaldehydes with lysine and arginine residues in proteins leads to the irreversible formation of AGEs (Thornalley, 1998). Glyoxal is derived from lipid peroxidation (Loidl-Stahlhofen and Spiteller, 1994) and autoxidation of glucose and glycated proteins (Glomb *et al*., 1995; Wells-knecht *et al*., 1995). MG is one of the substrates of the glyoxalase system, which serves to protect cells from α-oxoaldehyde-mediated AGE formation (Thornalley, 1998). Although present at low levels in the circulating blood, MG has a high specific glycating activity, in contrast with glucose, which is present at high levels but has a low specific glycating activity. Through the glyoxalase system, consisting of two enzymes, glyoxalase I and glyoxalase II, and a catalytic amount of glutathione, cells are capable of detoxifying α-oxoaldehydes. However, under conditions of oxidative stress, cellular concentrations of thiol are reduced, giving rise to an accumulation of α-oxoaldehydes and an increase in the formation of α-oxoaldehydes -mediated AGEs (Thornalley, 1998.). 3-DG, a hydrolysis product of fructose-3-phosphate, is a highly reactive carbonyl compound synthesized via the Maillard and polyol pathway. Detoxification of 3-DG to 3-deoxyfructose occurs via a reducing enzyme and the metabolite is excreted in the urine of healthy subjects (Niwa, 1999).

1.3 Structural identification of biologically relevant AGEs

The term AGE applies to a broad range of products of the Maillard reaction, including compounds which do not show a characteristic fluorescence or colour. The chemical structures of some physiological AGEs have been identified, including N^ε-(Carboxymethyl)lysine (CML) (Wells-knecht *et al*., 1995), N^ε-(Carboxyethyl)lysine (CEL) (Ahmed *et al*., 1997), pyrraline (Hayase *et al*., 1989), imidazolone (Niwa *et al*., 1997). In addition, some AGE -crosslinks have been identified, such as pentosidine (Dyer *et al*., 1991; Grandhee und Monnier, 1991), vesperlysine (Nakamura *et al*., 1997) and methyglyoxal – lysine – dimer (MOLD) (Nagaraj *et al*., 1996). Although some AGEs have been structurally characterised, several studies report the detection of uncharacterised AGEs in serum and tissue proteins, identified by enzyme-linked immunosorbent assay and radioreceptor assay (Bierhaus, *et al*., 1998).

1.4 AGEs in aging and degenerative diseases of the cardiovascular system

Recent progress in the understanding of this process has confirmed that AGEs play a significant role in the evolution of vascular complications in normal aging, especially in diabetes and end stage renal disease (Raj *et al*., 2000; Weiss *et al*., 2000). AGEs have been detected in a variety of vascular wall, lipoprotein and lipid constituents, where they lead to macroangiopathy, microangiopathy and amyloidosis. The detrimental effects of AGEs in pathological processes were originally only attributed to their physicochemical properties including protein crosslinking, but more recent studies increasingly emphasize the role of AGEs in cellular signaling events via specific receptors feeding into established signal transduction pathways (Kislinger *et al*., 1999).

In diabetes, accelerated AGE formation is caused primarily by a higher level of plasma glucose and, intracellularly, by activation of the polyol pathway. In hemodialysis patients, similar cardiovascular complications occur, presumably also caused by an increased level of AGEs (Floege and Ketteler, 2001).

1.5 AGEs in aging and in Alzheimer's disease (AD)

Alzheimer's disease (AD) is the most common type of dementia in the elderly. Dementia affects 5-8 % of the world's population over the age of 65 years, 15-20 % of those over 75 and 25-50 % of individuals over 85. AD accounts for 50-75 % of all cases of dementia in the western countries (American Psychiatric Association, 1997). The disease is characterised by an initial mild memory impairment that progresses unrelentingly to a total debilitating loss of mental and physical faculties. The cognitive decline is associated with the widespread loss of synapses, neuronal cell death, gliosis and the formation of amyloid plaques and neurofibrillary tangles. AGE modification and resulting crosslinking of protein deposits has been shown to occur in both plaques and tangles.

AGE accumulation has been demonstrated in senile plaques in different cortical areas, in primitive plaques, coronas of classic plaques and some glial cells of AD brain (Smith *et al.,* 1995). Furthermore, nucleation-dependent polymerization of ß-amyloid, the major component of senile plaques is significantly accelerated by AGE-mediated crosslinking (Münch *et al.,* 1997). Among many contributing factors including the ratio of the 1-42 vs. 1-40 ß-amyloid peptide isoform, AGEs may be an additional factor which accelerate ß-amyloid deposition and plaque formation in sporadic AD.

An interesting association between ApoE4, a susceptibility gene for AD (Roses *et al.,* 1997), and AGEs was described recently. ApoE exhibits AGE-specific binding

activity, with the dimeric form of apoE binding better than the monomeric form. ApoE4 exhibits a 3-fold greater AGE-binding activity than the apoE3 isoform. These results suggest that apoE may participate in aggregate formation in the AD brain by binding to AGE-modified plaque components with pathogenic consequences *in vivo* (Li and Dickson, 1997).

Neurofibrillary tangles (NFT) and neuropil threads are further histological characteristics of AD. The rate of progression of AD-related neurofibrillary changes is unknown, but initial changes occur decades before the disease is diagnosed (Braak and Braak, 1995). The major component of these tangles is the microtubuli associated protein tau (MAP-tau). MAP-tau in AD is glycated at its tubulin binding site, and MAP-tau glycated *in vitro* is capable of inducing oxidative stress (Ledesma *et al*., 1995). The protein constituents of NFT are resistant to proteolytic removal, possibly as a result of extensive cross-links. In addition to glycation, formation of specific disulfide bridges and hyperphosphorylation also contribute to the crosslinking process (Mandelkow *et al*., 1995).

1.6 AD and diabetes

Human populations show progressive age-related trends for increased blood glucose that are concurrent with the accelerating incidence of AD. The accumulation of AGEs in the AD brain, also found in peripheral tissues during diabetes, suggests that the pathological mechanisms of AD may be partially related to age-related changes in metabolism (Hoyer, 1998). AGEs may generally cause nerve dysfunction, since diabetic and end stage renal disease patients with AGE levels exhibit an increased incidence of peripheral neuropathy (Green *et al*., 1999; Brownlee, 2000). In addition, in two large population-based studies where the development of dementia was followed over a long time period, adult-onset diabetes increased the risk of both vascular dementia and Alzheimer's disease (Leibson *et al*., 1997; Ott *et al.,* 1998).

1.7 Evidence for a chronic sub-acute inflammatory process in AD

There is now considerable evidence that AD is characterized by a chronic, but silent, inflammatory process in affected brain regions. Involvement of the immune system in the pathogenesis of AD is evident by both presence of complement proteins in diseased tissue, and by the activation of cells of the immune system as well as the release of pro-inflammatory cytokines. AD tissue contains components of the classical, but not the alternative, complement pathway. The cytokines are important modulators of

inflammation, and accumulated evidence suggests that many occur at abnormal levels in brain regions affected by disease or injury (Akiyama *et al.*, 2000) Most importantly, various epidemiological studies indicate that anti-inflammatory drugs inhibit the onset and slow down the progression of AD (McGeer *et al.*, 1996).

1.8 Interaction of AGEs with cells of the CNS and subsequent oxidative stress

AGEs directly lead to activation of microglia and astroglia with the induction of oxidative stress, a further characteristic feature of AD (Fig. 1.2) (Markesbery and Carney, 1999; Smith *et al.*, 2000). Widespread signs of oxidative damage including nitration of tyrosine residues in proteins are evident in affected regions in AD suggesting that, among other radical species, nitric oxide (NO) production is upregulated (Smith *et al.*, 1997; Hensley *et al.*, 2000;). NO is catalytically produced by different isoforms of nitric oxide synthase during the oxidation of the terminal guanidino nitrogen of L-arginine to L-citrulline (Mayer and Hemmens, 1997). Three isoforms of NOS exist: the constitutive and calcium-dependent neuronal (nNOS or NOS1) and endothelial (eNOS or NOS3) forms and the inducible, non-calcium-dependent macrophage (iNOS or NOS2) form. NO derived from nNOS and eNOS has an important role in neural signaling and immunomodulation, whereas the NO due to iNOS activity is produced in greater amounts than nNOS or eNOS and is associated with cellular pathology (Calabrese *et al.*, 2000). Roles proposed for NO in CNS pathophysiology are increasingly diverse and range from intercellular signaling, through necrosis of cells and invading pathogens, to the involvement of NO in apoptosis (Lamas *et al.,* 1998; Bredt, 1999; Floyd, 1999). This radical challenge has been shown to cause "bystander-lysis" of neighbouring neurons in a coculture of microglia and PC-12 cells (Chang *et al.*, 2000). Thus a high level of NO generated in the brain is capable of inducing a chain of damaging reactions resulting in neuronal death. Due to the inability of cells to sequester this membrane-permeant molecule, it would be necessary to regulate the local concentration of NO and the most logical means of regulating NO activity would be to control its synthesis.

AGEs also induce the activation of peripheral macrophages and chemotaxis of mononuclear phagocytes, as well as the release of cytokines such as IL-1, IL-6 and TNF-α (Iida *et al.,* 1994; Morohoshi *et al.*, 1995; Westwood and Thornalley, 1996). Interestingly, IL-6 and TGF-ß immunoreactivity in the vicinity of neuritic plaques (Luterman *et al.*, 2000) and elevated concentrations of IL-6 and IL-1 receptor type II in the CSF (Garlind *et al.*, 1999) have been demonstrated in the brain of AD patients. This

supports the finding that an autodestructive process, involving overactive microglia and astroglia occurs at the characteristic lesions in AD (Akiyama *et al*., 2000). These overactive cells produce high levels of free radicals, which subsequently lead to an impaired glucose transport, which is downregulated in AD (Keller, 1997; Guo and Mattson, 2000). It is proposed that this involves the peroxidation of membrane lipids, which leads to a decreased membrane fluidity and loss of protein function including the glucose transporter in the brain (Mark *et al*., 1997). In summary, there is increasing evidence that the previously so-called "secondary factors" such as a disturbed glucose metabolism, oxidative stress, formation of AGEs and their interaction in a vicious cycle are also important for the onset and progression of AD (Finch and Cohen, 1997).

mitochondrial uncoupling	respiratory burst of microglia (and astroglia ?)	**SOURCES**
oxidative stress		EFFECTS
DNA strand breaks glycoxidation (AGEs) lipid peroxidation protein oxidation		*molecular level*
impairment of energy production neuritic dystrophy cell death		*cellular level*

Fig 1.2: Oxidative stress by microglia in the pathophysiological cascades in AD

1.9 AGEs and Parkinson's disease

Parkinson's disease (PD) is a progressive neurodegenerative disorder with an increasing incidence above 50 years of age. The motor dysfunction characteristic of PD results from a depletion in dopamine producing cells in the striatum (Forno, 1981). Current theories related to the pathogenesis of neurodegenerative diseases including Parkinson's disease focus on the formation of oxygen free radicals, which may in turn elicit neuronal damage. Postmortem studies have shown alterations in brain iron content, impaired mitochondrial function, changes in the ratio of superoxide dismutase to catalase and reduction of reduced glutathione. All these changes are suggested to play a part in the etiopathogensis of Parkinson's disease (PD) (Youdim and Riederer, 1997; Sian *et al.,* 1999). PD is characterized by neuronal cell loss in the Substantia Nigra (SN) pars compacta coupled with the presence of intracellular neuronal inclusion such as Lewy bodies and neuromelanin (Braak *et al*., 2000). It has been histochemically shown that

crosslinking by AGEs contributes to functional loss and insolubility of the proteins present in these deposits (Castellani *et al*., 1996).

In PD and Lewy body dementia, Lewy bodies predominantly contain neurofilament and cytoplasmic proteins, including α-synuclein (Spillantini *et al*., 1998; Gomez-Tortosa *et al*., 2000). Immunoreactivity to pentosidine and pyrraline, two specific AGEs, was seen in Lewy bodies in the SN of PD patients and the neocortex of diffuse Lewy body disease (Castellani *et al.,* 1996). However, it is still controversial, whether AGE crosslinking, promoted by the depletion of reduced glutathione (Shinpo *et al*., 2000) is a late or an early pathophysiologically relevant event.

1.10 Receptors for AGEs and AGE-induced signaling

In view of the close association of AGEs with cells in the body and their known adverse effects on cells, many studies have focused on searching for AGE binding proteins. Binding and internalization of AGE-modified proteins is facilitated through several AGE- specific cell surface receptors, including AGE-R1 (80K-H/p90), AGE-R2 (OST/p48), AGE-R3 (galectin-3), macrophage scavenger-receptor (MSR), and a receptor for AGEs (RAGE) (Li *et al*., 1998; Schmidt and Stern, 2000). RAGE can also interact with amphoterin to regulate neurite outgrowth during nerve development (Huttunen 2000 JBC). Thus, cellular signaling of AGEs has emerged as an important link in the pathophysiological events of AD, showing activation of cellular transcription mechanisms in the response to an elevated AGE level, such as in the vicinity of a neuritic plaque. AGE-RAGE interaction has been shown to activate two major signal transduction pathways: a redox-sensitive pathway involving the transcription factor NFκB (Kislinger *et al*., 1999; Mohamed *et al*., 1999) and a mitogenic pathway involving protein kinases including ERK-2 and the transcription factor AP-1 (Lander *et al.,* 1997). Both signal transduction pathways could be involved in the pathophysiological events of AD.

The redox-sensitive pathway involves NFkB, a three-subunit complex consisting of two subunits of 50kDa (p50) and 65 kDa (p65) and an inhibitory subunit, IkB. The NFkB is located in the cytosol and upon activation, induced by the dissociation of IkB, the p50-p65 dimer translocates to the nucleus (Mattson, 2000). This pathway is likely to be important in neurons, astroglia and microglia where AGEs or ßA4 might cause the release of cytokines and free radicals (Yan *et al.,* 1997). This pathway can be initiated by both AGEs and ßA4 and uses reactive oxygen intermediates as messengers.

AGEs are able to activate p21(ras) as well as the mitogen-activated protein kinases (MAP-kinase or ERK) ERK 1 and ERK 2 and their downstream target, the AP-1 complex via a RAGE-dependent pathway. MAP kinases are able to phosphorylate MAP-tau, thereby generating abnormally hyperphosphorylated tau species that are similar to PHF-tau found in AD (Shea, 1997). Thus it is likely that the activation of the MAP kinase cascade by AGEs is critically involved in the processes of neurodegeneration and aberrant repair.

1.11 Combinatorial approaches to immunogenic AGE-structures. (AGE-peptide spot libraries)

Despite the structural elucidation of a few specific AGEs and their biological significance, the exact chemical structure for many AGEs is still unknown, due to their heterogeneity and the complexity of their routes of formation. Furthermore, limited understanding of the structures of AGEs hinders research into the identification of the more physiologically relevant/harmful AGES and their exact mechanism of toxicity. Since most AGE-modified proteins used as antigens contain a mixture of various substructures, antibodies raised against these AGE-modified proteins recognise a variety of AGE epitopes (Ling *et al.*, 1998). One method of classification of anti-AGE antibodies divides these antibodies into three groups according to their CML-specificity (Ikeda *et al.*, 98). However, a more systematic approach in mapping the amino acid specificity of AGEs would assist in the standardisation of histochemical results as well as the quanitification of AGEs in biological fluids.

Combinatorial peptide libraries represent one of the best technical approaches for the systematic mapping of antigenic epitopes. They can be efficiently synthesised on paper sheets ('SPOT' libraries) (Frank, 1995; Rudiger *et al.*, 1997; Reineke *et al.*, 1998). Such a library, consisting of dipeptides chemically crosslinked to sugars, has been recently applied to systematically assay the relative reactivities of amino acid side chains and the N-terminal amino group towards sugars as well as towards crosslinking to preformed protein-AGEs (Münch *et al.*, 1999). Peptide libraries have been intensively used to determine immunogenic protein epitopes, i.e. which amino acids are part of the epitope recognised by an antibody.

1.12 Aims

      The overall aim of this study was to reach a closer understanding of the mechanisms underlying the role of AGE-related oxidative stress in neurodegenerative diseases such as AD and PD. In particular, the induction of oxidative stress via the release of NO by activated microglia and the effects of membrane permeable antioxidants as inhibitors of this inflammatory response were examined. The role of AGEs in the induction of NO was compared with ßA4, one of the main components of the amyloid plaque in AD. The localisation of AGEs and Aß with iNOS was immunohistochemically compared in the brains of normal aged individuals and AD cases. The presence of AGEs was also examined in the brain tissue of non-demented patients whose pathological diagnosis showed Lewy bodies in the SN, i.e so-called cases of incidental Lewy body disease. Finally, a recently novel technique involving a peptide SPOT library was used to determine the relative reactivities of amino acid residues toward reducing sugars and map the specificity of four different anti-AGE antibodies.

2. MATERIAL AND METHODS

2.1 Material

2.1.1 Chemicals

Chemicals were obtained from the following companies: Amersham Life Science, Calbiochem, Fluka, Merck, Sigma, Riedel de Haen, Roche Diagnostics, Roth.

2.1.2. Peptide synthesis

Amino acids and chemicals for peptide synthesis were obtained from Novabiochem (Table 2.1.1). Amine derivatised cellulose and polypropylene membranes (APEG) were purchased from AIMS Scientific Products, Hartmann Analytic.

Table 2.1 - Amino acids used for peptide spot synthesis

Code	Designation	MW g/mol
ß-Ala	Fmoc-ßAla-OH	311.3
A	Fmoc-Ala-OH	311.3
R	Fmoc-Arg(Pmc)-OH 98%	662.8
N	Fmoc-Asn-(Trt)-OH	596.7
D	Fmoc-Asp-(OBu)-OH	411.5
C	Fmoc-Cys-(Trt)-OH	585.7
Q	Fmoc-Gln-(Trt)-OH	610.7
G	Fmoc-Gly-OH	297.3
H	Fmoc-His-(Trt)-OH	619.7
K	Fmoc-Lys-(Boc)-OH	468.6
F	Fmoc-Phe-OH	387.4
W	Fmoc-Trp-(Boc)-OH 95%	526.6
Y	Fmoc-Tyr-(tBu)-OH	459.5

2.1.3. Antibodies

The following antibodies were used:

a) polyclonal anti-AGE (Hb-CML, K1933, Dr Stahl, Dr Kientsch-Engel, ROCHE Diagnostics)

b) polyclonal anti-AGE (KLH-CML, K2002/4, Dr Stahl, Dr Kientsch-Engel, ROCHE Diagnostics)

c) polyclonal anti-AGE (Hb-peptide-CML, K2013, Dr Stahl, Dr Kientsch-Engel, ROCHE Diagnostics)

d) monoclonal anti-AGE (Hb-CML, M-4G9, Alteon, New York)

e) polyclonal anti-AGE (RNAse-AGE K1935, Dr Stahl, Dr Kientsch-Engel, ROCHE Diagnostics)

f) polyclonal anti-AGE (RNAse-AGE, K1936, Dr Stahl, Dr Kientsch-Engel, ROCHE Diagnostics)

g) polyclonal anti-AGE (RNAse-AGE, K1937, Dr Stahl, Dr Kientsch-Engel, ROCHE Diagnostics)

h) monoclonal anti-Imidazolone Mab AG1 (KLH-AGE, Dr. T. Niwa, Nagoya)

i) monoclonal anti-CML-peroxidase (Alteon, New York)

j) polyclonal anti-iNOS antibody (BIOMOL, ALEXIS),

k) monoclonal anti-ß-amyloid (DAKO)

l) monoclonal anti-PHF 1 (P. Davies, New York)

m) monoclonal anti-monocyte (BIOLOGO)

n) anti-RAGE (Dr J. Li, New York)

o) monoclonal anti α-synuclein (Transduction Laboratories)

p) monoclonal anti-neurofilament SMI 32, SMI 311, SMI 312 (Sternberger Monoclonals).

Preparation of anti-AGE-antibodies

The polyclonal antibody used for histochemistry (RNAse-AGE, K1936, ROCHE Diagnostics) was prepared by incubation of RNAse (10 mg/ml) with a solution of 500 μM glucose and 1 μM Cu^{2+} in 100 μM phosphate buffer, pH 7.4 for 4 weeks at 37°C under sterile conditions.

The anti-imidazolone (AG-1) antibody was selected from several clones of monoclonal antibodies, which were produced against AGEs by immunising mice with AGE-keyhole limpet hemocyanine (KLH). The AG-1 clone reacted specifically with imidazolones A and B.

The anti-AGE antibody raised against AGE-keyhole limpet hemocyanine (KLH) was prepared by incubating KLH (10 mg/ml) with 1 M glucose for 3 months at 50°C. New Zealand white rabbits were immunized subcutaneously with 100 μg KLH-AGE. Booster injections were given with 50 μg KLH-AGE after 2 weeks. Blood was collected 2 weeks after the booster injection and coagulated overnight. The supernatant was centrifuged at 8000 g for 10 min and filtered through a 0.45 μm cellulose filter. Serum was frozen and

stored in aliquots at -70°C. Specificity of the antibody for AGEs was tested with various AGE-proteins such as AGE-chicken egg albumin, AGE-lysozyme and AGE-BSA both in ELISA and Western blot. Although affinity purified antibody was preferred for histological staining to reduce background, no differences in staining pattern compared to unpurified serum were observed. This antibody has been previously used for AGE staining in dog brain and in human AD cases (Münch *et al*., 1998; Weber *et al*., 1998), and preferentially recognizes arginine-derived AGEs (unpublished observation).

2.1.4 Antioxidants

Antioxidants were obtained from: ASTA Medica AG, Frankfurt (R-(+)-thioctic acid), Centaur Pharmaceuticals (PBN, N-tert.-butyl-α-phenylnitrone), Tebonin ® forte, Dr Willmar Schwabe Arzneimittel, Karlsruhe (*Gingko biloba* extract EGb 761 extract), and Sigma (17β-estradiol).

2.1.5 Cell culture

Cell culture medium and supplement solutions were obtained from Gibco. Sterile flasks, plates and other cell culture labware were purchased from Greiner, Falcon and Becton-Dickinson.

2.1.6 Cases used for immunohistochemistry

Alzheimer's Disease (AD)

Brains used in the present study were obtained from 8 controls, subdivided into an older (65-90 years, 4 males) and a younger (30-50 years, 4 males) group and from 12 patients with AD, subdivided into an advanced (Braak stage III-VI; 1 male, 8 females) and early (Braak stage I-II; 3 males) stage of the disease (Braak and Braak, 1992) (Table 2 and Table 3). The AD cases were matched with respect to age (mean age: aged controls; 79.3 +/- 8.1 years; AD, 83.8 +/- 6.6 years; $p > 0.20$, Student's t-test), postmortem interval (old controls: 64 +/- 30 h; AD: 47 +/- 33 h; $p > 0.20$) and the "Premortem Severity Index" (PMSI) by Monfort *et al.* (1985) ($p > 0.20$) to minimize the likelihood of an artificial influence by premortem hypoxia and hypovolemia. The young control group (mean age: 39) was used to evaluate age-related changes as well as to compare with changes found in early stage AD. The whole procedure of case recruitment, acquisition of patients' personal data, performing the autopsy, and handling the autoptic material was performed in accordance with the Helsinki Declaration in its latest version and the convention of the council of

Europe on Human Rights and Biomedicine and was approved by the responsible Ethical Committee of Leipzig University.

Brains used for the group of controls were obtained at routine autopsy from patients who died without a history of neuropsychiatric disorder or mental impairment or diabetes mellitus. There had to be clear evidence that the patient was alert, well oriented, and capable of functioning relatively independently shortly before death. No pathological signs were detected by neuropathological examination. The clinical diagnosis of AD was based on the occurrence of significant intellectual dysfunction i.e. the presence of deficits in at least four aspects of cognitive and social behaviour. Other causes of dementia were excluded by medical, psychiatric and paraclinical examination (Diagnostic and Statistical Manual of Mental Disorders, DSM-IIIR, American Psychiatric Association). Cases with a history of diabetes mellitus were excluded. Each case met the National Institute of Neurologic and Communicative Disorders and Stroke (NINCDS) and Alzheimer's Disease and Related Disorders Association (ADRDA) criteria for definite diagnosis of Alzheimer's disease (McKhann *et al*., 1984), based on the presence of NFTs and neuritic plaques observed in the hippocampal formation and neocortical areas, as recommended (Khatchaturian ,1984).

Table 2.2 - summary of control (used for comparison with AD) cases in immunohistochemistry

CASE NO.	NEUROPATHO - LOGICAL DIAGNOSIS	AGE (yr)	SEX	BRAIN MASS (g)	POST - MORTEM DELAY (h)	CAUSE OF DEATH
1	NORMAL	33	m	1280	96	mycotic pneumonia
2	NORMAL	36	m	1630	96	multiorgan failure septic shock
3	NORMAL	38	m	1430	96	multiorgan failure
4	NORMAL	49	m	1480	48	multiorgan failure septic shock
5	NORMAL	68	m	1400	24	septic shock
6	NORMAL	79	m	1250	96	chronic ischaemic heart disease
7	NORMAL	84	m	1100	72	pulmonary carcinoma liver metastases
8	NORMAL	86	m	1220	64	bronchopneumonia

Table 2.3 - summary of AD cases used in immunohistemistry

CASE NO.	NEUROPATH-OLOGICAL DIAGNOSIS	BRAAK STAGE	AGE (yr)	SEX	BRAIN MASS (g)	POST-MORTEM DELAY(h)	CAUSE OF DEATH
9	AD	I - II	74	m	1350	105	acute myocardial infarct
10	AD	I - II	82	m	1250	26	gastric carcinoma
11	AD	I - II	85	m	1390	32	acute myocardial infarct
12	AD	V -VI	76	f	1350	105	acute myocardial infarct
13	AD	V -VI	79	f	1195	32	heart failure
14	AD	V -VI	79	f	1060	19	pulmonary embolus
15	AD	V -VI	83	f	1110	14	heart failure
16	AD	V -VI	85	f	1100	29	tumor intoxication
17	AD	V -VI	86	f	1305	48	cerebral insufficiency
18	AD	V -VI	88	f	1085	84	Morgani-Adam-Stokes (MAS) attack
19	AD	III - IV	90	m	990	39	gastric carcinoma
20	AD	III - IV	98	f	1065	25	chronic heart insufficiency

Incidental Lewy body disease

The brains were obtained via a rapid autopsy system of the Netherland Brain Bank (NBB) of patients who were donors and signed informed consent for brain donation and autopsy. The patients had no previous history of either neurological or psychiatric disorders or mental impairment (Tab. 2.4). Based on the presence of Lewy bodies in the SN (frequency of about 1 to 2 neurons out of 400 to 600 affected), four cases (mean age: 76.5 +/- 5.3 years) were diagnosed as having incidental Lewy body disease, which might be considered to be a preclinical stage of PD. There was no indication of depigmentation, but a moderate neuronal cell loss (20 - 30 %) in the SN of these patients. Four cases without any neuropathological changes served as control (77.2 +/- 6.3 years). The entire procedure of recruitment was performed to conform to the ethical code of conduct of the NBB.

Table 2.4 - summary of Lewy body disease cases

case	sex	age	diagnosis
1	m	71	non-demented control
2	m	73	non-demented control + Lewy bodies
3	f	80	control + Lewy bodies
4	m	82	control + Lewy bodies

2.2 Methods

2.2.1. Production of AGEs

2.2.1.1 BSA and chicken egg albumin AGE

AGEs were produced by incubation of BSA or chicken egg albumin at a concentration of 1 mM with 1 M glucose in 100 mM phosphate buffer, pH 7.4 at 50°C for 6 weeks. Since a steady and nearly linear increase in both fluorescence (370 nm excitation/440 nm emission) and absorbance at 400 nm was observed after 6 weeks and the increase thereafter was only marginal, the BSA was assumed to be maximally modified by AGEs. Unbound sugars were removed by dialysing for 1 week in 2 l distilled water, changed daily. Model-AGEs were lyophilised and resuspended in PBS (pH 7.4). Protein content was determined by the Bradford-assay, using BSA as a standard. Optical densities were determined at 400 nm and 360 nm and fluorescence was measured (Exc.370 nm / Em. 440 nm). AGE preparations were heated at 70°C for 20 min immediately before applying to cell culture. Methylglyoxal (MG)-AGE was prepared accordingly to Westwood *et al*. (1995).

2.2.1.2. ß-amyloid AGE

The ß-amyloid peptide (ßA4) (1-40) was produced in our laboratory (Prof. Dr. Palm) with a Zinsser simultaneous multiple-peptide synthesiser using a Fmoc protection and diisopropylcarbodiimide/hydroxybenzotriazole (DIC/HOBT) activating chemistry with routine double-coupling steps. Deprotection and cleavage was achieved with trifluoroacetic

acid/anisol/ethanedithiol/water (93: 5: 2.5: 2.5, by vol.). After precipitation in ether, the peptide was redissolved in 10% formic acid and purified on a preparative RP-HPLC C$_{18}$ column. Purity of the peptide was confirmed by comparison with commercial ßA4 (1-40) standards by analytical HPLC, and its molecular mass by matrix-assisted laser desorption ionisation (MALDI) MS.

Sequence of the peptide:

ßA4 (1-40)	DAEFRHDSGYEVHHQKLVFFAEDVGSNKGAIIGLMVGGVV

ßA4 (1-40) was dissolved in water at a concentration of 1 mg/ml and incubated for 1 week at 37°C. ßA4-AGE were produced by incubation of the ßA4 peptide (1-40) in the dark at a concentration of 10 mg/ml in 100 mM phosphate buffer, pH 7.4 with 500 mM glucose for 2 weeks or 2 mM methylglyoxal for 2 days. In contrast to the protein–modified AGE, removal of unbound sugars in ßA4-AGE preparations is more difficult, due to adhesion of the aggregated amyloid to the dialysis membrane. Hence, frequent washings of the ßA4-AGE in distilled water was carried out in order to minimise the presence of unbound sugars. The ßA4-AGE solution was then centrifuged for 15 min at 15 000 rpm, the supernatant removed and the ßA4-AGE pellet redissolved in water. This step was repeated three times, after which the pellet was redissolved in 1 x PBS. AGE - and ThioT- fluorescence were measured and accumulation of AGE was confirmed by their characteristic fluorescence (Exc. 370nm, Em. 440nm) using FPLC.

2.2.2. CML-content

The CML-content of the AGE preparations was determined by competitive ELISA (ROCHE Diagnostics) using a monoclonal CML-antibody. This technique measures the ability of the AGE in the samples to compete with the immobilised AGE on the microtitre plate surface for binding to the first AGE antibody.

2.2.3. Endotoxin Assay

All BSA and AGE preparations were tested for bacterial contamination using the Limulus Amebocyte Lysate (QCL-1000, Biowhittaker). This method detects endotoxin chromogenically from the reaction between a modified Limulus Amebocyte Lysate (LAL) and a synthetic colour producing substrate. 25 µl of the sample solution was mixed with 25 µl LAL and incubated at 37 °C for 10 min in a 96-well ELISA-plate. 50 µl of substrate

solution was then mixed with the LAL-sample and incubated at 37 °C for an additional 6 min. The reaction was stopped by adding 50 µl of 10 % SDS. The absorbance of the samples were determined spectrophotometrically at 404 nm. Since this absorption is directly proportional to the amount of endotoxin present, the concentration of endotoxin was calculated from a standard curve.

2.2.4. Protein determination

The concentration of protein in samples was measured with the Bradford assay which relies on the binding of the Coomassie Brillant Blue dye with protein. The dye binds more readily with the free NH_2-groups of arginyl and lysyl residues. An aliquot of the sample was mixed with 500 µl of the reagent and the absorption read after 5 min at 595 nm. Incubations were made against a reagent blank consisting of distilled water. Protein concentration was calculated by comparing the values of the samples with a BSA standard.

Bradford - Reagents

Coomassie Brillant Blue	100 mg
Ethanol abs.	50 ml
Phosphoric acid 85%	100 ml
distilled water	ad 1 l

2.2.5. Fluorescence measurements
2.2.5.1 AGEs

At an excitation wavelength of 370 nm, AGEs show a characteristic emission maximum of 440 nm (Nagaraj and Monnier, 1992). For fluorescence measurements AGEs were diluted in 1 x PBS or distilled water. Reagent blanks contained 1 x PBS or distilled water only.

2.2.5.2 Detection of βA4 fibrils using Thioflavin T - Fluorescence

Growth of βA4 aggregates leads to the formation of β-pleated sheets (Lansbury, 1992). These form adducts with the fluorescence dye Thioflavin T and increase its emission maximum to 480nm.

Testbuffer

Phosphate buffer, pH 6	50 mM

Thioflavin T	3 µM

Excitation 450 nm, Emission maximum 480 nm

2.2.6. Cell culture

2.2.6.1 Production of cell culture medium

DMEM (Dulbeccos modified Eagles Medium) was prepared by combining the powder with sodium carbonate according to the instructions provided and steril-filtered through a 0.2 µm mediumfilter (Spektrum).

The following substances were added to the medium prior to use in cell culture:

L-Glutamine	2 mM
Penicillin	100 µg/ml
Streptomycin	100 U/ml
FCS	10 % or 1 %

FCS : Fetal calf serum was heat-inactivated at 56 °C for 30 min., aliquoted und stored at −20°C.

2.2.6.2 Cell line

Since a clonal human microglia cell line is still lacking, the monocyte cell line, THP - 1, is widely used as a test system to assess AD specific inflammatory responses. Alternatively, rodent microglia cells are routinely used. We have selected the N-11 microglia cell, derived from primary mouse microglial cells, which expresses the full set of pro-inflammatory cytokines upon stimulation and has been used as a model cell line of microglial constitutive and inducible functional activities (Corradin *et al*., 1993). Microglia cells (N-11 cell line) were derived from transfection of primary mouse microglia (Dr Paola Ricciardi-Castagnoli, Centre of Cytopharmacology, Milan, Italy). In addition, the J774A.1 murine macrophage (ATCC TIB-67) cell line was used as a control for production of NO and expression of iNOS, as these responses are well established in this cell line (Kiemer and Vollmar, 1997; Lui, 1998).

2.2.6.3 Cell culture techniques

Cells were grown in 75 cm^2 sterile tissue flasks for 24 - 36 h until confluency in DMEM/10 % FCS, supplemented with penicilline/streptomycine (100 U/ml, 100 µg/ml) and l-glutamine (2 mM) at 37°C, 5 % CO_2. Before incubation with test substances, the cell culture medium was replaced with medium containing 1 % serum for 24 h to minimise the

interference of growth factors in the serum with signal transduction. Fresh medium with 1 % serum was added 1 h before the start of the experiment. For experiments with BSA-AGEs, cells were seeded onto 6-well tissue culture plates at a density of 1×10^6 cells per well. NO production was induced by the addition of BSA-AGEs (2.0 μM) for 4, 8, 12, 16, 20 and 24 h. For experiments with ßA4-AGE, MG, and 3-DG, cells were seeded onto 96-well tissue culture plates at a density of 1×10^4 cells per well. The induction of NO production was measured following the addition of fibrillar ßA4 (2.5 – 80 μM), ßA4-Glu (2.5 – 80 μM), ßA4-MG (2.5 – 80 μM), BSA-Glu (0.4 – 10 μM), BSA-MG (0.4 – 10 μM), MG (0.4 – 250 μM), and 3-DG (0.4 – 250 μM) for 24 h. As a positive control for NO production, LPS (*Salmonella typhimurium*, Sigma Aldrich; 50 μg/ml) was added to one of the wells for 24 h. Negative control wells contained BSA or medium only.

2.2.6.4 Cell counts

Cells were washed with 1 x PBS and incubated for 3-5 min in 1 x trypsin (Gibco) to detach cells from the plate. Cell culture medium was added to inactivate the trypsin and the cell suspension centrifuged for 5 min at 4000 rpm. Cells were re-suspended in fresh medium and 10 μl of the suspension was pipetted onto a Neubauer counting chamber for determination of the number of cells per volume. This chamber contains 4 large grids, consisting of 16 smaller grids. The area of one of the large grids is 1 mm^2 and the height of the chamber is 0.1 mm^2. Hence, the volume of one large grid is 0.1 mm^3, which corresponds to 0.4 mm^3 for the 4 large grids together.

A factor of 2.5×10^3 per ml of cell suspension (achieved by dividing the volume of cell suspension, 1000 mm^3, by the volume of the 4 large grids, 0.4 mm^3) was accounted for in the calculations. The total number of cells is given by:

Number of cells counted in the 4 large grids x 2.5 x 10^3 x volume (ml) of cell suspension.

2.2.6.5 Freezing and thawing of cells

Cells are able to be stored for several months at –80 °C and for several years in N_2 at –170 °C. For freezing, cells grown confluently in a Petri dish were divided and placed into 1.5 ml of freezing medium (20 % FCS, 10 % dimethylsulfoxide, DMSO, in DMEM) in sterile cryotubes. Cells were frozen for 1 h at –20 °C and for 12 h at –80 °C, then stored

in liquid N_2. Cells were thawed by placing the cryotubes in a 37 °C water bath, then transferring the suspension to Falcon tubes containing fresh, warmed medium and centrifuging the suspension for 5 min at 1200 rpm. After resuspension in fresh medium, cells were seeded onto cell culture plates.

2.2.7. MTT (3-(4,5-dimethylthiazol-2-yl)2,5-diphenyl tetrazolium bromide) Assay

This test measures the metabolic activity of cells via the intracellular reduction of a yellow, soluble tetrazolium salt (MTT) to a violet, insoluble product (formazan) with an absorption maximum of 550 nm (Mosmann, 1983). The reaction takes place in the inner mitochondrial membrane of intact cells via the respiratory enzymes, succinate dehydrogenase and cytochrome dehydrogenase. The amount of formazan produced is proportional to the number of living cells.

3×10^5 cells/well were seeded onto 96- well cell culture plates and grown for 2 days. The medium was then changed and test substances added (100 µl end volume). Following incubation, the medium was removed and the cells washed with 1 x PBS. 100 µl of medium without phenol red and 25 µl of a MTT stock solution (1.5 mg / ml) was added. The use of medium without phenol red is crucial for two reasons. Firstly, the colour of the medium may affect consequent absorption measurements at 550 nm and secondly, phenol red may act as an electron acceptor. After 4 h incubation, the supernatant was removed and the formed formazan crystals dissolved by addition of EtOH / DMSO (1:1). Dissolution of the crystals was maximised by placing the plates on a rotary shaker for 10 min or in an ultrasonic bath for 3 min. Absorption of the formed dye was measured with a 96 well plate Elisa-Reader at 550 nm using a reference filter set to 630 nm. The reduction in cell activity of treated cells was calculated as a percentage of untreated control cells, taken as 100 %. All MTT assays were performed in triplicate.

2.2.8. Incubation with antioxidants

A variety of antioxidants were tested for their effects on the BSA-AGE induced NO production and NO synthase expression. R-(+)-thioctic acid (ASTA Medica AG, Frankfurt), N-tert.-butyl-a-phenylnitrone (PBN, Centaur Pharmaceuticals), of *Gingko biloba* extract EGb 761 extract (Tebonin ® forte, Dr Willmar Schwabe Arzneimittel, Karlsruhe), and 17β-estradiol (Sigma), an estrogen derivative, were added to the cell wells at concentrations ranging from 0.002 µM - 2 mM, 30 min prior to a 10 h incubation with 2 µM BSA-AGE. A stock solution of R-(+)-thioctic acid was prepared in sterile PBS and

stock solutions of PBN, *Gingko biloba* extract EGb761 and 17β-estradiol were prepared in ethanol. Incubation of cells with the compounds alone or their solvent ethanol had no effect on iNOS expression nor NO production (data not shown). Following incubation for 10 h, the supernatant was collected for nitrite analysis and the cells lysed for Western blotting and iNOS detection.

2.2.9. NO determination

At the specified time points, 1 ml of supernatant was collected for assay of nitric oxide, measured as nitrite. Nitrite concentration in the supernatant was measured by transferring 100 µL of supernatant to a 96-well plate to which 100 µL of Griess Reagent was added. After 15 min, formed colour was measured in a ELISA plate reader at 550 nm with a reference at 630 nm.

2.2.10. Cell lysis and SDS - Polyacrylamide Gel Electrophoresis (SDS-PAGE)

Cells were lysed with lysis buffer containing 2 % SDS and 1 mM sodium vanadate after incubation with BSA-AGEs or LPS. Protein separation was achieved by SDS – Polyacrylamide Gel Electrophoresis (SDS-PAGE, first described by Lämmli, 1970). An acrylamide gel consisting of a separating and stacking gel with different pH-values was set up. Proteins were completely denatured by boiling for 3 min at 95 °C in sample buffer pH 6.8 (4 % SDS, 12 % glycerol, 85 % 50 mM Tris, 2 % mercaptoethanol, 0.01 % Coomassie Brilliant Blue). SDS is an anionic detergent which binds strongly to, and denatures proteins as well as conferring to them a large negative charge. Protein separation occurs on the basis of molecular weight in the direction of the anode. 10 µg of total protein from each sample was added to a loading buffer, and pipetted into separate lanes of a 8 % SDS polyacryamide gel. A high range Color Marker (Sigma) was used as a molecular mass standard for the SDS-PAGE.

Pipetting volumes for 1 minigel:

	Separating gel	Stacking gel
Polyacrylamide 30%	1.33 ml	417.5 µl
Bisacrylamide 2%	325 µl	165 µl
Tris 1 M, pH 8,7	1.86 ml	-
Tris 250 mM, pH 6,8	-	1.25 ml
20 % SDS	50 µl	25 µl
distilled water	1.06 ml	452.5 µl
APS 40%	50 µl	25 µl
TEMED	10 µl	5 µl

10 x gel buffer, pH 8.4

Tris	0.25 M
Glycin	1.92 M
SDS	1 %

2.2.11. Western blot for detection of inducible NO synthase

After gel electrophoresis, the proteins were transferred from the gel onto a nitrocellulose membrane via the wet transfer method (in transfer buffer pH 8.3: 24.8 mM Tris, 192 mM glycine, 10 % methanol). Following an overnight block in 3 % BSA/TBS-Tween 20 (0.1 %) at 4°C, the membrane was incubated in rabbit polyclonal anti-iNOS (BIOMOL, 1:2,000 in block buffer) or goat polyclonal anti-RAGE antibody (J.Li, 1:2,000) for 2 h at room temperature. The membrane was then washed 6 x 5 min in TBS-Tween (0.1 %), incubated with anti-rabbit IgG peroxidase conjugate (ROCHE Diagnostics, 1:10,000) or anti-goat IgG peroxidase conjugate (Boehringer Mannheim, 1:2,500) for 1 h at room temperature, washed again 6 x 5 min in TBS-Tween (0.1 %) and drained. Detection was done by enhanced chemiluminescence (ECL Western blotting, Amersham).

2.2.12. RNA isolation

N-11 microglial cells were grown in cultured medium (same conditions as for Western blotting) in tissue culture flasks (1 x 10^7 cells per flask and incubated with BSA

(2.4 μM), BSA-AGEs (2.4 μM) or LPS (50 μg/ml) for 1-4 h, then lysed with 1 ml of guanidinium thiocyanate solution (TRIZOL, BRL). The cell lysates were mixed with 2 M sodium acetate, pH 4, phenol, and chloroform/isoamyl alcohol and the suspension incubated at 4°C for 15 min. After centrifugation at 15,000 rpm for 15 min at 4 °C, RNA was precipitated twice. The pellet was resuspended in 75 % ethanol, vortexed, dried, and dissolved in DEPC-treated water. The concentration and purity of the RNA were determined by the absorbance at 260 and 280 nm.

2.2.13. RT-PCR

Reverse transcription of total RNA and consequent cDNA amplification were performed using the Stratagene RT-PCR Kit (Stratagene Inc., La Jolla, USA). 10 μg of total RNA were transcribed to cDNAs by first adding DEPC-treated water and 300 ng of oligo (dT) primer and incubating this mixture at 65°C for 5 min, then adding 5 μl of 10 x first-strand buffer, 40 U of RNase Block Ribonuclease Inhibitor, 4 mM dNTPs and 50 U of MMLV-RT and incubating the reactions at 37 °C for 1 h, followed by 90°C for 5 min. Primers specific for iNOS (up: 5´ -CGT-GGA-GGC-TGC-CCG-GCA-GAC-TGG- 3´; down: 5´ -TGC-CCG-GAA-GGT-TTG-TAC-AGC-CCA- 3´) (Amore *et al*., 1997) and β-Actin (up: 5´- TGA CGG GGT CAC CCA CAC TGT GCC CAT CTA -3´; down: 5´- CTA GAA GCA TTT GCG GTG GAC GAT GGA GGG -3´) were obtained from ROTH (Karlsruhe, Germany). 1 μl of cDNA was added to the following components: Taq DNA polymerase buffer, 0.8 mM dNTPs, 0.2 μM of each iNOS primer and sterile water to a final volume of 99.5 μl. 0.5 μl of Taq DNA polymerase (5 U/μl) was added to the mixture just before amplication (1 cycle at 95°C for 5 min, 32 cycles at 95°C for 1 min, 54°C for 1 min, 72°C for 1 min, 1 cycle at 72°C for 5 min). 16 μl of the PCR products were loaded and run on a 1 % agarose gel and the bands visualised after ethidium bromide staining on a UV transilluminator.

2.2.14. Data analysis

In all cases for the analysis of NO production and iNOS expression, the mean values were calculated from data taken from at least 3 separate experiments performed on separate days. Analysis of iNOS expression was made by comparing the relative densities of the bands on the ECL/Western blot with the corresponding molecular weight of the protein. X-ray films were scanned and analysed by NIH image 1.57. IC_{50} values were estimated from the graphs.

2.2.15. Immunohistochemistry

2.2.15.1 Preparation of tissue for cases with Alzheimer's disease

Tissue blocks were taken from the temporal cortex (Brodmann area 22) and immersed in 4 % paraformaldehyde / 0.5 % glutaraldehyde in phosphate buffer (0.1 M; pH 7,4) for four days at 4°C. Blocks were subsequently immersed in 15 % sucrose in phosphate buffered saline (PBS) for 24 h, followed by 30 % sucrose in PBS for 48 h. Coronal sections, 30 μm thick, were cut on a freezing microtome and processed for the immunohistochemical detection of AGE, iNOS, ß-amyloid, microglia, and the microtubule associated protein tau (anti-PHF 1). The Thioflavin S staining method for demonstration of neuritic plaques, neurofibrillary tangles and neuropil threads was performed (Guntern *et al.*, 1992).

Table 2.5 - protocol for staining with Thioflavin S

Steps
1   place frozen tissue sections on gelatined slides
2   wash in EtOH 100 %, 96 %, 85 %, 70 %, dH$_2$0 (10 min each)
3   place in Haemalaun for 2 min
4   rinse briefly in tap water
5   dry the slides between 2 sheets of filter paper
6   incubate in 100 - 200 μl Thioflavin S (1 % solution) for 20 min.
7   2 x rinses in dH$_2$0
8   incubate in 80 % EtOH 20 – 40 min for differentiation
9   2 x rinses in dH$_2$0
10   allow to air-dry

2.2.15.2 Immunohistochemistry for cases with Alzheimer's disease

Free floating sections were briefly boiled in sodium citrate buffer (NaCl 150mM, Na-citrate 100mM, pH6) to maximise antibody accessibility. Sections were pre-incubated with 1 % H$_2$O$_2$ in methanol for 30 min to destroy endogenous peroxidase, followed by blocking of unspecific binding sites with 5 % normal goat serum (Sigma), 0.5 % Triton X 100 (FERAK, Berlin) in 0.1 N Tris buffered saline (TBS, pH 7.4) for 1 h. Next, sections were incubated with one of the following primary antibodies overnight at 4 °C: polyclonal anti-AGE (1:750, RNAse-AGE K1936, Dr. Stahl, Dr. Kientsch-Engel, ROCHE Diagnostics), polyclonal anti-iNOS (1:500, ALEXIS, clone L05074), monoclonal anti-ß-

amyloid (1:50, DAKO, clone 6F/3D), monoclonal anti-PHF-1 (1:15 000, P. Davies)**,** monoclonal anti-monocyte (1:2, BIOLOGO, MAC 387). Primary antibodies were detected by (a) biotinylated goat anti-rabbit IgG or biotinylated goat anti-mouse IgG (1:200, Vector Laboratories) in combination with avidin-biotin-peroxidase complex (1:200, Vector Laboratories) or (b) biotinylated goat anti-mouse Ig (1:1000, Dianova) in combination with the Extravidin-peroxidase conjugate (1:1000, Sigma). Immunoreactivity was visualized with 3,3`-diaminobenzidine/H_2O_2. Primary antibodies were omitted in control incubations.

For simultaneous detection of AGE with iNOS, sections were first incubated with anti-AGE antibody, then with a green CyDye (fluorescent) labelled species-specific secondary antibody, goat anti-rabbit IgG-Cy2 (1:100, Dianova) and reblocked. The sections were then incubated with anti-iNOS antibody, followed by a red CyDye (fluorescent) labelled species-specific secondary antibody, goat anti-rabbit IgG-Cy3 (1:1000, Dianova). For simultaneous detection of AGE and ß-amyloid/microglia or iNOS and ß-amyloid/microglia, sections were incubated with a cocktail containing anti-AGE and the corresponding antibody. Immunodetection was carried out accordingly with a cocktail of the CyDye labelled species-specific secondary antibodies goat anti-rabbit IgG-Cy2 (1:100, Dianova) and goat anti-mouse IgG-Cy3 (1:1000, Dianova). All incubation steps were separated by intensive washing with TBS. Sections were mounted, covered with Entellan (Merck) and scanned with a laser scanning microscope (LSM 510, Zeiss). The Cy2 channel collected the anti-AGE immunolabelled structures, while the Cy3 channel collected the anti-ß-amyloid, anti-microglia or anti-iNOS structures. For the green fluorescence (Cy2) the Argon Laser (excitation 488 nm) and the emission filter 3P (505 – 530 nm) were applied. For Cy3 an excitation of 543 nm and emission filter LP 560 nm were used. Sections were also examined and digitalised by the use of an Axiophot fluorescence microscope equipped with a SL XRS CCD camera and appropriate Zeiss filter combinations for red Cy3 (no. 15) and green Cy2 (no. 09) fluorescence.

2.2.15.3 Preparation of tissue for cases with incidental Lewy body disease

Tissue blocks containing the SN were fixed in 4 % buffered formaldehyde, paraffin-embedded and cut in the coronal plane at a thickness of 12 μm. After deparaffination, sections were stained with Haematoxylin and Eosin (H&E), silver impregnated according to Switzer-Campbell or processed for immunohistochemistry.

Table 2.6 - Protocol for staining with Haematoxylin and Eosin (H&E)

Steps
1   place tissue sections in Haematoxylin, 15 min
2   3 x 2 min, in warm tap water, for differentiation of cell nuclei
3   in Eosin, 1 min
4   dH$_2$0, EtOH 70%, 85%, 96%, 100% (3 min), Xylene I-IV (5 min each)
5   cover with coverslip

Table 2.7 - Protocol for staining with Switzer-Campbell

Steps
1   wash sections in EtOH 100 %, 96 %, 85 %, 70 %, dH$_2$0 (10 min each)
2   pyridine-silver solution (40 min., with agitation)
60 ml 1 % silver nitrate (AgNO3) + 5 ml pyridine (variable, 2.5 – 5 ml)
+ 45 ml 1 % potassium carbonate (K$_2$CO$_3$)
3   0.5 % acetic acid (6 Min.)
4   1 – 3 min 0.5% physical developer
5   3 – 5 min 0.5% acetic acid
6   3 min. dH$_2$0
7   0.1% gold chloride
8   2 x 5 min. dH$_2$0
9   5 min. sodium thiosulfate
10   5 min. dH$_2$0
11   70 %, 85 %, 96 %, 100 % EtOH
12   cover with coverslip

2.2.15.4. Immunohistochemistry for cases with incidental Lewy body disease

Sections were treated for 15 minutes with 0.3 % H$_2$O$_2$ in methanol and preincubated in 0.3 % non-fat dried milk and 0.1 % gelatine in 0.1 M PBS for blocking. They were incubated overnight (4 °C) in one of the following primary antibodies: polyclonal anti-AGE (1:300), monoclonal anti α-synuclein (1:200; Transduction Laboratories) or monoclonal anti-neurofilament SMI 311, SMI 32, SMI 312 (1: 500; Sternberger Monoclonals). Immunoreaction was visualized using biotinylated secondary antibodies (1:1000, Amersham) and the Extravidin-peroxidase conjugate (1:2000, Sigma)/DAB. Co-localization of AGE and α-synuclein was analyzed by double

immunofluorescence using Cy3- and Cy2-conjugated secondary antibodies. Primary antibodies were omitted in control incubations. Sections were rinsed, mounted on chrome-alum-coated slides, dehydrated and cover slipped with Entellan (Merck, Darmstadt, Germany).

<u>2.2.16. Synthesis of the dipeptide/tripeptide library.</u>

<u>2.2.16.1 General description</u>

The assembly of peptide libraries forming an array of spots of membrane-bound peptides follows essentially the methods described by Frank and Overwin (1996), using an automated pipetting system (Auto-Spot Robot ASP 222, ABIMED, Langenfeld, Germany). Using the Auto-Spot Robot, 1-1600 peptides on up to four membranes of the microtiterplate formate (9 cm x 13 cm) are able to be produced. Three types of membranes were used and compared for their stability and capacity of binding amino acids: conventional Whatman 540 filter-paper sheets (W540) and commercially available amine derivatised cellulose and polypropylene membranes (APEG). The latter additionally contain a polyethylene glycol (PEG) spacer to optimise accessibility of immobilised ligands and should have a capacity of up to 400 nmol/cm^2 compared with 250 nmol/cm^2 for W540 membranes. "Amino-functionalized" membranes were prepared from W540 sheets by esterification of N-Fmoc protected ßAla to the sheets, followed by Fmoc-cleavage, and the coupling of another Fmoc-ßAla. This provided the W540 membranes with a ßAla-ßAla anchor, onto which the peptides could be added. As the APEG membranes were already amine derivatised and contained a linker compound, no pretreatment was necessary prior to amino acid spotting. Grids consisting of 9 x 8, 12 x 12 or 20 x 20 spots representing complete libraries or subsets consisting of combinations of 8, 9, 12 or 20 amino acids were then spotted onto the membranes. Fig 2.1 displays the arrangement of a dipeptide library consisting of 12 x 12 dipeptides, H$_2$N-AA$_1$-AA$_2$-. The first (N-terminal) amino acid is displayed horizontally in a row array and the second (C-terminal) amino acid displayed vertically in a column array. Peptide synthesis on membranes, like conventional solid phase peptide synthesis, proceeds from the C-terminus to the N-terminus. When synthesizing dipeptides, H$_2$N-AA$_1$-AA$_2$-, the C-terminal amino acid (AA$_2$), elongating the ß-Ala anchor, was applied first followed by the N-terminal amino acid (AA$_1$). To build tripeptides an Ala was added N-terminally. Three separate experiments under the same conditions for glycation/ribosylation were performed. For the first two experiments, 9 amino acids with the following side chain–protected Fmoc amino acid derivatives were

used: Ala, Arg(Pmc), Cys(Trt), Gly, His(Trt), Lys(Boc), Phe, Trp(Boc), Tyr(tBu). As three important amino acids for the first two experiments were overlooked, 12 amino acids with the following side chain–protected Fmoc amino acid derivatives were used for the third experiment: Ala, Arg(Pmc), Asn(Trt), Asp(OtBu), Cys(Trt), Gln(Trt), Gly, His(Trt), Lys(Boc), Phe, Trp(Boc), Tyr(tBu).

		1	2	3	4	5	6	7	8	9	10	11	12
	2.1.	A	R	N	D	C	Q	G	H	K	F	W	Y
1	A												
2	R												
3	N												
4	D												
5	C												
6	Q												
7	G												
8	H												
9	K												
10	F												
11	W												
12	Y												

Fig 2.1 − Synthesis and array of a dipeptide SPOT library. Activated amino acids are spotted onto a derivatised membrane consisting of a ßAla- ßAla grid. Synthesis starts at the C-terminus. The first (N-terminal) amino acid is displayed horizontally in a row array and the second (C-terminal) amino acid displayed vertically in a column array.

2.2.16.2 Protocol for synthesis of the ßAla-ßAla anchor

W540 sheets were treated with an amino-linker by esterification with activated Fmoc-ßAla (2.5 ml/membrane of 0.2 M Fmoc-ßAla, 0.24 M *N,N'*-diisopropylcarbodiimide (DIC), 0.4 M *N*-methylimidazole (NMI) in dimethylformamide (DMF) for 3 h (see Table 2.8). After washing with DMF, the membranes were incubated in 15 ml 20 % piperidine in DMF for 20 min for Fmoc deprotection, then washed in DMF and EtOH. Membranes were blow-dried with warm air for 5 min, followed by 1 h in a vacuum. Spotwise distribution of 0.25 M activated Fmoc-ßAla (in 0.375 M 1-hydroxybenzotriazole (HOBT) and 0.3 M DIC in *N*-methyl-pyrrolidinone (NMP)) was performed by the Auto-Spot Robot. After 20 min incubation, spotting was repeated with the same volume of activated Fmoc-

ßAla to maximise peptide yield. Residual amino functions on and between the spots formed by incomplete coupling as well as underivatized hydroxyl groups on the cellulose membrane were capped by acetylation with 2 % acetic anhydride in DMF. The membranes were washed with DMF, incubated in 15 ml 20 % piperidine in DMF for 5 min for Fmoc deprotection and rewashed with DMF to completely remove piperidine. Optionally, spots were stained with a 373 μM bromphenol blue (Merck) solution in DMF. The membranes were washed in DMF and EtOH, then dried as usual. All steps were carried out at room temperature and are summarised in Table 2.8 (volumes refer to use with one membrane).

A grid of ßAla spots was generated on APEG membranes by applying 0.25 M activated Fmoc-ßAla using the protocol for elongation of amino acids (described below).

Table 2.8 - Synthesis of the ß-Ala - ß-Ala anchor (volumes refer to use with one membrane)

Steps
1   Derivation of filter paper (9 x 13 cm) with 2.5 ml 0.2 M ß alanine (156 mg Fmoc - ß-Ala, 93.0 µl DIC and 80 µl NMI in DMF for 3 h)
2   3 x 2 min washes with 15 ml DMF
3   15 ml 20 % piperidine in DMF for 20 min
4   3 x 2 min washes with 15 ml DMF
5   2 x 2 min washes with 15 ml EtOH
6   Dry the filter paper for 5 min with cold air, then 1h at 10 mbar
7   Spot 0.2 –1.0 µl of amino acids (activated for ½ h in following solution: 78 mg Fmoc - ß-Ala, 56 mg HOBT and 47 µl DIC in 1 ml NMP), using the Auto - Spot Robot ASP 222. For volumes see Table 3.6. When using the repeat function see instructions. Incubate for 20 min.
8   3 x 2 min washes with 15 ml DMF
9   15 ml 2% acetanhydride in DMF for 30 min
10   2 x 2 min washes with 15 ml DMF
11   15 ml 20 % piperidine in DMF für 5 min
12   4 x 2 min washes with 15 ml DMF
13   Staining of spots with 15 ml Bromphenolblue solution (25 mg Bromphenolblue in 100 ml DMF) for 2 min; colour change of spots from from yellow to dark blue
14   2 x 2 min washes with 15 ml DMF
15   2 x 2 min washes with 15 ml EtOH
16   Dry the filter paper for 5 min with cold air, store at - 20 °C

<u>2.2.16.3 Protocol for synthesis of the di/tripeptide library</u>

Amino acids were spotted onto the ßAla-ßAla anchor of W540 or directly onto APEG membranes. A stock solution was prepared from 0.5 mmol Fmoc amino acid derivatives and 0.75 mmol HOBT in 1 ml NMP in 2 ml Eppendorf caps. After dissolution of the amino acid, the volume was adjusted to 2 ml with NMP, resulting in an end concentration of 0.25 M. Stock solutions could be stored for up to 6 weeks at −20 °C. Amino acid stock solutions were activated with 1.1 mmol/ml DIC in NMP at a dilution of 4 parts amino acid to 1 part DIC for 30 min at room temperature, giving an end concentration of 0.2 mmol/ml. Aliquots (0.2 - 0.4 μl) were spotted (repeatedly if required) onto the membranes by the Auto-Spot Robot, with 20 min incubation after each coupling. Residual amino groups were capped with 2 % acetic anhydride in DMF and membranes washed and dried. The second and third (N-terminus) amino acids were added in aliquots of the same volume under the same conditions onto the membranes. Following the final cycle of elongation, the N terminus was acetylated, and membranes washed in DMF, EtOH, then dried as usual (Table 2.9). Selective deprotection of the amino acid side chains was achieved by treating the membranes in 50 % trifluoroacetic acid (TFA), 45 % dichloromethane (DCM), 3 % triisobutylsilane, and 2 % water for 2 h, and by careful washing in DMF and ethanol, while the peptides remained attached to the membrane (Table 2.10). In this manner, the amino acid side chains, but not the N-terminals, were made selectively available for reaction with sugars (Fig 2.2). All steps were carried out at room temperature. Quantification of the yield of spotted peptides was calculated from the incorporation of ^{14}C – acetic or ^{14}C – benzoic acid applied after the final cycle of elongation (see below). Selected tryptophan-containing peptides, isolated after aminolysis of the paper spots, were analyzed by matrix-assisted laser desorption/ionization time-of-flight mass spectrometry (MALDI-TOF) and showed the correct molecular mass.

Table 2.9 - Synthesis of the di-/tripeptide library (volumes refer to use with one membrane)

Steps

1   Activate amino acid stock solutions by mixing with DIC/NMP solution. Incubate for 20 min, centrifuge 1 min. Load the Autospotter or perform spotting manually.

2   spot activated amino acid solutions; for volumes see Table 3.6, incubate for 20 min

3   repeat step 2, (after incubating for 20 min, the spots should change colour from blue to a greenish-yellow)

4   2 x 15 ml 2% acetanhydride in DMF for 30sec, 10 min

5   2 x 2 min washes with 15 ml DMF

6   15 ml 20 % piperidine in DMF für 5 min

7   7 x 2 min washes with 15 ml DMF

8   Staining of spots with 15 ml bromphenol blue solution (25 mg bromphenol blue in 100 ml DMF) for 2 min; colour change of spots from from yellow to dark blue

9   2 x 2 min washes with 15 ml DMF

10   2 x 2 min washes with 15 ml EtOH

11   Dry the filter paper for 5 min with cold air, store at - 20 °C

Table 2.10 – Deprotection of side chain Fmoc groups (volumes refer to use with one membrane)

Steps

1   2 x 15 ml of the following solution: 7.5 ml TFA, 450 µl Triisobutylsilane, 300 µl H_2O and 6.75 ml DCM, for 1 h

2   4 x 2 min washes with 15 ml DCM

3   3 x 2 min washes mit je 15 ml DMF

4   2 x 2 min washes mit je 15 ml EtOH

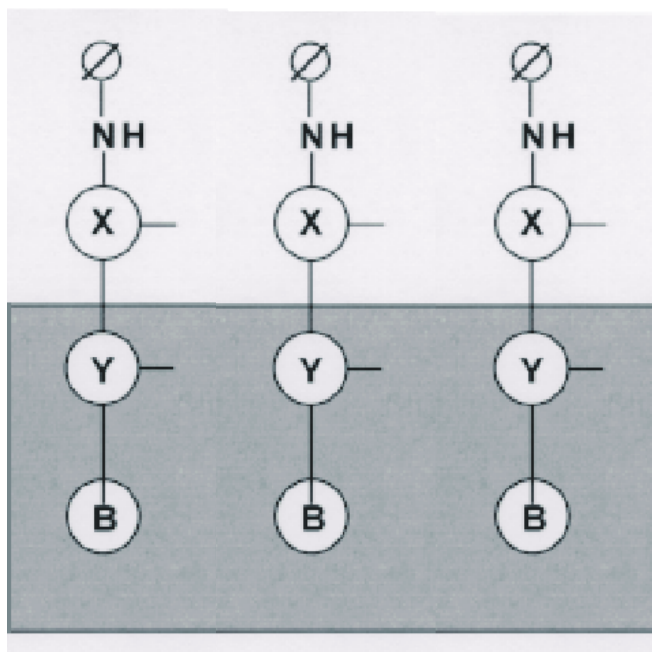5   Dry the filter paper for 5 min with cold air

Fig 2.2 – schematic representation of dipeptides (amino acids X and Y) bound via ßAla to a membrane. Selective deprotection of side chains and acetylation of the N-terminus of dipeptides is shown. (∅ refers to acetylated/ blocked N-terminus)

2.2.16.4 Glycation/ribosylation of the di/tripeptide library

Glycation/ribosylation was performed with 50 – 500 mM glucose or ribose in 0.4 M phosphate buffer, pH 7.5. Glycation/ribosylation of the side-chains of di/tripeptides was analysed by incubation with radioactive glucose/ribose. Membranes were incubated with 50 - 500 mM glucose/ribose or with 15 µCi [^{14}C] D(+)glucose, 15 µCi [^{14}C] D(-)ribose in 50 mM non-radioactive glucose/ribose in 10 ml 0.4 M sodium phosphate buffer pH 7.5 containing 0.02 % sodium azide. Incubations with [^{14}C] D(+)glucose were for 96 h at 50°C, and with [^{14}C] D(-)ribose or non-radioactive ribose for 24 h at 37 °C, followed by replacement of the [^{14}C] D(-)ribose solution with 0.4 M sodium phosphate buffer pH 7.5, and a further 72 h incubation at 37°C. In this way, ribosylation was "interrupted" to remove excess and reversibly bound (Schiff base) sugars by dialysis against frequent cold buffer changes at 4°C (Khalifah *et al*., 1997). The supernatant from radioactive incubations was collected and the radioactivity measured as a control for peptide binding. After extensive washing steps (twice in PBS, twice in 100 mM acetate buffer, pH 4.0, and twice in 100 mM ammonia buffer, pH 9.0) to remove loosely bound radioactive sugars, the dried membranes were exposed to an X-ray film for up to 12 days. Membranes without glycation were used as controls for anti-AGE antibody recognition (see below). Quantification of the yield of glycation of peptides was calculated from the incorporation of ^{14}C sugars onto spots excised after several rounds of immunoassays and stripping.

2.2.16.5. Epitope mapping with anti-AGE antibodies

AGE formation due to reactions between glucose/ribose with the free side-chains of N-terminal acetylated di/tripeptides was analysed by immunodetection using specific monoclonal and polyclonal anti-AGE antibodies. The following anti-AGE antibodies were used:

a) monoclonal Imidazolone Mab AG1 (T. Niwa, Nagoya)
b) monoclonal CML-Peroxidase (ROCHE Diagnostics)
c) polyclonal AGE K1935 (ROCHE Diagnostics)
d) polyclonal anti-KLH-AGE (D.Palm, G. Münch 1996-1998)

Anti-mouse or anti-rabbit peroxidase-conjugated secondary antibodies (BioRad, Roche Diagnostics, Sigma) were used for the detection of a), c) and d), respectively. A fluorescent luminol substrate (ECL Western blotting, Amersham-Pharmacia) was then applied to the membranes, which were exposed to an X-ray film in a darkroom.

Following a 2 h block in 5 % BSA in PBS, pH 7.4, with 0.1 % Tween 20 (PBS-T) at room temperature, membranes were incubated in primary antibodies (1: 5000 for b), 1:1000 for a) and c)in 2 % BSA/PBS-T) for 2 h at room temperature, then washed 3 x 10 min in PBS-T. Membranes incubated with a) or c) were further incubated with anti-mouse/rabbit IgG peroxidase conjugate (1: 10 000) for 1 h at room temperature. After 3 x 10 min washes with PBS-T, a solution of chemiluminescent detection reagents (ECL Western blotting, Amersham) was applied to the membranes, which were then exposed to an X-ray film in a darkroom. To allow for the application of several antibodies to the same membrane, complete removal of primary and secondary antibodies was achieved by incubation in stripping buffer (100 mM 2-mercaptoethanol, 2 % sodium dodecyl sulphate, 62.5 mM Tris-HCL pH 6.7) at 50 °C for 30 min on a vibrating tray. This was followed by 2 x 10 min washes in PBS-T and reblocking and reprobing with a different primary antibody as described. Non-glycated membranes incubated with primary and secondary antibodies and glycated membranes incubated without primary antibodies were used as controls.

<u>2.2.16.6 Stability of ^{14}C-labeled SPOTS</u>

The ability of W540 and APEG membranes to retain the attached peptides was tested under the same conditions as used for the preparation of the libraries and glycation. Following synthesis of "tripeptide" spots on APEG or W540, the N-terminal H_2N-groups were acetylated with 0.2 M acetate/DIC/HOBT containing ^{14}C- acetic acid or ^{14}C benzoic acid. For the generation of the grid, two concentrations of ßAla were used: 0.2 M and one tenth of the concentration ie. 0.02 M.

<u>2.2.17. Other buffers and solutions</u>

<u>10 x PBS pH 7.4</u>

NaCl	80 g
KCl	2 g
Na_2HPO_4	14.4 g
KH_2PO_4	2.4 g

in a total of 1l distilled water

<u>10 x TBS</u>

Tris HCl, pH 7.5	500 mM
NaCl	1.5 M

<u>100 mM Acetate buffer pH 4.0</u>

Sodium acetate	8.203 g
Acetic acid	0.1 M pH 4,0

in a total of 1l distilled water

<u>100 mM Ammonium buffer pH 9,0</u>

Ammonium hydrogencarbonate	7.906 g

10 % NH_3 - solution pH 9.0

in a total of 1l distilled water

Physical developer (Switzer-Campbell):

Solution. A: 50 g sodium carbonate   9 ml

                in a total of 1l distilled water

Solution B: 2 g ammonium nitrate   10 ml

                2 g silver nitrate

                10 g Wolfram silicic acid

                in a total of 1l distilled water

Solution C: 2 g ammonium nitrate   1 ml

                2g silver nitrate

                10 g Wolfram silicic acid

                7.3 ml 35 % Formol

                in a total of 1l distilled water

2.3 Equipment

Autospot Robot ASP 222	Abimed Analysis Technic GmbH
Bench centrifuge	Eppendorf
Blot chamber	BRL
Fine scales	Sartorius
Cell counter	Casy Coulter Counter
Centrifuge	Hettich; Sorvall
Cleanbench	Heraeus
Coarse scales	Sartorius
Elisa Reader	Labsystems, Multiscan Ascent
FPLC	BioRad BioLogic
Gel chamber	Laboratory workshop
Incubator	Heraeus
Luminometer	Bertold
pH-Meter	Hanna Instruments
Photometer	Varian Cary
Pipettes	Gilson; Brand
Power supplies	Consort; Pharmacia
Scintillation counter	Wallace System, Pharmacia
Spectrophotometer	Spex Fluoromax
Thermocycler	Techne ProGene
Vacuum chamber	BioRad

2.4. Software

Adobe Photoshop D1 – 3.0
MS - Office 97 (Word, Excel)
Canvas 3.5.4
Corel Photo Paint 8.0
Corel Draw 8.0
Endnote Plus 2.0.2
Image Quant
Grafit 3.0
NIH – Image 1.57
XRS 2.2 (Jena, Germany)

3. RESULTS

3.1. AGE-modified proteins induce the expression of iNOS, leading to the production of NO in microglia

3.1.1 Characteristics of BSA and AGE preparations

Calculations for absorption, fluorescence and protein and CML content of the AGE preparations are summarised in Table 3.1. In addition, as BSA and AGE-modified preparations were incubated for 2-6 weeks, endotoxin contamination was tested in order to confirm that the effects described were due to AGE-modification and not bacterial contamination of the compounds (Table 3.2). Endotoxin levels for BSA and BSA-AGEs were less than 1 Unit / mg. Interestingly, the amount of endotoxin measured in BSA (Sigma) incubated for 6 weeks in the absence of sugars did not differ from that found in freshly prepared BSA (Sigma, 1 Unit / mg). βA4-Glc and βA4-MG samples contained 38 and 94 endotoxin Units / mg, respectively.

Table 3.1 – Characteristics of AGE preparations

	BSA-AGE	βA4-Glc
Protein (mg/ml)	25	2
OD_{360} /mg	1.12	0.36
OD_{400} /mg	0.56	0.32
Fluorescence (AU/mg)	8×10^6	3.2×10^6
CML (ng/mg)	4.4×10^5	20

Table 3.2 - Endotoxin content of BSA, Aβ and AGE preparations

	Total Endotoxin Units/mg protein
LPS (Sigma)	500 000
BSA (Sigma); freshly prepared	1
BSA; incubated in the absence of sugars	1
fibrillar βA4	0.6
βA4-Glc	38
βA4-MG	94
BSA-AGE	0.2

3.1.2 AGE-modified model proteins induce NO production in microglia

AGE-modified bovine serum albumin – AGE (BSA-AGE), but not the unglycated protein, induced the production of NO (17 fold-increase; measured as nitrite) in the murine macrophage cell line J774A.1 (ATCC TIB-67) (Fig. 3.1). Similar results were obtained by incubation of the murine microglia cell line N-11 (Corradin et al., 1993) with BSA-AGE and chicken egg albumin – AGE (CEA-AGE) (Fig. 3.2). NO synthesis peaked at a concentration of 10 µM BSA-AGE (12 fold-increase) and 2 µM CEA-AGE (15 fold-increase), respectively, and nitrite concentration reached up to 30 µM in confluent N-11 cultures. Maximal levels of nitrite were also induced by bacterial lipopolysaccharide (LPS) (2 µg/ml, 10 µg/ml, 50 µg/ml) in N-11 microglia.
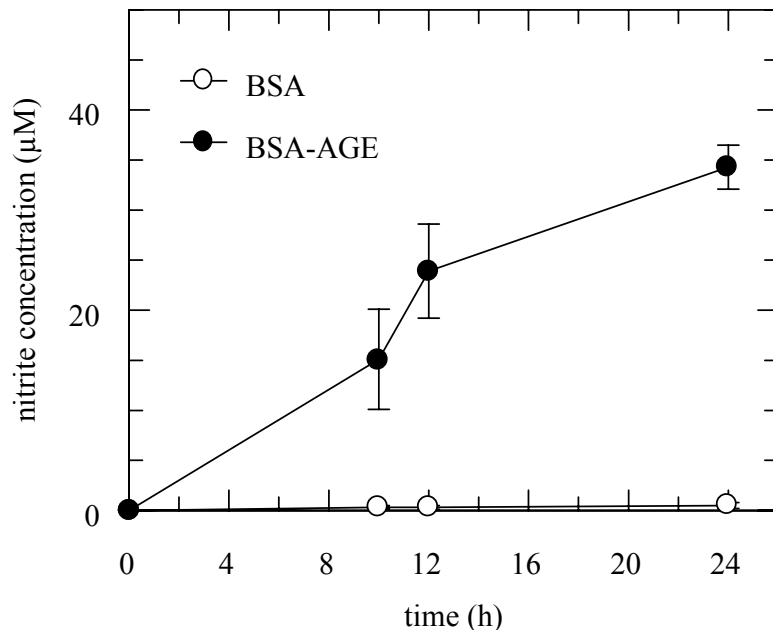
Fig. 3.1: Induction of NO production by BSA - AGE in J774A.1 macrophages. Macrophages were incubated with BSA-AGE (2 µM) for 0 - 24 h, after which the medium was removed for nitrite determination. NO production increased with the time of incubation.
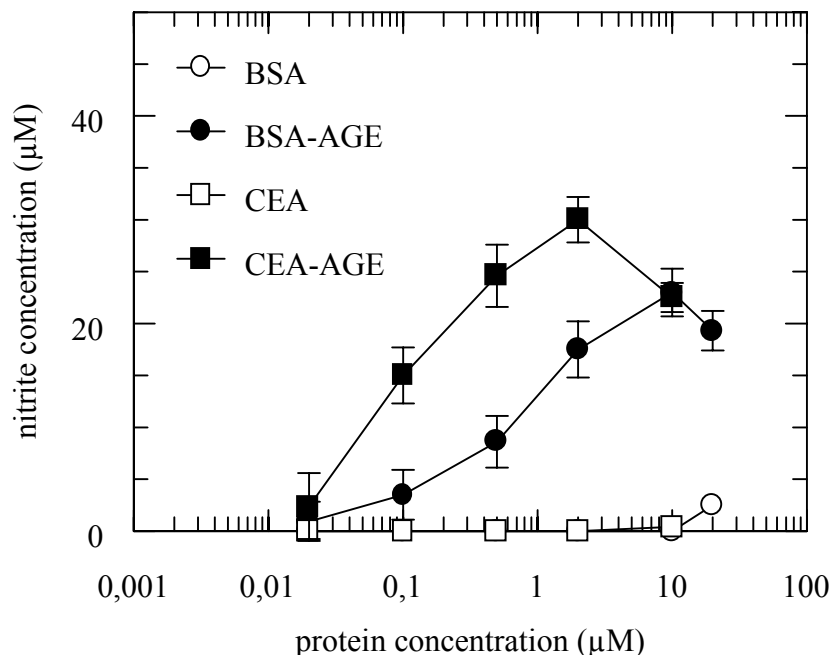

Fig. 3.2: Induction of NO production by AGE-modified model proteins in N-11 microglia. Microglia were incubated with various concentrations of BSA-AGE or CEA-AGE for 24 h, after which the medium was removed for nitrite determination.

3.1.3 α-Oxoaldehydes do not induce NO production in microglia

α-Oxoaldehydes, MG and 3-DG, have been reported to induce oxidative stress and neurotoxicity in vitro (Abordo *et al.,* 1999, Kikuchi *et al.,* 1999). In order to test the effect of these compounds for the induction of NO, N-11 microglia were incubated with MG and 3-DG (0.4 – 250 µM) for 24 h, after which the medium was removed and analysed for the presence of nitrite. However, neither compound caused significant changes in the level of nitrite in the cell culture medium. Furthermore, since MG is known to bind and modify a number of proteins, including BSA (Nagai *et al.,* 2000), lysozyme (Kato *et al.,* 1986) and collagen (Paul and Bailey, 1999), MG - modified BSA (BSA-MG) was also tested to see whether it caused a difference in the induction of NO compared with MG alone. However, there were no changes in nitrite levels following incubation of N-11 cells with BSA-MG (0.4 – 10 µM).

3.1.4 AGE-modification increases the potency of βA4 for NO production

Activated microglia have been shown to be associated with β-amyloid plaques in AD and it has long been suggested that these protein deposits contain the active pro-inflammatory ligand. However, it appears to depend on cell type and culture conditions, whether β-amyloid peptide (βA4) alone can sufficiently activate macrophages and microglia, whether it induces only a limited repertoire of "early" cytokines like IL-1β or whether the additional presence of pro-inflammatory cytokines is required for a more complex inflammatory response (Klegeris *et al*., 2000). Thus we were particularly interested to test the potency of unmodified βA4 vs βA4-AGE in terms of NO production. Three different βA4 batches were compared: "Aged", fibrillar βA4 (containing β-sheeted fibrils, confirmed by a 10 fold increase in fluorescence at 480 nm, 20 000 versus 500 000 arbitrary units) and two βA4-AGE preparations modified by glucose (Glc) or MG, respectively. Both βA4-AGE preparations caused a concentration-dependent increase in NO production similar to the one observed with BSA- or CEA-AGE, whereas unmodified "aged" βA4 did not increase NO production above control levels in the same concentration range (Fig. 3.3). Maximal NO production induced by βA4-AGEs occurred at 10 - 15 fold higher peptide concentrations than that required with the larger model proteins, suggesting that the absolute number of AGE-modified residues present in solution determines the dose response curve.
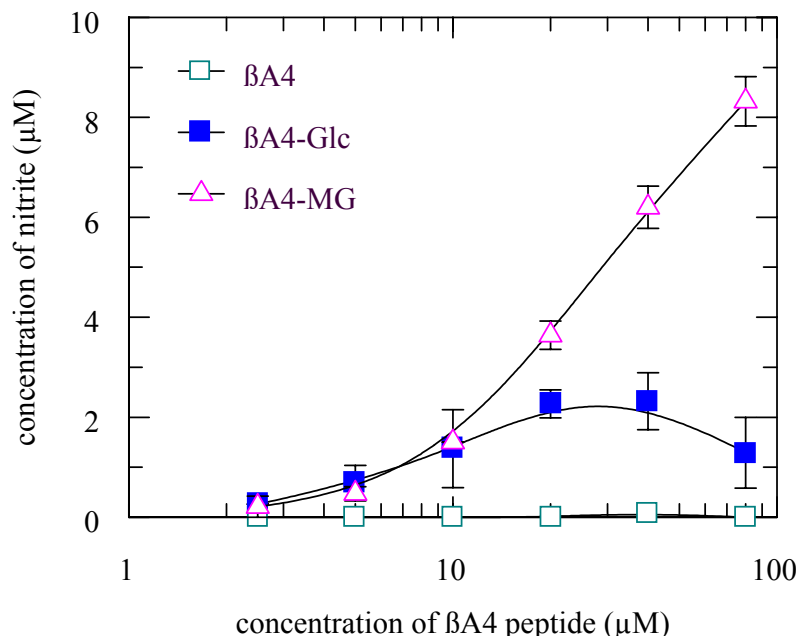
Fig. 3.3: NO induction by AGE-modified Aβ peptides. Incubation of microglia for 24 h with AGE-modified βA4 resulted in a strong increase in NO production compared to unmodified βA4, as determined by nitrite levels in the medium, using the Griess assay. A higher potency of βA4-MG compared with βA4-Glc is evident at concentrations greater than 10μM.

3.1.5 Inducible nitric oxide synthase (iNOS) is the AGE-induced NOS isoform

Having established that AGE-modification of proteins/peptides leads to microglial NO production, we investigated whether the inducible, non-calcium-dependent NO synthase (iNOS) which is upregulated upon stimulation with LPS and certain cytokines (Knowles, 1997), is the responsible isoform. A first indication that this assumption was correct came from time course experiments. When cells were incubated with 2 μM BSA-AGE, a steady increase in the concentration of nitrite was observed up to 24 h after an initial lag phase of 4 h (Fig. 3.4). The 4 h delay in the response to the stimulus suggests that the respective NO synthase had to be synthesized *de novo*, indicating iNOS to be the active isoform. Thus, iNOS induction by AGEs was studied on the mRNA (by RT-PCR) and protein level (by Western blotting). Indeed, BSA-AGE induced the synthesis of iNOS mRNA after 4 h (Fig. 3.5A), which was comparable to the time course observed for LPS mediated induction (data not shown). The expression of iNOS protein (130 kDa) began after 4 h and continued up to 24 h (Fig. 3.5B). BSA-AGE also induced the expression of iNOS in macrophages (J774 cell line) (Fig.3.6).
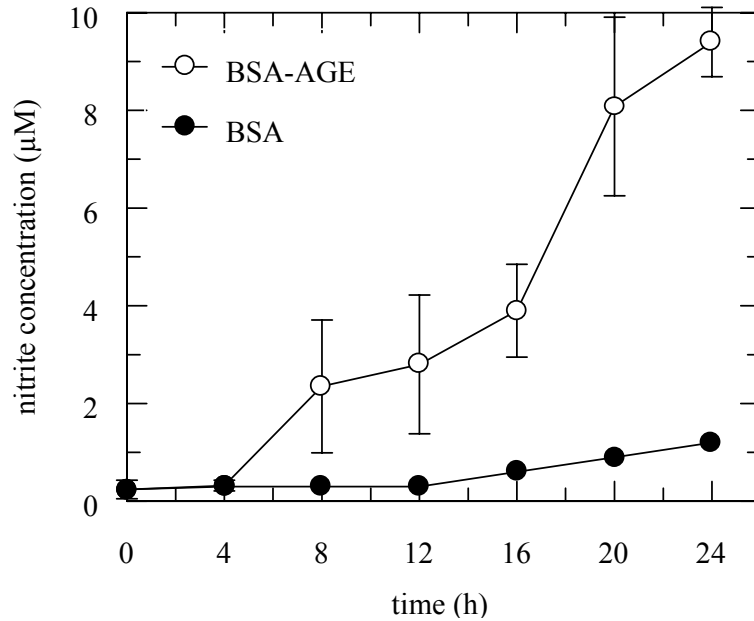
Fig. 3.4: Timecourse of BSA vs BSA-AGE-induced NO production. At a concentration of 2 μM BSA/BSA-AGE, increasing concentrations of nitrite in the medium was detected from 4 to 24 h of incubation with BSA-AGE.A lag period of between 4-8 h in NO production suggests *de novo* synthesis of nitric oxide synthase.
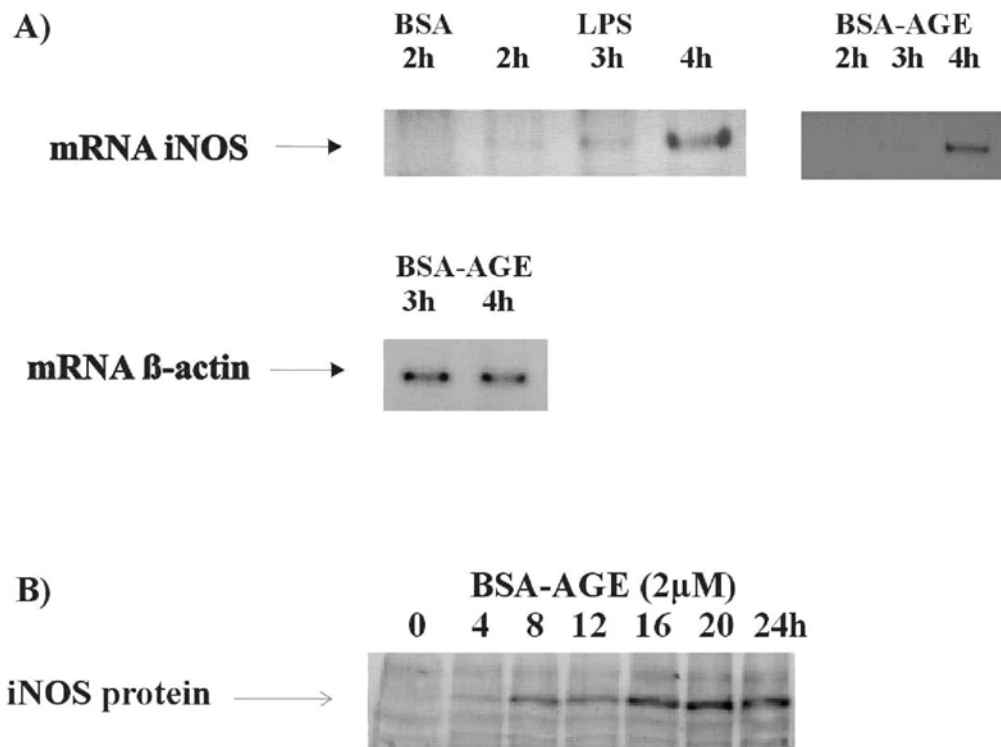

Fig. 3.5: Timecourse of AGE induced iNOS mRNA and protein expression in N-11 microglia cells. A) Induction of mRNA iNOS (bands at 663 bp) after 4 h incubation of microglia with 2 μM BSA-AGE and (in comparison) LPS. Actin mRNA was used as a loading control. B) Expression of iNOS was induced by incubation of microglia with 2 μM BSA-AGE from 0 to 24 h and detected with Western blot, using a rabbit polyclonal anti-iNOS antibody.

BSA-AGE

| LPS | 0 | 10 | 12 | 24 h |

iNOS
130 kDa

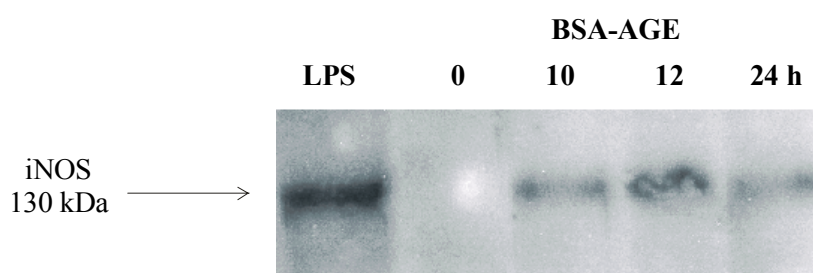Fig. 3.6 Detection of the iNOS protein in J774A.1 macrophages with Western blot after incubation with 2 µM BSA-AGEs for 10 – 24 h and with LPS for 24 h.

3.1.6 Antioxidants inhibit AGE-induced iNOS expression and NO production

AGEs have been reported to activate redox-sensitive transcription factors including AP-1 and NF-kB, with superoxide radicals, hydrogen peroxide and hydroxyl radicals acting as parts of the second messenger cascade (Kislinger *et al.*, 1999; Lander *et al.*, 1997). Since the mouse iNOS gene promoter contains several binding sites for NF-κB and AP-1, it is likely that upregulation of iNOS expression by AGEs occurs via redox-sensitive signal transduction, suggesting antioxidants as possible inhibitors of this signal transduction cascade (Kikumori *et al.*, 1998). Thus, we tested various classes of membrane-permeable radical scavengers / antioxidants for both inhibition of iNOS expression and of NO production. The compounds used represent three different classes of antioxidants: phenolic antioxidants (e.g. estrogen derivatives such as 17β-estradiol and flavonoids which are contained in *Gingko biloba* extract EGb761), thiol antioxidants (e.g. R-(+)-thioctic acid) and spin traps (e.g. PBN) (Fig. 3.7). Expression of the iNOS protein was determined using the relative densities of the iNOS bands at 130 kDa from the ECL / Western Blot and was compared to nitrite levels in the cell culture medium. All antioxidants tested inhibited both iNOS expression and NO production (Fig. 3.8, Fig. 3.9, Table 3.3). 17β-estradiol, *Gingko biloba* extract EGb 761 and R-(+)-thioctic acid showed dose-dependent responses, whereas only partial inhibition was observed for PBN. 17β-estradiol was the most potent of the antioxidants ($IC_{50} = 0.2$ µM for nitrite and iNOS). The curves for NO and iNOS inhibition with *Gingko biloba* extract EGb 761 showed IC_{50} values in similar ranges ($IC_{50} = 350$ µg/ml for nitrite, $IC_{50} = 500$ µg/ml for iNOS). In comparison, a large shift was noted between the two curves with R-(+)-thioctic acid ($IC_{50} = 65$ µM for nitrite, $IC_{50} = 500$ µM for iNOS). The difference might be caused by the ability of this thiol antioxidant to bind NO directly as a nitrosothiol. PBN also inhibited

NO production, though this appeared to be a rather biphasic response with increases in NO production at high PBN concentrations. This effect, however, was not simply caused by chemical decomposition of the compound and resulting NO release, since no nitrite could be detected in PBN solutions incubated for 24 h at 37 °C (data not shown).
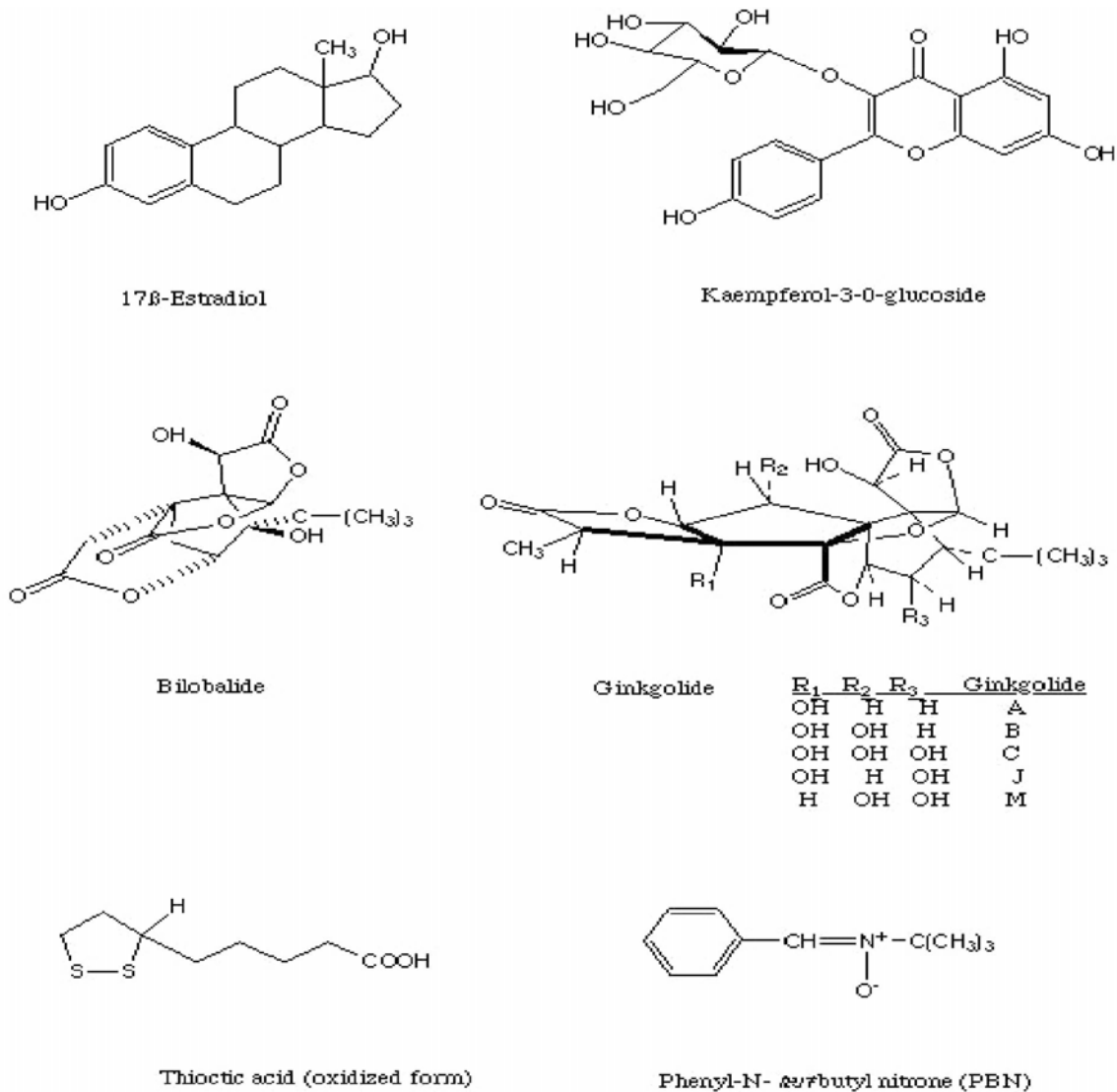

Fig. 3.7: Chemical structures of the antioxidants used to inhibit AGE-mediated signal transduction. 17β-estradiol, kaempferol-3-0-glucoside (flavonoide), bilobalide, gingkolide (active ingredients found in the leaves of the *Gingko biloba* plant), R-(+)-thioctic acid, and N-tert.-butyl-α-phenylnitrone. Note the common phenolic A ring found in estradiol and kaempferol-3-0-glucoside.
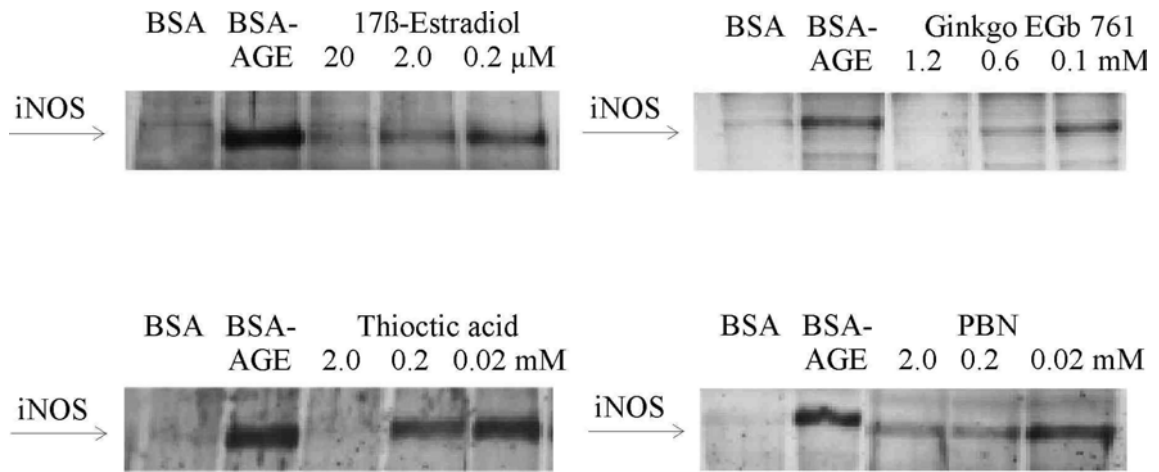
Fig. 3.8: Inhibition of BSA-AGE-induced expression of the iNOS protein (130 kDa) by antioxidants. All antioxidants were able to inhibit iNOS expression in the following order from most to least effective: 17β-estradiol > *Gingko biloba* extract EGb 761 (concentrations calculated as kaempferol-3-0-glucoside) > R-(+)-thioctic acid > PBN.
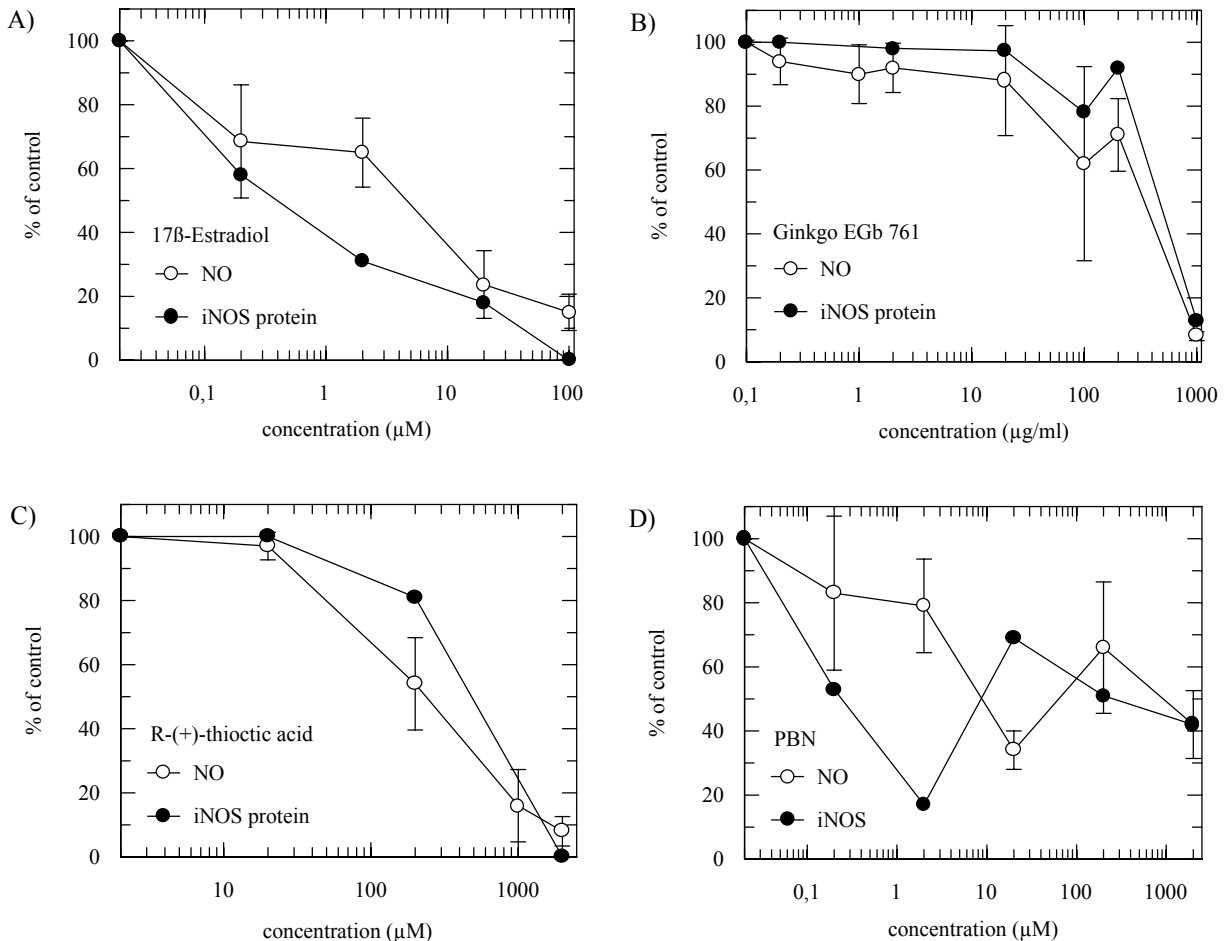

Fig. 3.9: Dose-dependent inhibition of BSA-AGE-induced NO production and iNOS expression by antioxidants. Values on the y-axis are represented as percentages of the control, where cultures were incubated in 2 μM BSA-AGE without addition of antioxidant. The antioxidants A) 17β-estradiol, B) *Gingko biloba* extract EGb761 and C) R-(+)-thioctic acid produced a dose-dependent and complete inhibition of BSA-AGE-induced NO production and iNOS expression, whereas D) PBN showed a limited efficacy above 10 μM.

50

3.1.7 Toxicity of AGEs and α-oxaldehydes on N-11 microglia

Since no effects on nitrite levels were induced by MG, 3-DG, nor BSA-MG, cell vitality was tested using the MTT assay after 24 h of incubation with these substances. AGE MG was the most toxic substance, causing a 90 % (250 µM) and 60 % (50 µM) reduction in cell activity. Neither BSA-MG (0.4 – 10 µM) nor 3-DG (0.4 – 250 µM) caused a reduction in cell activity. Mitochondrial respiration was reduced by 20 % with LPS (stock solution 1 mg/ml, diluted 20 fold) and 30 % with BSA-AGE (2 µM), βA4-MG (40 µM), and βA4-Glc (40 µM). An 8 % reduction in cell activity was detected with fibrillar βA4 (40 µM). The addition of antioxidants did not alter cell activity.

3.1.8 BSA.-AGE induce activation of RAGE

Cell lysates from N-11 microglia were obtained following incubation with BSA-AGE (2 µM) for 4 - 24 h and LPS (50 µL/ml) for 24 h. Lysates were run on an SDS-PAGE and immunoblotted to test for upregulation of one of the known receptors for AGEs, namely RAGE (35 – 50 kDa). Two different sized bands within the range for the RAGE protein were detected. Bands at around 50 kDa were visible with LPS and BSA-AGE at all time points of incubation. Control lysates incubated in medium only also showed bands of this molecular weight. In addition, there were fainter bands at around 35 kDa for LPS and for BSA-AGE, with increasing intensities at longer incubations. This band was absent with control lysates. The latter band could represent soluble RAGE, which contains the extracellular two-thirds of the receptor (Schmidt and Stern, 2000)(Fig 3.10).
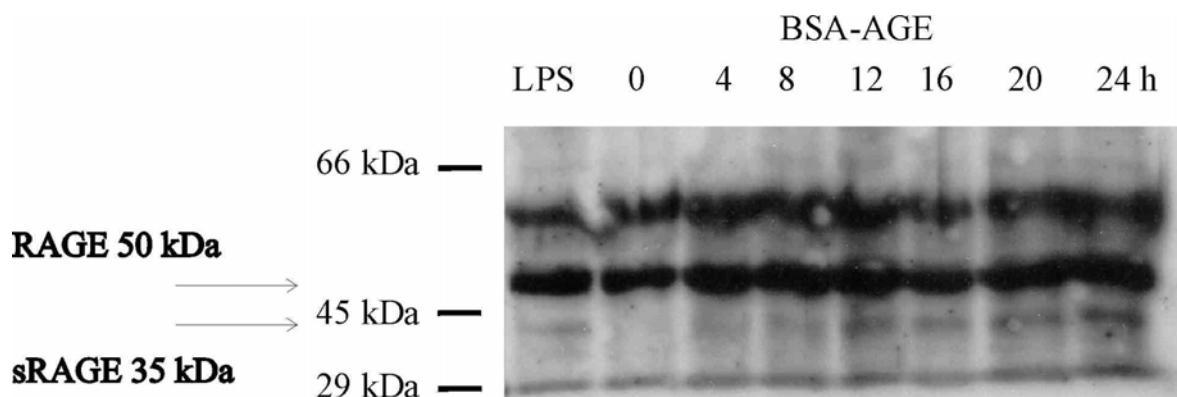

Fig. 3.10: BSA-AGE (2 µM) induction of RAGE (50 kDa) and soluble RAGE (35 kDa) in N-11 microglia, detected by Western blot.

Table 3.3 – Effect of potential inhibitors on AGE-induced iNOS expression and NO production

compound tested	inhibition of nitrite production IC$_{50}$ [µM]	% nitrite at 100 µM inhibitor	inhibition of iNOS expression IC$_{50}$ [µM]
estrogens			
17β-estradiol	~ 0.2	10 ± 6	~ 0.2
17-α estradiol	~ 1	7 ± 4	n.d.
J 861	~ 0.1	2 ± 0.6	n.d.
flavonoids			
Gingko biloba extract EGb761*	~ 350 µg/ml (~ 203 µM *)	60 ± 27	~ 500 µg/ml (~ 290 µM)*
thiol antioxidants			
N-acetylcysteine	~ 5000	98 ± 3	n. d
(R+)-thioctic acid	~ 65	36 ± 6	~500
spin trap			
PBN	> 500	41 ± 12	> 500

* Since the *Gingko biloba* EGb 761 extract consists of a heterogenous mixture of compounds isolated from the leaves of the *Gingko* tree, the IC$_{50}$ value in µM was estimated assuming that the flavone glycoside, kaempferol-3-0-glycoside (MW 423 g/mol) is the most active compound and represents 24 % of the extract (manufacturers specification).

3.2. Immunodetection of AGE and iNOS in the brains of normal aged individuals and cases with Alzheimer's and incidental Lewy body disease.

The progression of AD is manifested in the brain by a spread of the neurofibrillary pathology from the trans- and entorhinal cortices, in the early stages of the disease, to the neocortical regions such as the temporal and frontal cortices, and later to the association areas, in the more advanced stages (Braak and Braak, 1992). To examine whether this regional difference in pathology is accompanied by corresponding differences in the distribution of AGE and iNOS reactivity, sections from the entorhinal (Area 28, 34) and temporal cortices were compared in control and AD cases.

3.2.1 Comparison of AGE antibodies

Seven anti-AGE antibodies (Dr Stahl, Dr Kientsch-Engel; ROCHE Diagnostics) were compared for the structures which they recognise in both AD and control brain sections. The results are listed in Table 3.4. In summary, of the 3 polyclonal CML-specific antibodies tested, 2 showed non-specific staining and the other stained blood vessels and neurons in both AD and control brain sections. The monoclonal CML-specific antibody (Alteon) also stained blood vessels and neurons in AD and control brain sections. In comparison, the three polyclonal anti-AGE antibodies showed clear differences in the structures stained between AD and control sections. In summary, all three anti-AGE antibodies stained blood vessels and neurons in both AD and control brain sections. In addition, plaques and astroglia were detected in AD tissue. Although minimal differences in the structures stained between the lysine- and arginine-specific anti-AGE antibodies were seen, the arginine-specific anti-AGE antibody worked optimally and was used for all further experiments.

Table 3.4 – Specificity and structures stained in the temporal cortex by the anti-AGE antibodies (ROCHE Diagnostics)

ANTIBODY	IMMUNOGEN	AGE SPECIFICITY (unpublished observations)	CASE TYPE	STRUCTURES STAINED IN TEMPORAL CORTEX
K1933 (polyclonal)	Hb-CML	lysine	aged control	non-specific
			AD	non-specific
K2002/4 (polyclonal)	KLH-CML	lysine	aged control	non-specific
			AD	non-specific
K2013 (polyclonal)	Hb-peptide-CML	lysine	aged control	blood vessels, neurons
			AD	blood vessels, neurons
M-4G9 (monoclonal)	AGE-CML	lysine	aged control	blood vessels, neurons
			AD	blood vessels, neurons
K1935 (polyclonal)	RNAse-AGE	lysine	aged control	blood vessels, punctate clusters in WM and GM, neurons
			AD	blood vessels, punctate clusters in WM and GM, neurons, some astroglia
K1936 (polyclonal)	RNAse-AGE	arginine	aged control	blood vessels, punctate clusters in WM and GM, neurons
			AD	blood vessels, punctate clusters in WM and GM, neurons, some astroglia, diffuse plaques
K1937 (polyclonal)	RNAse-AGE	lysine	aged control	blood vessels, punctate clusters in WM and GM, neurons
			AD	blood vessels, punctate clusters in WM and GM, neurons, some astroglia, diffuse plaques

3.2.2 Distribution of iNOS and AGE in young and old control temporal cortex

In the 4 young control brains, AGE reactivity was observed in blood vessels only (Fig. 3.11B). Immunofluorescence with the anti-iNOS antibody showed no specific staining of structures (Fig. 3.11B'). Neither AGE nor iNOS was detected in nerve or glial cells. In the 4 aged control brains, AGE reactivity was observed in blood vessels and in the soma and proximal dendrites of a few neurons (Fig. 3.11A, 3.11C). Sections immunostained with the anti-iNOS antibody showed no specific staining of structures (Fig. 3.11C'). In one of the aged control cases, there was some AGE immunoreactivity observed in the soma and processes of a few astroglia (Fig.3.12A. Table 3.5). Some faint iNOS immunoreactivity in AGE - positive astroglia was detected (Fig. 3.12A'). Co-localisation of AGE and iNOS in astroglia was evident (Fig. 3.12A'')

3.2.3 Distribution of iNOS and AGE in early AD temporal cortex

In brains diagnosed with early AD (Braak stage I-II), a few pyramidal neurons were diffusely AGE but not iNOS reactive. Aggregations of astrocytes in the upper and deeper neuronal layers showed immunoreactivity for AGE (Fig 3.12B) and iNOS (Fig. 3.12B') in the cell processes. Some co-localisation of AGE and iNOS in astroglia was evident (Fig. 3.12B'') (Table 3.5)

3.2.4 Distribution of iNOS and AGE in advanced AD temporal cortex

An abundance of astrocytes were found immunoreactive for AGEs (Fig. 3.13A, Fig. 3.13B, Fig. 3.14A) and iNOS (Fig. 3.13B') in the temporal cortex of medium to severely affected (Braak stages III-VI) AD brains. Whereas most of the reactive astrocytes were located in the upper (I and II) layers and grouped in clusters, some single astrocytes were also distributed in the deeper neuronal layers. AGE staining appeared more diffuse in the processes compared with iNOS staining, which was observed in the cell soma as well as processes of astrocytes. Some co-localisation was observed in astrocyte processes (Fig. 3.13B''). Plaques throughout the neuronal layers were stained AGE positive (Fig. 3.14B). Parts of NFT contained AGE immunoreactivity (Fig. 3.15B). The soma, apical and proximal basal dendrites of numerous and selective pyramidal neurons in the deeper layers of the temporal cortex showed diffuse AGE- but not iNOS- reactivity (Fig 3.11A', Fig. 3.18C)(Table 3.5).
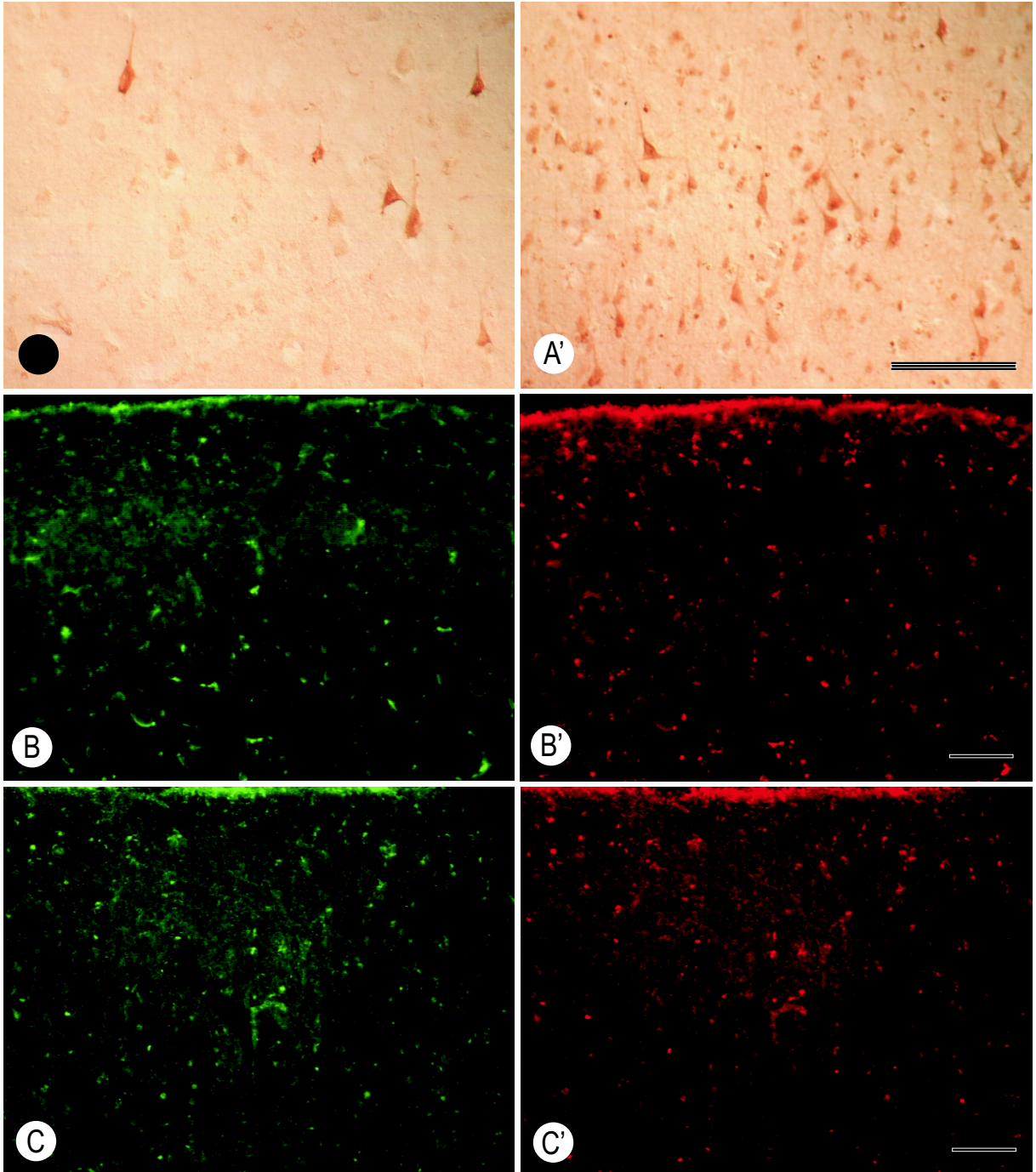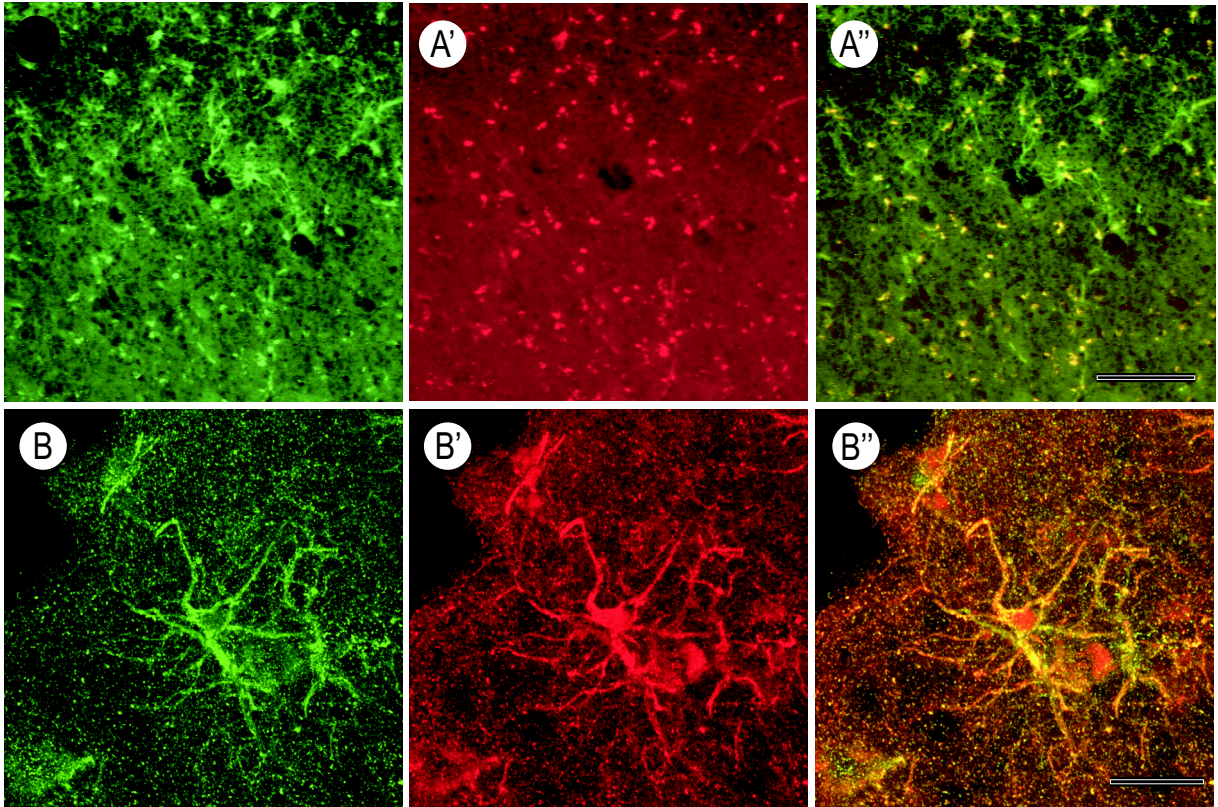
Fig. 3.11: Photomicrographs of sections of human cerebral cortex (Area 22) with immunohistochemical demonstration of AGE and iNOS. **A** - Section from an aged control brain (years old) stained with a polyclonal antibody to AGE, showing AGE   immunoreactivity in the peri   arya of a few neurons. **A'** - Section from an AD brain (years old) stained with a polyclonal antibody to AGE, showing a greater number of neurons with AGE   immunoreactivity compared with the aged control (scale bar = 100 μm). **B** - Single immunofluorescence for AGE (green; Cy2) from a young control (33 years old), showing a few blood vessels with AGE   immunoreactivity. **B'** - Single immunofluorescence for iNOS (red; Cy3) from the same section as B. Although some iNOS-reactivity appears in this section, there was a rather high intensity of autofluorescence from blood vessels and glial cells (scale bar = 100 μm). **C** - Single immunofluorescence for AGE (green; Cy2) from an aged control (years old), showing a few blood vessels with AGE   immunoreactivity. **C** - Single immunofluorescence for iNOS (red; Cy3) from the same section as C (scale bar = 100 μm).
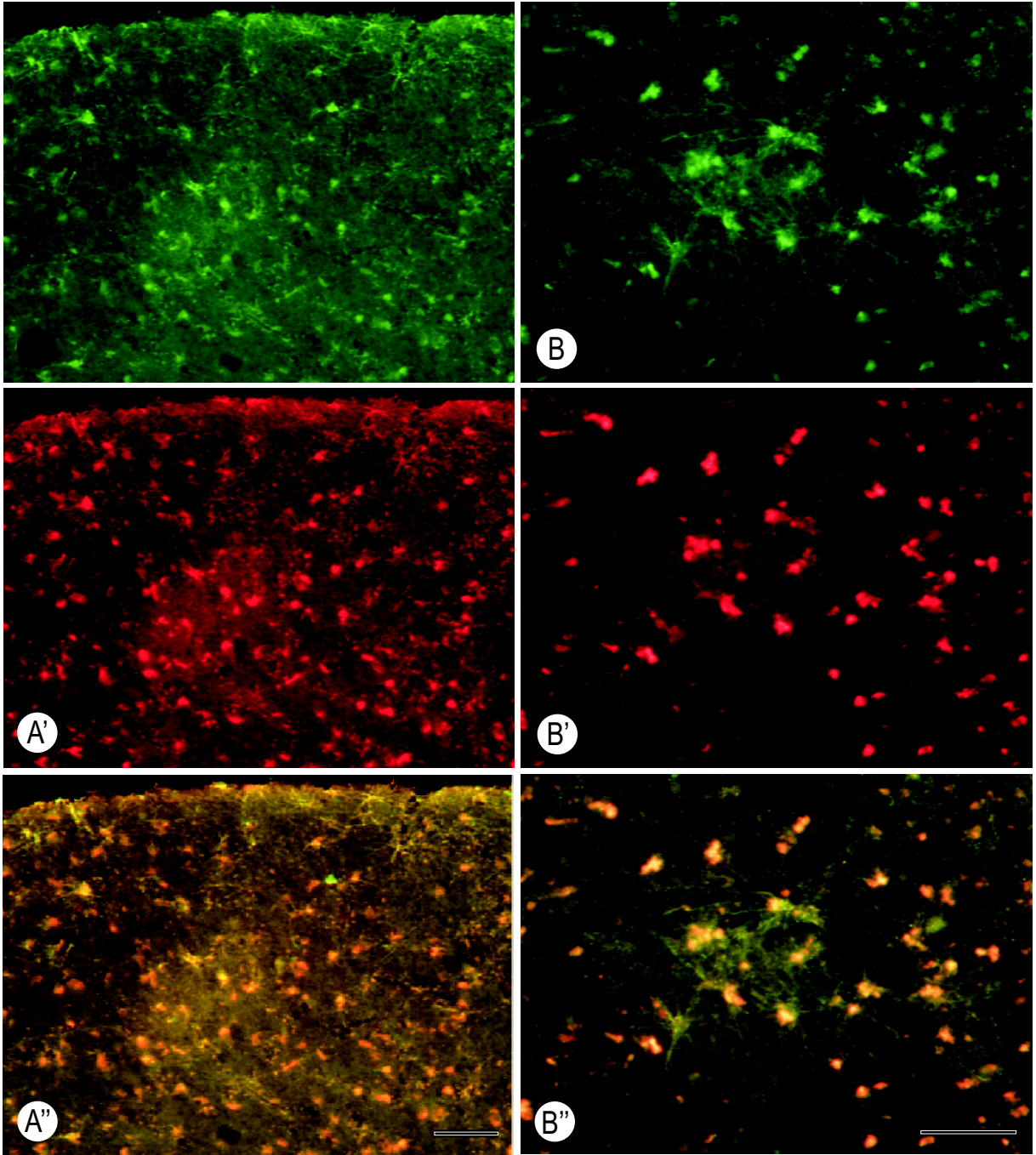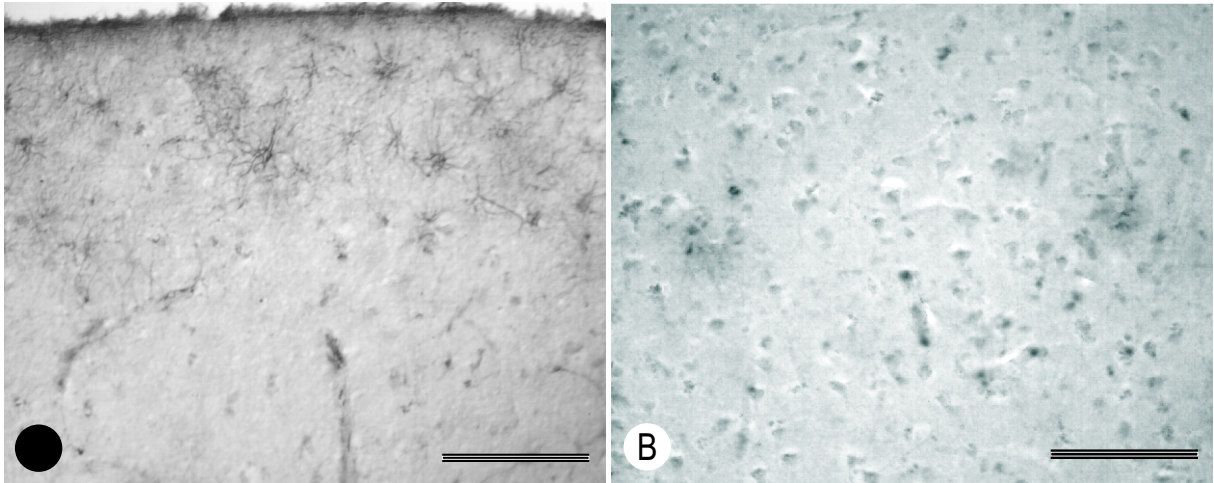
Fig. 3.1 Photomicrographs of sections of human cerebral cortex (Area 22) with immunohistochemical demonstration of AGE and iNOS in astrocytes of an aged control (years old) and early AD (5 years old) brain. **A** - Single immunofluorescence for AGE (green; Cy2) from an aged control brain, showing some AGE immunoreactivity in single astroglia near the pial border and in astrocytes associated with a pla ue in layer - . **A'** - Single immunofluorescence for iNOS (red; Cy3) from the same section as A, showing some positive staining in astroglia near the pial border and in a pla ue in layer - . **A''** - Double immunofluorescence showing co-localisation (yellow) of AGE iNOS in astrocytes (scale bar = 100 µm). **B** - Single immuno-fluorescence for AGE (green; Cy2) from an early AD brain, showing some AGE immunoreactivity in an aggregation of astroglia in layer - . **B'** - Single immunofluorescence for iNOS (red; Cy3) from the same section as B, showing some positive staining in astroglia in a pla ue in layer - . **B''** - Double immuno-fluorescence showing co-localisation (yellow) of AGE iNOS in astrocytes (scale bar = 100 µm).
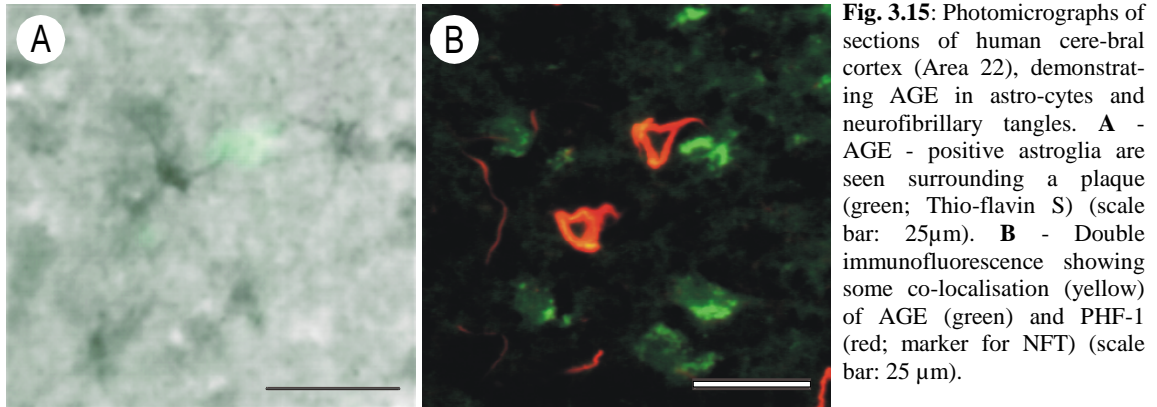
Fig. 3.13: Photomicrographs of sections of human cerebral cortex (Area 22) with immunohistochemical demonstration of AGE and iNOS in astrocytes of the late AD brain (years old). **A** - Single immuno-fluorescence for AGE (green; Cy2), showing some AGE   immunoreactivity, particularly in the processes, of numerous astroglia in layer   - . **A'** - Single immunofluorescence showing iNOS (red; Cy3) in the same astrocytes from A. **A''** - Double immunofluorescence showing co-localisation (yellow) of AGE iNOS in astrocytes (scale bar = 100 μm). **B -** Single immunofluorescence showing AGE (green; Cy2) in an astrocyte. **B'** - Single immunofluorescence showing iNOS (red; Cy3) in the astrocyte from B. **B''** - Double immunofluorescence showing co-localisation (yellow) as well as differential distribution of AGE iNOS in an astrocyte (scale bar = 20 μm).

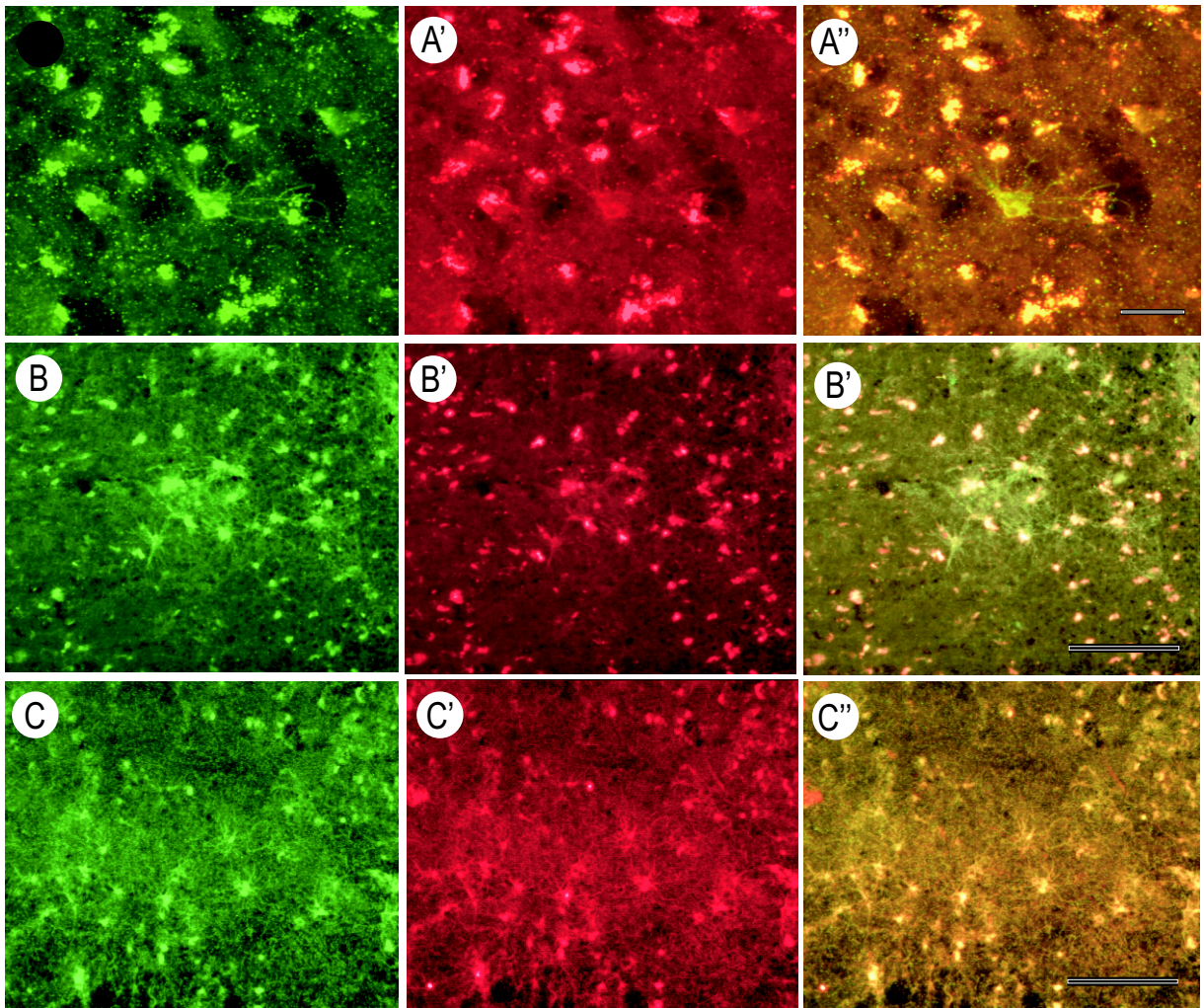**Fig. 3.1** Photomicrographs of sections of human cerebral cortex (Area 22) with immunohistochemical demonstration of AGE in astrocytes and pla ues of the late AD brain (years old). **A** - Section showing AGE immunoreactivity in astroglia in layer   (scale bar = 100 µm). **B** - Section showing AGE   immunoreactivity in astroglia associated with pla ues in layer   (scale bar = 100 µm).

Fig. 3.15: Photomicrographs of sections of human cere-bral cortex (Area 22), demonstrating AGE in astro-cytes and neurofibrillary tangles. **A** - AGE - positive astroglia are seen surrounding a plaque (green; Thio-flavin S) (scale bar: 25µm). **B** - Double immunofluorescence showing some co-localisation (yellow) of AGE (green) and PHF-1 (red; marker for NFT) (scale bar: 25 µm).

3.2.5 Comparison between the distribution of iNOS and AGE in temporal and entorhinal cortices in AD and controls

In the aged control group, only one case showed very few astroglia with AGE- and iNOS-reactivity in the entorhinal cortex (Fig 3.16A, Fig. 3.16A'). Similar findings were seen in the temporal cortex of this case, as mentioned previously (Fig. 3.12A, 3.12A'). There were no astrocytes detected in the entorhinal cortex of the other aged controls. In the two early AD cases examined, there were a few astrocytes detected in the entorhinal (Fig 3.16B, Fig. 3.16B') and temporal (Fig. 3.12B, 3.12B') cortices and a few astrocytes in the cortex, showing AGE- and iNOS-reactivity. In comparison, in the five late AD cases examined numerous astrocytes with AGE- and iNOS-reactivity were demonstrated in the superficial and deeper layers of the entorhinal cortex (Fig 3.16C, 3.16C'). In summary, no detectable quantitative differences in astrocytes staining positive for AGE and iNOS were evident between the entorhinal and temporal cortices within the control nor AD groups. However, marked differences were noted between the various groups. AGE and iNOS reactive astrocytes were absent from both the entorhinal and temporal cortices of all except one of the control brains. There were a few astrocytes staining positive for AGE and iNOS in both regions of early AD, compared with a much larger accumulation of astrocytes seen in the late AD brain.

Fig. 3.1 : Photomicrographs of sections of human cerebral cortex (entorhinal, Area 2 and 3) with immuno-histochemical demonstration of AGE and iNOS in astrocytes of control and AD brains. **A** - Single immuno-fluorescence for AGE (green; Cy2) from an aged control brain (years old), showing some AGE immunoreactivity in a single astroglia layer - . his was the only astrocyte detected in the entorhinal cortex of this case. **A'** - Single immunofluorescence for iNOS (red; Cy3) from the same section as A, showing some faint staining in an astrocyte. **A''** - Double immunofluorescence showing co-localisation (yellow) of AGE iNOS in an astrocyte (scale bar = 25 µm). **B** - Single immunofluorescence for AGE (green; Cy2) from an early AD brain (5 years old), showing some AGE immunoreactivity in an aggregation of astroglia in layer - . **B'** - Single immunofluorescence for iNOS (red; Cy3) from the same section as B, showing some positive staining in astroglia in a pla ue in layer - . **B''** - Double immunofluorescence showing co-localisation (yellow) of AGE iNOS in astrocytes (scale bar = 100 µm). **C** - Single immunofluorescence for AGE (green; Cy2) from a late AD brain (years old), showing some AGE immunoreactivity, particularly in the processes, of numerous astroglia in layer - . **C'** - Single immunofluorescence showing iNOS (red; Cy3) in the same astrocytes from C. **C''** - Double immunofluorescence showing co-localisation (yellow) of AGE iNOS in astrocytes (scale bar = 100 µm).

3.2.6 Differential pattern of AGE/iNOS staining according to plaque development

Brain sections were stained with an anti-AGE antibody-and counterstained with the fluorescent marker, Thioflavin S, to visualise plaques. AGE-positive astrocytes were detected in the vicinity of mature plaques (Fig. 3.15A). Senile plaques in the temporal cortex of AD brains in the advanced Braak stages (III-VI) were stained with an antibody against the β-amyloid peptide. Double immunofluorescence with anti-AGE and anti-β-amyloid antibodies showed AGE-positive astrocytes surrounding mature but not diffuse β-amyloid plaques (Fig. 3.17A). In some of these AGE-positive astrocytes, co-localisation with β-amyloid was seen. Furthermore, double immunofluorescence with anti-AGE and anti-iNOS antibodies showed accumulation of iNOS-positive astrocytes around mature β-amyloid plaques (Fig. 3.17B). No co-localisation with β-amyloid and iNOS was seen in these astrocytes. In fluorescent as well as DAB preparations, some light AGE- as well as iNOS- staining of plaques was evident. In summary, localisation of iNOS and AGE was evident in astroglia associated with mature but not diffuse plaques.
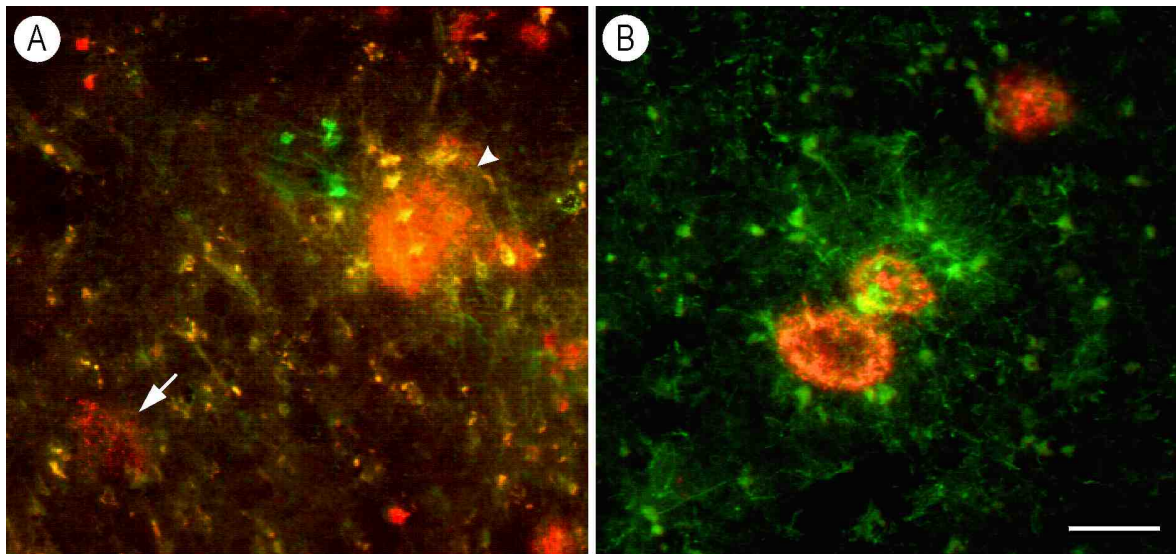
Fig. 3.17: Immunohistochemical demonstration of AGE, iNOS and beta-amyloid in Area 22 of AD brains.
A - Double immunofluorescence showing beta-amyloid plaques (red; Cy3) and AGE-reactive astrocytes (green; Cy2). AGE-reactive astrocytes can be seen surrounding a mature (arrowhead) but not diffuse plaque (arrow).
B- Double immunofluorescence showing iNOS-reactive astrocytes (green; Cy2) clustered around two beta-amyloid plaques (red; Cy3) (scale bar = 100 μm).

3.2.7 Distribution of iNOS and AGE in microglia in advanced AD temporal cortex

       Since iNOS expression and AGE-mediated activation is known to occur in microglia as well as astrocytes, a monoclonal antibody against reactive macrophages was used to verify microglial involvement. Using this antibody, the presence of numerous microglia was observed in the middle to deeper neuronal layers of the AD temporal cortex (Fig. 3.18A', Fig. 3.18B', Fig. 3.18C'). In some of these microglia, AGE reactivity was detected (Fig 3.18A). In addition, we were able to demonstrate that some reactive microglia contain iNOS (Fig. 3.18B) . AGE and iNOS staining in the soma and processes of reactive microglia appeared granular and sparse, compared with the more diffuse staining in the astrocytes. Some reactive microglia not co-localised with AGE were found adjacent to AGE-positive pyramidal neurons (Fig. 3.18C''). No reactive microglia were detected in the older control group (Table 3.5).

Table 3.5 – Summary of immunohistochemical findings in control and AD brains (Area 22).

| CASE TYPE	astrocytes	microglia	neurons	blood vessels
young controls	no astrocytes detected	-	AGE (-) iNOS (-)	AGE (+) iNOS (-)
aged controls	few astrocytes AGE (+) iNOS (+)	no microglia detected	few neurons AGE (+) iNOS (-)	AGE (+) iNOS (-)
early AD	few astrocytes AGE (+) iNOS (+)	-	few neurons AGE (+) iNOS (-)	AGE (+) iNOS (-)
late AD	abundant astrocytes AGE (+) iNOS (+)	some microglia AGE (+) iNOS (+)	numerous neurons AGE (+) iNOS (-)	AGE (+) iNOS (-)
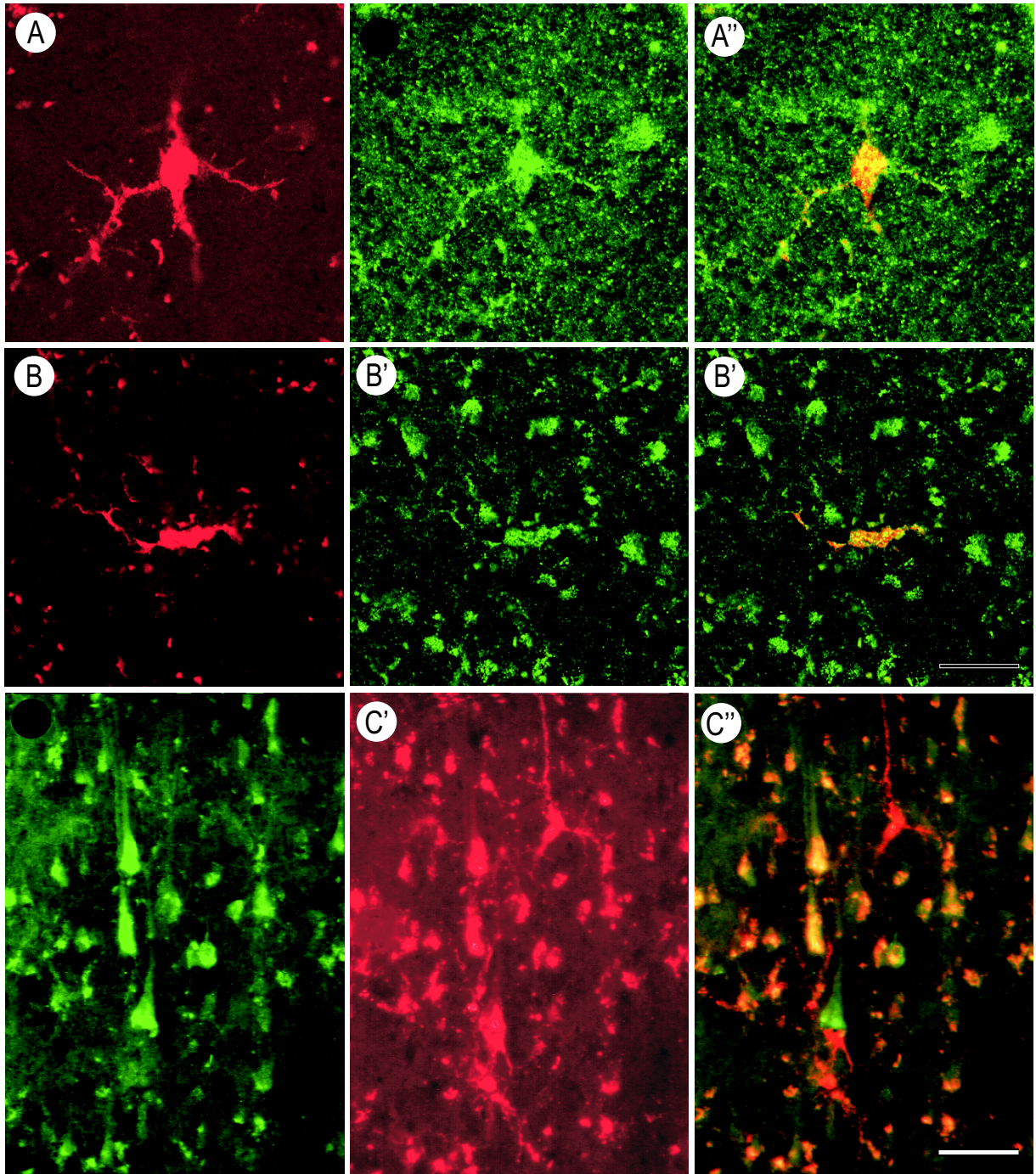
Fig. 3.18: Photomicrographs of sections of human cerebral cortex (Area 22) stained with anti-AGE, anti-iNOS and anti-macrophage antibodies in the late AD brain. **A -** Reactive microglia (red; Cy3). **A'**- AGE-immunoreactivity (green; Cy2) in the microglia depicted in A. **A''** - Double immunofluorescence showing co-localisation of AGE in microglia. **B -** Reactive microglia (red; Cy3). **B'**- iNOS-immunoreactivity (green; Cy2) in the microglia shown in B. **B''** - Double immunofluorescence showing co-localisation of iNOS in microglia (scale bar = 10 µm). **C** - Double immunofluorescence showing a reactive microglia (red; Cy3) adjacent to an AGE-staining pyramidal neuron (green; Cy2) (scale bar = 50 µm).

3.2.8 AGE colocalises with α-synuclein in the Substantia Nigra in incidental Lewy body disease

The cases examined had no clinical signs of Parkinson's disease. Although this clinical diagnosis was confirmed by the absence of late changes of PD such as depigmentation and extensive cell death, Lewy bodies appeared as the first signs of PD specific changes in the S. nigra. Among 400 - 600 neurons counted per section, about 1-2 neurons showed the presence of Lewy bodies by H&E staining and the Switzer-Campbell-method (Figure 3.19 A/B). Lewy bodies appeared as intracytoplasmic spherical inclusions, 5μm to 20μm in diameter, with a dense eosinophilic core and a clearer surrounding halo. All Lewy bodies displayed immunoreactivity against neurofilament (not shown) and α-synuclein (Figure 3.19E). Typically, α-synuclein immunostaining had a ring-like appearance with a denser outer zone. α-synuclein-reactive Lewy neurites were only rarely observed in these early cases. The anti-AGE antibody clearly labeled Lewy bodies. Similar to the α-synuclein staining, reactivity was most dense in the outer zone of the Lewy bodies (Figure 1C/D). Using double immunofluorescence, AGEs were highly colocalized with α-synuclein in Lewy bodies (Figure 3.19F/F'). This suggests that they are actively involved in the chemical crosslinking and resistance of the protein deposit to proteolytic degradation. In three of the four incidental Lewy body disease cases, a few Lewy-bodies were detected in the cortex, which stained for both α-synuclein and AGEs (data not shown). One case had numerous Lewy bodies in the locus coeruleus. The fact that cortical Lewy-bodies and brainstem Lewy bodies displayed identical features points to a similar process of formation involving covalent crosslinking by AGEs.
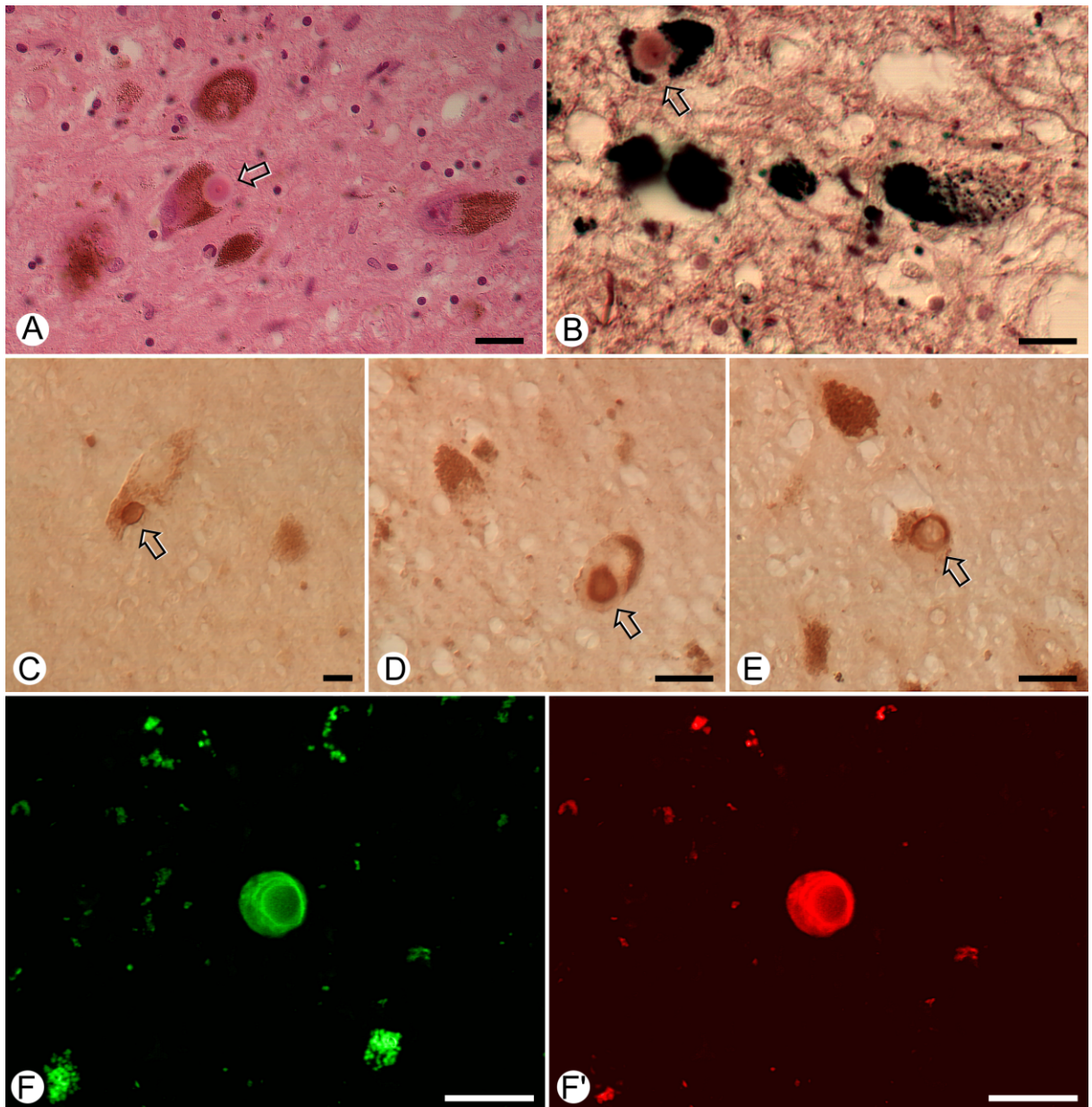
Figure 3.19: Lewy bodies in the SN of incidental Lewy body disease disease (preclinical stage of Parkinson's disease). **A** - H&E, **B** Switzer-Campbell, **C/D** - Immunostaining for AGE; **E** - Immunostaining for α-synuclein; **F/F'** - Double-immunofluorescence for the simultaneous detection of AGE (F, Cy2-labelled secondary antibody) and α-synuclein (F', Cy3-labelled secondary antibody). (Scale bars: 20µm)

3.3. Characterization of anti-AGE antibodies with glycated peptide libraries on cellulose membranes (AGE-peptide spot libraries).

In order to investigate the reactivities of proteins, glycated by reducing sugars, di- and tri-peptide libraries were produced. Of the 20 naturally occurring amino acids, 8-12 were selected, which included non-reactive and reactive amino acids, defined from a previous study (Münch *et al,* 1999). The membrane-bound di- and tri- peptides were selectively deprotected and N-terminally acetylated to expose free side chains for glycation/ribosylation.

3.3.1 Assembly of peptides on membranes

Some standard configurations for the synthesis of peptides on cellulose membranes (W540) or amino-polyethylene glycol derivatized membranes (APEG) used in the present experiments are summarized in Table 3.6. Depending on spot volume and spot size libraries or sublibraries from the combinations of the 20 proteinogenic amino acids were synthesized on membranes in the microtiterplate formate. Münch *et al*., (1999). used 2 membranes to arrange 20 x 20 = 400 combinations of amino acids. In the present work in a more economical way up to two libraries of 12 x 12 = 144 amino acid combinations or a total of 288 spots were arranged on 1 membrane. The yield of peptides per spot was experimentally determined by ^{14}C-labelling (acetylation or benzoylation) of the underivatized peptides and is referred to as synthesis scale in Table x. The synthesis scale or loading may be increased by double or triple spotting. For comparison two types of grids were used, with high or low capacities for peptide-binding. The standard (with high capacity and high density) grid was produced by singly applying 0.4 µl of 0.2 M βAla per spot; the capacity of each spot was 27 nmol on APEG and 19 nmol of peptides on W540B membranes. In contrast, the low capacity grid was produced with 0.4 µl of 0.02 M βAla (one tenth of the concentration on the high capacity grid) per spot; the capacity per spot was 5.3 nmol on APEG and 7.3 nmol of peptides on W540B membranes. The capacity did not correlate with the spot volume and concentration of
the spotted amino acid.

Table 3.6 - Configuration and synthesis scale of SPOT peptides on cellulose (W540) and APEG membranes

Membrane Type	Capacity nmol/cm^2	Spotted volume (µl)	Spot size $\varnothing$ mm	Calculated (maximal) capacity	Synthesis scale nmol/spot	Useful format of grid
W540	200 – 400[1]	0.5/0.7	7	96	25[1]	8 x 12 = 96
	292	0.3/0.4	5	57	17[2]	10 x 20 = 200; 12 x 24 = 288
	40	0.2/0.3	4	5	2.1 – 5.4	12 x 24 = 288; 16 x 25 = 400
	40	0.4/0.5 (0.2 M βAla)	6	11	19	10 x 16 = 160
		0.4/0.5 (0.02 M βAla)	6		7.3	10 x 16 = 160
APEG	334 (400[3])	0.2/0.3	3	24	19-29	12 x 24 = 288; 16 x 25 = 400
	340	0.4/0.5 (0.2 M βAla)	5	62	27	10 x 16 = 160
		0.4/0.5 (0.02 M βAla)	5		5.3	10 x 16 = 160

[1] Frank *et al.* 1996
[2] Muench *et al.* 1999
[3] AIMS-Products, Hartmann Analytic, Braunschweig, Germany (Supplier)

The total capacity of peptides on W540 membranes measured in our experiments, by ^{14}C acetylation (^{14}C-labelled acetate), varied from 40 to 292 nmol/cm^2. The total capacity of peptides (334 - 340 nmol of peptide/cm^2) on APEG membranes lay closer to the expected value (400 nmol of peptide/cm^2) and was more reproducible with APEG membranes than on W540 membranes. On W540 membranes, the quantity of peptides formed on individual spots derived from 0.2 µl of amino acid aliquots was 2 - 5 nmol and from 0.4 µl of amino acid it was 19 nmol. On APEG membranes, the quantity of peptides

formed on each spot was higher than on W540 membranes; from 0.2 μl amino acid aliquots, it was 19 – 29 nmol and from 0.4 μl amino acid, it was 27 nmol. (Table 3.7)

Table 3.7 – Yields of non-glycated and glycated (with glucose and ribose) peptides

A) Spots derived from the single spotting of **0.4 μl** of 0.2 mol/l βAla on **W540** membranes

Peptide		glucosylation		ribosylation	
Composition (*) of A*β-Ala	Yield nmol	Yield nmol	Fraction of peptide (%)	Yield nmol	Fraction of peptide (%)
K	19	0.55	2.9	1.2	6.3

B) Spots derived from the single spotting of **0.4 μl** of 0.2 mol/l βAla on **APEG** membranes

Peptide		glucosylation		ribosylation	
Composition (*) of A*βA	Yield nmol	Yield nmol	Fraction of peptide (%)	Yield nmol	Fraction of peptide
K	27	5.3	20	2.5	9

3.3.1 Glycation reactivities of amino acid side chains

The yield of glycated peptides on APEG and W540 membranes was calculated by comparing the amount of radioactivity of incorporated ^{14}C sugars on peptide spots. In general, the yields of glycated/ribosylated peptides were higher on APEG compared with W540 membranes, which was expected from the higher yields of non-glycated peptides (per spot and in total) on APEG membranes. In addition, for both membranes the fraction of peptides which reacted with ribose was higher that the fraction which reacted with glucose. The yield of glycated/ribosylated peptides was selective for different peptides on both membranes. The amino acids which were shown to react more strongly with sugars on both APEG and W540 membranes, as determined by autoradiographs, were cysteine, lysine and arginine (Fig 3.20). On both membranes the order of reactivity of amino acid residues with glucose or ribose was similar. The order of reactivity from strongest to weakest was lysine ≥ cysteine > arginine. In addition, histidine and asparagine showed some reactivity with ribose. Arginine was only weakly marked by ^{14}C ribose compared with ^{14}C glucose. Slight differences in the amino acids glycated were also found between the membranes. On W540 membranes, higher yields of glycated cysteine and arginine residues were measured compared with APEG membranes. On APEG membranes, asparagine was additionally glycated. As a control, calculations were repeated after blocking the membranes with 5 % BSA in PBS/0.1 % Tween-20 and several rounds of

"stripping", necessary for re-probing with different antibodies. There were no significant differences in the results for reactivities before and after handling of the membranes. Since glycated cysteine is generally not recognized by the anti-AGE antibodies currently available, cysteine was not further considered for the classification of glycated peptides. Table 3.8 shows the relative glycation reactivities of acetylated peptides (ac-Ala * βAla), including 11 amino acids and a reference (Ala), whose reactivities with glucose were apparent from previous experiments.

In general, membranes were incubated in 10 ml 50 mM glucose or ribose. This corresponds to a total of 500 µmol sugar available per membrane. The total number of spots represented on one membrane was 16 x 10 = 160. W540 membranes incubated with 500 µmol ^{14}C glucose and a total of 3040 nmol (160 x 19 nmol) tripeptide would contain an excess of sugar versus peptide in the proportion of 164:1. In contrast, APEG membranes incubated with 500 µmol ^{14}C ribose and a total of 4320 nmol (160 x 27 nmol) tripeptide would contain an excess of sugar versus peptide in the proportion of 115:1.

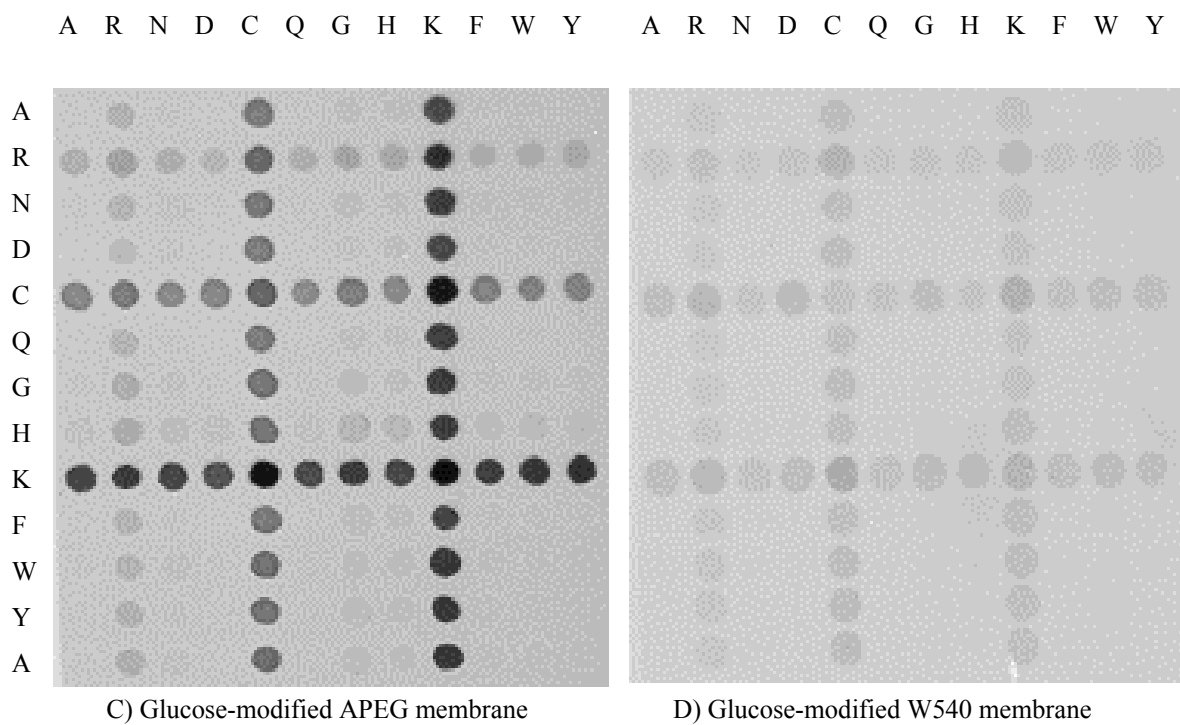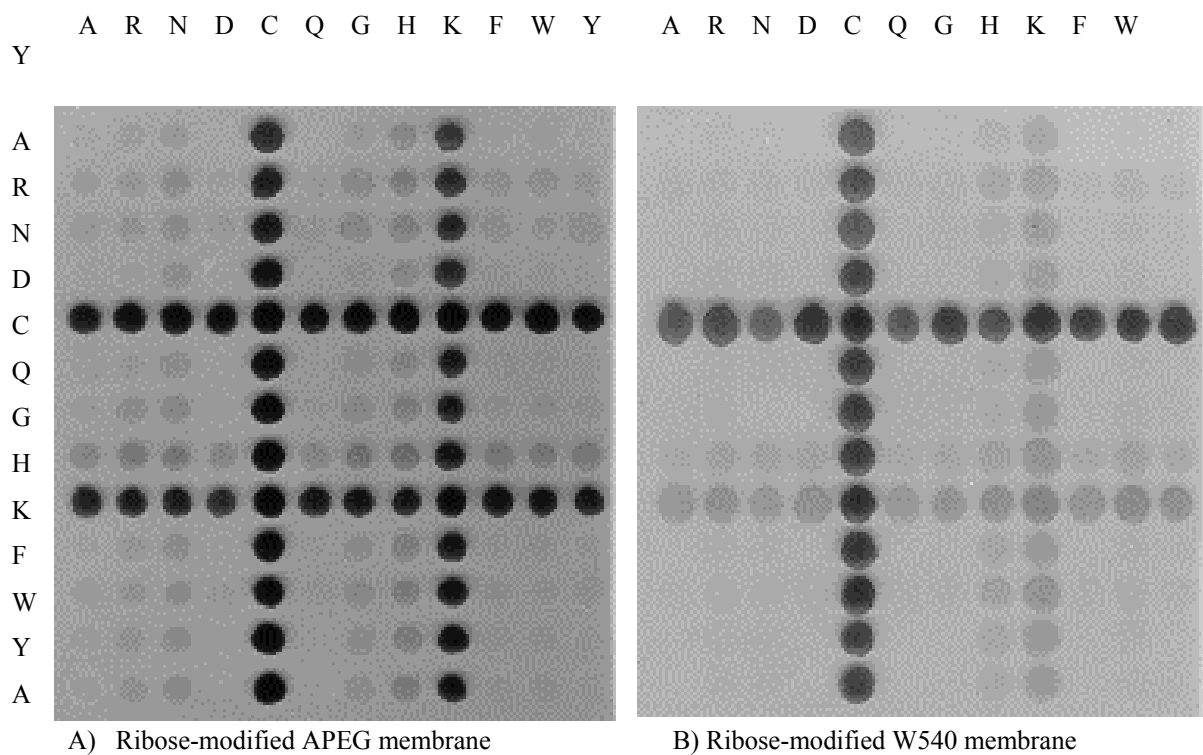Fig 3.20: Autoradiographs of glycated (with glucose and ribose) peptides on **W540 and APEG** membranes. First (C-terminus) amino acids are shown on the left-hand column and 2nd (N-terminus) amino acids on the top row.

Table 3.8. – Yields of non-glycated and glycated (with glucose and ribose) peptides

A) Spots derived from the single spotting of **0.2 µl** of 0.2 mol/l βAla on **W540** membranes

Peptide		glucosylation		ribosylation	
Composition (*) of A*β-Ala	Yield nmol	Yield nmol	Fraction of peptide (%)	Yield nmol	Fraction of peptide (%)
A	3.0	-	-	-	-
R	2.9	0.09	3.1	0.20	6.9
N	2.8	-			
D	3.4	-			
C	2.7	0.14	5.2	2.62	97
Q	2.6	-			
G	5.4				
H	4.3				
K	2.1	0.14	6.6	0.33	15.7
F	3.1				
W	2.6				
Y	3.1				
Average	3.2	0.0 – 0.14	Max 6.6	0 – 0.33 (2.62)	Max 15.7

B) Spots derived from the single spotting of **0.2 µl** of 0.2 mol/l βAla on **APEG**-membranes

Peptide		glucosylation		ribosylation	
Composition (*) of A*β Ala	Yield nmol	Yield nmol	Fraction of peptide (%)	Yield nmol	Fraction of peptide (%)
A	19	-	-	-	-
R	23	0.19	0.8	0 – 0.11	0.5
N	21	-		0.20 – 0.40	1.0 – 2.0
D	26	-		0.12	0.8
C	22	0.97	4.4	8.50	38.6
Q	24	-		0 – 0.16	0.7
G	29	0.08	0.3	0.34	1.2
H	22	0.16	0.7	0.48	2.2
K	22	1.64	7.6	5.40	25.1
F	26	0.08	0.3	0.24	0.9
W	27	0.09	0.4	0.35	1.2
Y	25	0.10	0.5	0.28	1.1
Average	24	0.0 – 1.64	Max 7.6	0 – 5.40 (8.5)	Max 25.1

3.3.2 Epitope mapping using anti-AGE antibodies

In addition to analysing the reactivities of di/tripeptides with glucose and ribose, membranes were incubated with anti-AGE antibodies to characterise their specific epitopes. As expected, all four anti-AGE antibodies tested bound preferably with AGE-modified amino acids with nucleophilic side chains i.e. lysine and arginine. In our experiments, the anti-CML antibody recognised glycated and ribosylated lysine on both APEG and W540 membranes (Fig. 3.21)(compared with lysine and arginine, using 1000 mM glucose on W540 as reported by Schicktanz (2000). The anti-imidazolone antibody exhibited affinity towards glycated and (500 mM) ribosylated arginine on both APEG and W540 membranes (Fig. 3.22) (also found by Schicktanz, 2000). In additional, affinity towards lysine after incubation with 50 mM ribose was evident and this was of equal intensity to arginine (Fig. 3.23). The predominant epitopes of the anti-AGE (K1935) antibody were glycated and ribosylated lysine and arginine on APEG membranes. (Fig. 3.24). The anti-KLH-AGE antibody showed strong affinity towards lysine and arginine and some weak affinity towards glutamine-phenylalanine, glutamine-trytophan and glutamine-tyrosine (compared with only lysine and asparagine, detected by Schicktanz, 2000) (Fig. 3.25). Results are summarised in Table 3.9.
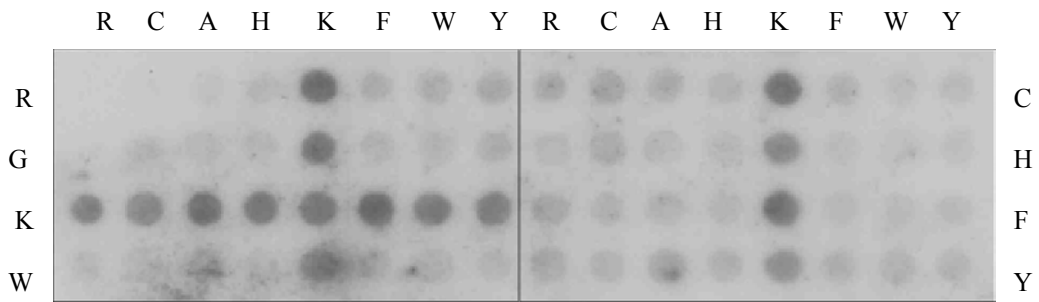
A) ECL blot (APEG membrane) of glycated (50 mM glucose) tripeptide library.
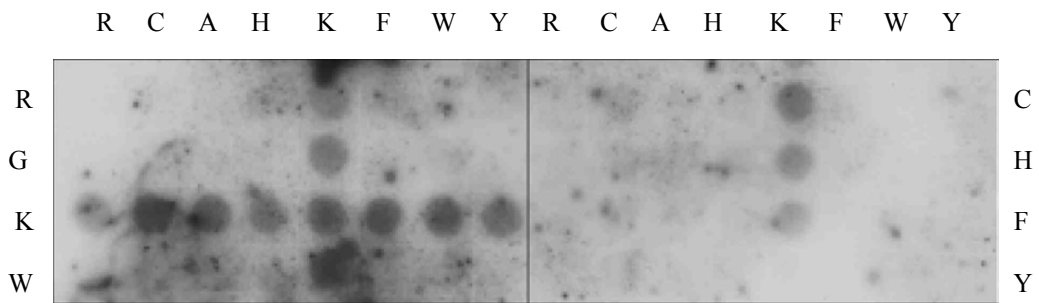
B) ECL blot (W540 membrane) of glycated (50 mM glucose) tripeptide library.
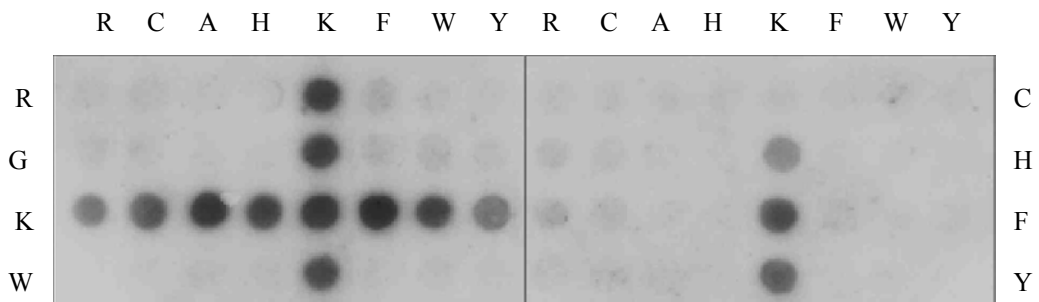
C) ECL blot (APEG membrane) of riboslyated (50 mM ribose) tripeptide library.
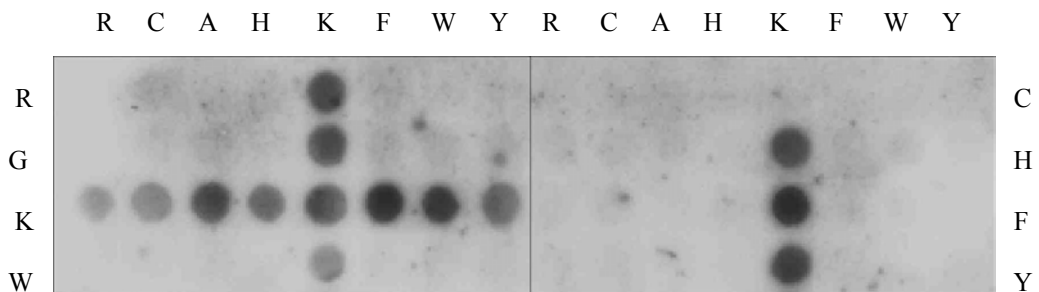
D) ECL blot (W540 membrane) of riboslyated (50 mM ribose) tripeptide

Fig. 3.21: ECL blots of glycated/riboslyated tripeptide libraries on APEG and W540 membranes incubated with the anti-CML-POD (1:5000) antibody. 1st (C-terminus) amino acids are shown on the left- and right-hand columns and 2nd (N-terminus) amino acids are shown on the top rows.
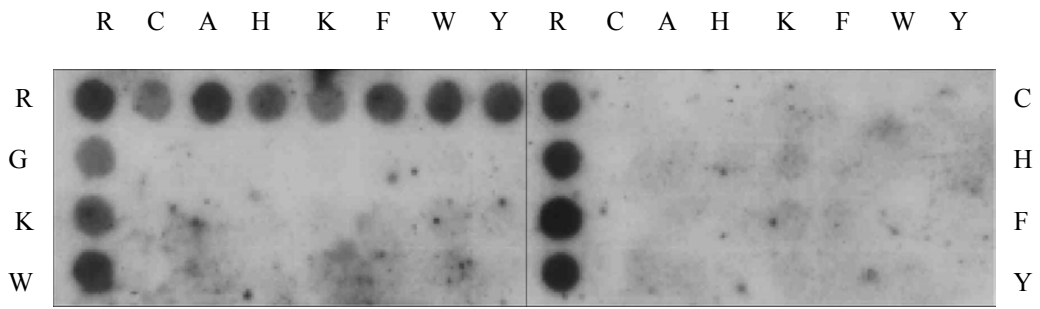
A) ECL blot of glycated (50mM) tripeptide library.
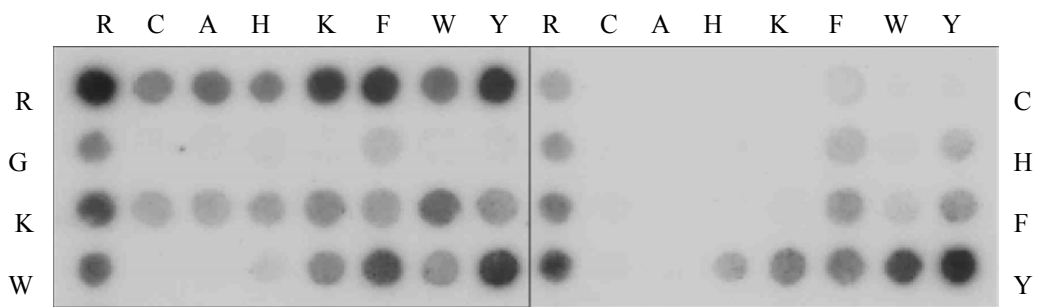
B) ECL blot of riboslyated (500mM) tripeptide library.

C) ECL blot of riboslyated (50mM) tripeptide library.

Fig. 3.22: ECL blots of glycated/riboslyated tripeptide libraries on APEG membranes incubated with the anti- anti- AG1 (1:1000) antibody. 1st (C-terminus) amino acids are shown on the left- and right- hand columns and 2nd (N-terminus) amino acids are shown on the top rows.
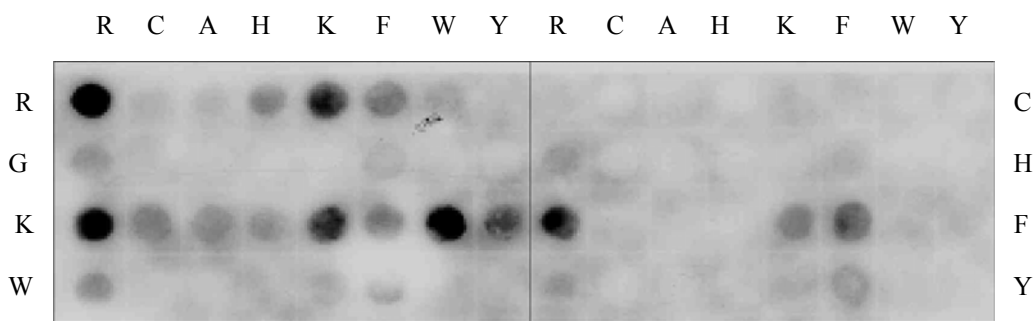
A) ECL blot of glycated (50mM) tripeptide library.
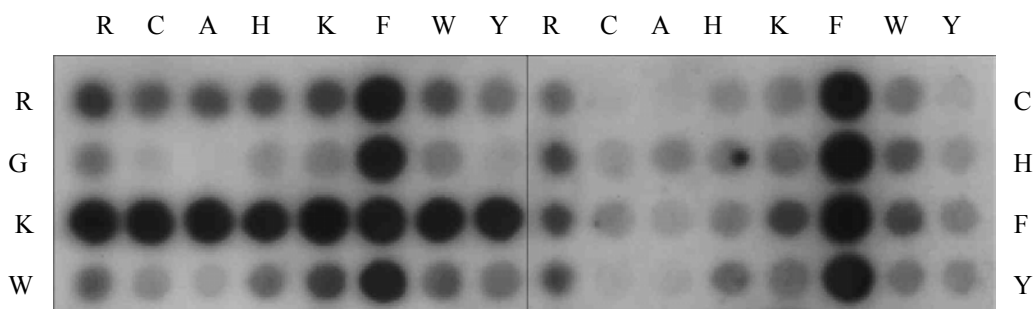
B) ECL blot of riboslyated (500mM) tripeptide.
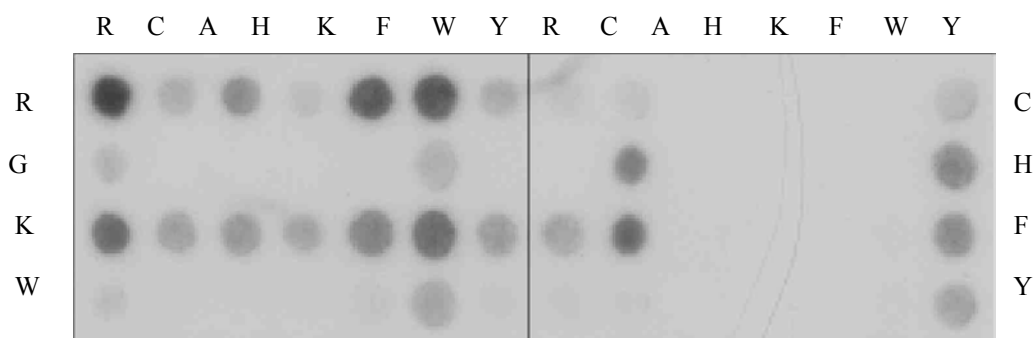
C) ECL blot of riboslyated (50mM) tripeptide library.

Fig. 3.23: ECL blots of glycated/riboslyated tripeptide libraries on APEG membranes incubated with the anti-AGE K1935 (1:1000) antibody. 1st (C-terminus) amino acids are shown on the left- and right- hand columns and 2nd (N-terminus) amino acids are shown on the top rows.
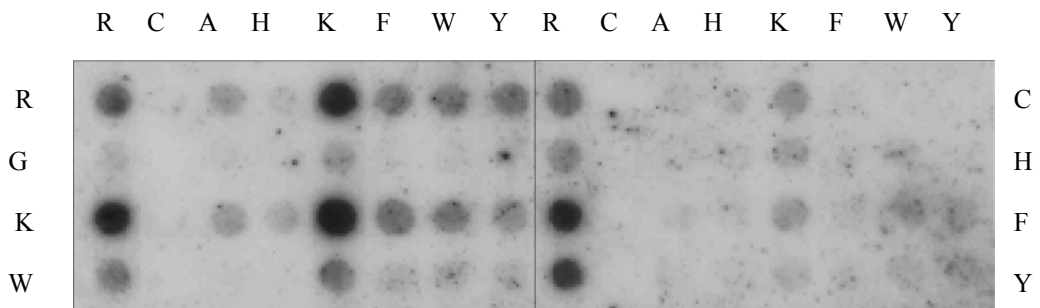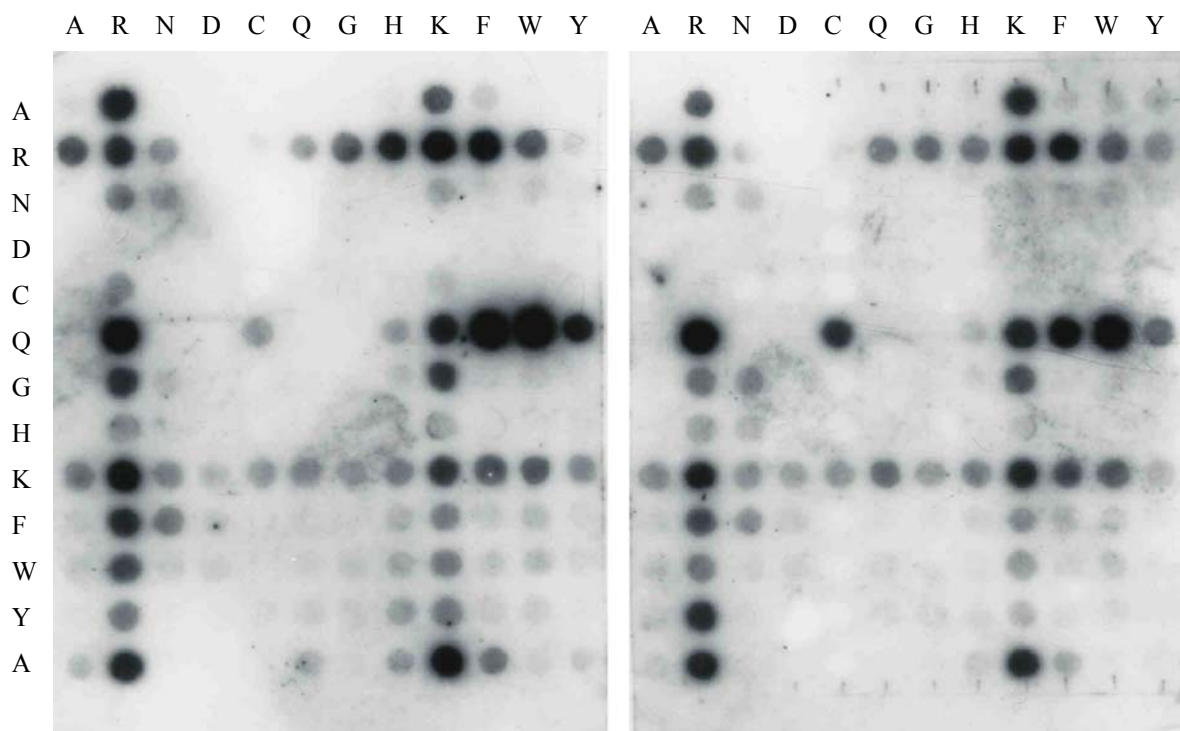
A) With ribose (50 mM)   B) With glucose (50 mM)

Fig. 3.24: ECL blots of glycated/riboslyated tripeptide libraries on APEG membranes incubated with the anti-KLH-AGE (1:1000) antibody. 1st (C-terminus) amino acids are shown on the left-hand column and 2nd (N-terminus) amino acids are shown on the top row.

Table 3.9 – Summary of amino acid epitopes recognised by anti-AGE antibodies (comparison with the results of Schicktanz et al (2000)

SUGAR	Anti-CML-POD (Roche) monoclonal antibody		AG-1 (selected for imidazolone), monoclonal antibody		Anti-AGE (AK 1935) polyclonal antibody	Anti-KLH-AGE polyclonal antibody
	W540B	APEG	W540B	APEG	APEG	APEG
glucose 1000 mM 50°C	**R,** K >> W, F (Schicktanz 2000, K1932)	n.d.	R > N, Q > W (Schicktanz 2000)	n.d.	n.d.	n.d.
glucose 50 mM 50°C	K	K	R	R	R, K	R and K, QF,QW,QY
ribose 50 mM 37°C	K	K	**K**, R >> W, Y	**K** > R	R, K	R and K, QF,QW,QY
ribose 500 mM 37°C	n.d.	K	n.d.	R >> K R= KW, WW, YY	R, K	R, K
Dipeptide membranes on Whatman 540-βAla (Schicktanz, 2000)						
W540B only	K1001 KLH-AGE	K1936 RNAse-AGE	KLH-AGE selected for imidazolone	K1937 RNAse-AGE	K1935 RNAse-AGE	K1932 Hb-CML
glucose 1000 mM 14 days at 50°C	R, N (WW, YY, WY, YW)	R, N (WW, YY, WY, YW)	R (WW ,YY, WY, YW)	K (WW, YY, WY, YW)	K >> W, Y	**R**, K (WW, YY, WY, YW)

3.3.3 Non-specific antibody reactivity

Non-glycated membranes were incubated with primary and secondary antibodies to confirm antibody specificity. Some binding of both anti-AGE and secondary antibodies to non-glycated W540 but not APEG membranes was seen. The anti-CML-POD antibody showed some very weak affinity towards lysine, arginine and tyrosine residues (Fig. 3.25). The anti-AG1 antibody detected some lysine residues (Fig 3.26A) and the anti-mouse-POD detected arginine (weak) and tyrosine residues (Fig 3.26B). The anti-AGE (K1935) antibody did not recognise any specific non-modified amino acid residues (Fig 3.27A), but there was some affinity of the anti-rabbit-POD IgG towards lysine, arginine and tyrosine residues (Fig 3.27B).

The control experiments with non-glycated peptide libraries showed that the primary and secondary antibodies have affinity towards some non-modified amino acids. As the anti-CML antibody was conjugated with a secondary antibody, it was difficult to assess whether the amino acid residues detected were due to the primary or secondary antibodies.

Fig. 3.25: ECL blot (W540 membrane) of non-glycated tripeptide library incubated with anti-CML-POD antibody (1:5000), showing some faint detection of lysine, arginine and tyrosine residues. 1st (C-terminus) amino acids are shown on the left- and right- hand columns and 2nd (N-terminus) amino acids are shown on the top rows.
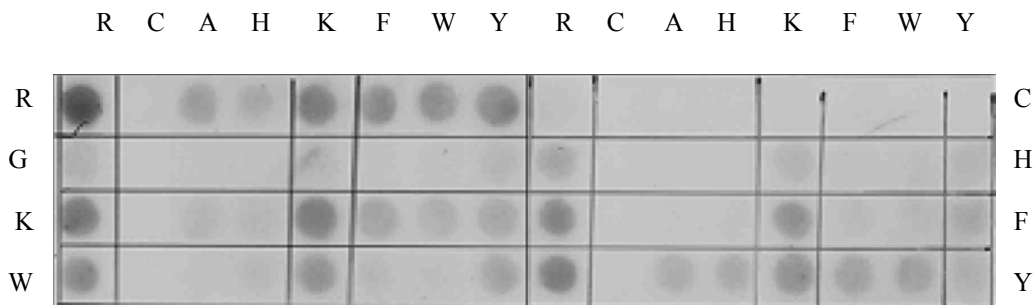
Fig. 3.26: A) ECL blot (W540 membrane) of non-glycated tripeptide library incubated with anti-AG1 (1:1000). Although some lysine, arginine and tyrosine residues are marked, the actual amino acid detected by the anti-AG1 antibody would be lysine (after subtraction of the amino acids detected by the anti-mouse-POD IgG). 1st (C-terminus) amino acids are shown on the left- and right- hand columns and 2nd (N-terminus) amino acids are shown on the top rows.
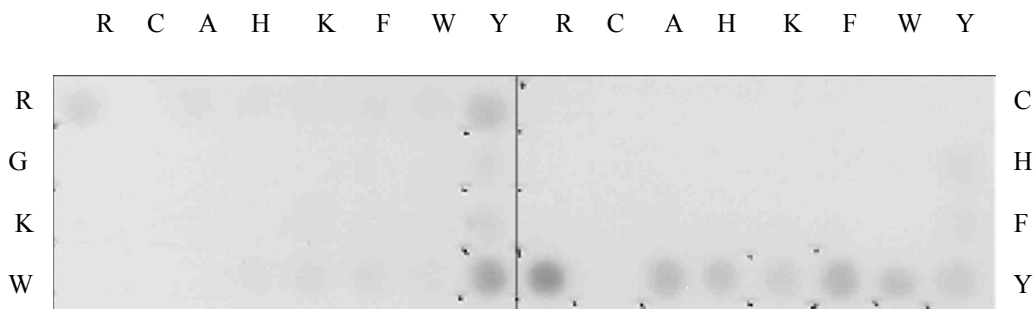
Fig. 3.26: B) ECL blot (W540 membrane) of non-glycated tripeptide library incubated with anti-mouse-POD (1:5000) IgG. The secondary antibody shows some affinity towards non-modified tyrosine and arginine (faint). 1st (C-terminus) amino acids are shown on the left- and right- hand columns and 2nd (N-terminus) amino acids are shown on the top rows.
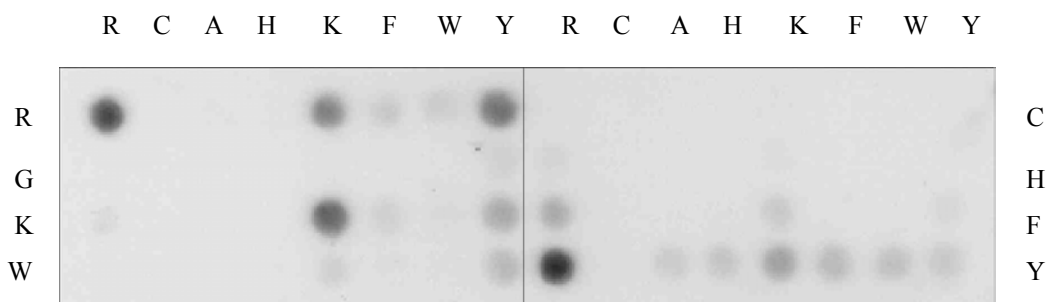
Fig. 3.27: A) ECL blot (W540 membrane) of non-glycated tripeptide library incubated with the anti-AGE (K1935) (1:5000) antibody, showing immunodetection of lysine, arginine and tyrosine residues, which were actually recognised by the anti-rabbit (1:5000) IgG. 1st (C-terminus) amino acids are shown on the left- and right- hand columns and 2nd (N-terminus) amino acids are shown on the top rows.
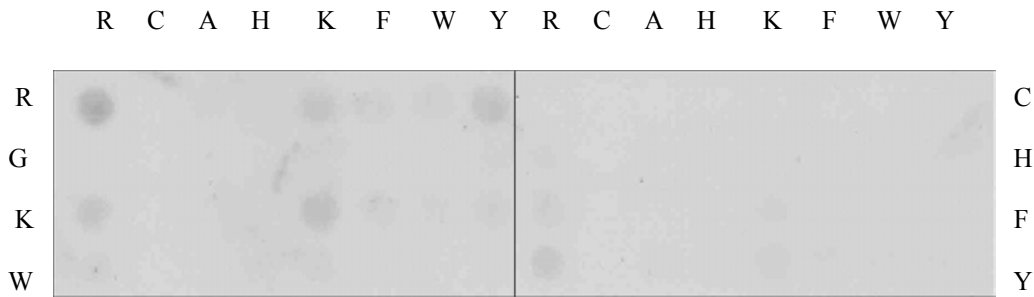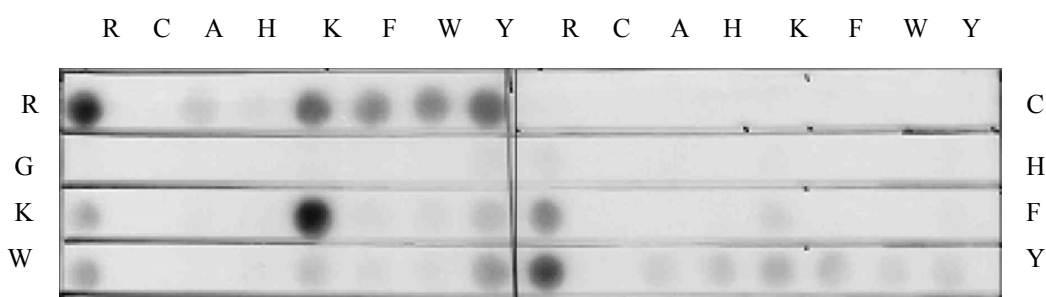

Fig. 3.27: B) ECL blot (W540 membrane) of non-glycated tripeptide library incubated with the anti-rabbit (1:5000) IgG, showing immunodetection of lysine, arginine and tyrosine residues. 1st (C-terminus) amino acids are shown on the left- and right- hand columns and 2nd (N-terminus) amino acids are shown on the top rows.

3.3.4 Stability of ^{14}C-labeled SPOTS

The stability of anchoring peptides to the solid phase support (membranes) was determined by measuring the specific reactivity of ^{14}C-acetylated spots. Whereas APEG membranes can be considered essentially stable (maximal loss of ^{14}C-acetylated glycated peptides was 13 % at 37 °C, and 22 % at 50 °C) , W540-βAla membranes lost up to 76 % in PBS, pH 7.4 and more than 50 % after 24 h at 50 °C or up to 85 % after 96 h in 0.4 M phosphate buffer, pH 7.5. Nevertheless the remaining percentage of glycated peptides appeared to be fixed (by crosslinking during glycation) and of sufficient quantity to allow immunodetection. The results for the stability of spots under various conditions is summarised in Table 3.10.

Table 3.10 – Comparison of the stabilities of APEG and W549 membranes during the various conditions for glycation and immunoblotting

CONDITIONS	STABILITY OF APEG-MEMBRANES	STABILITY OF W540B MEMBRANES
In "block bufffer" (PBS-0.1 % Tween, 5 % BSA, pH 7.4), 96 h	100 %	92 %
After 4 antibody assays and 4 times stripping in "stripping buffer"	1. non-glycated: 100 % 2. glycated, pH 7.5: 96 %	1. non-glycated: 80 % 2. glycated, pH 7.5: 24 % (0.02 M loading : 43 %)
During and after glycation in 0.4 M phosphate buffer, pH 7.5 at 37 °C at 50 °C	 after 24 h: 94 %; 96 h: 87 % after 24 h: 96 %; 96 h: 78 %	 after 24 h: 77 %; 96 h: 55 % after 24 h: 42 %; 96 h: 15 %

4. DISCUSSION

4.1 AGE-mediated oxidative stress in the ageing and diseased brain

The brain is particularly susceptible to oxidative damage, owing to its high rate of oxygen consumption, high rate of glucose turnover, high content of polyunsaturated fatty acids and elevated levels of the redox-active iron in certain regions (Samson and Nelson, 2000). Moreover, there are relatively low levels of antioxidants such as glutathione and vitamin E and antioxidant enzymes such as GSH peroxidase, catalase and superoxide dismutase (Schulz *et al.,* 2000). An impairment of the glutathione antioxidant system and mitochondrial function and an increased iron load are reported to occur in the AD (Mecocci *et al.,* 1997; Sayre *et al.,* 2000) and PD (Grunblatt *et al.,* 2000) brains. These factors contribute to a state of oxidative stress, creating an ideal environment for the formation of AGEs. Indeed, the AGEs CML, pentosidine (Kimura *et al.,* 1998; Takeda *et al.,* 1998) and pyrraline (Smith *et al.,* 1994) have been immunohistochemically localised in the AD brain. AGE formation is not only a marker of oxidative stress, but AGEs themselves may mediate the production of reactive oxygen intermediates (Kislinger *et al.,* 1999; Schmidt and Stern, 2000).

4.2 AGEs induce NO production in J774A.1 macrophages and N-11 microglial cells

NO is a small, diffusable molecular messenger in the central nervous system. Unlike conventional neural transmitters, NO is not stored in synaptic vesicles, but rather is synthesized on demand. As a free radical, NO reacts readily with other species containing unpaired electrons. For instance, NO reacts with metalloproteins such as cis-aconitase, thus regulating cellular iron metabolism (Miranda *et al.,* 2000). NO also reacts with the superoxide anion to produce peroxynitrite ($ONOO^-$), a potent oxidant (Fig 4.1). Peroxynitrite mediates most of the cytotoxic effects following overproduction of NO by inducing membrane lipid peroxidation (Rubbo *et al.,* 1994), nitration of tyrosine residues (Souza *et al.,* 1999) and oxidation of DNA (Burney *et al.,* 1999*).*
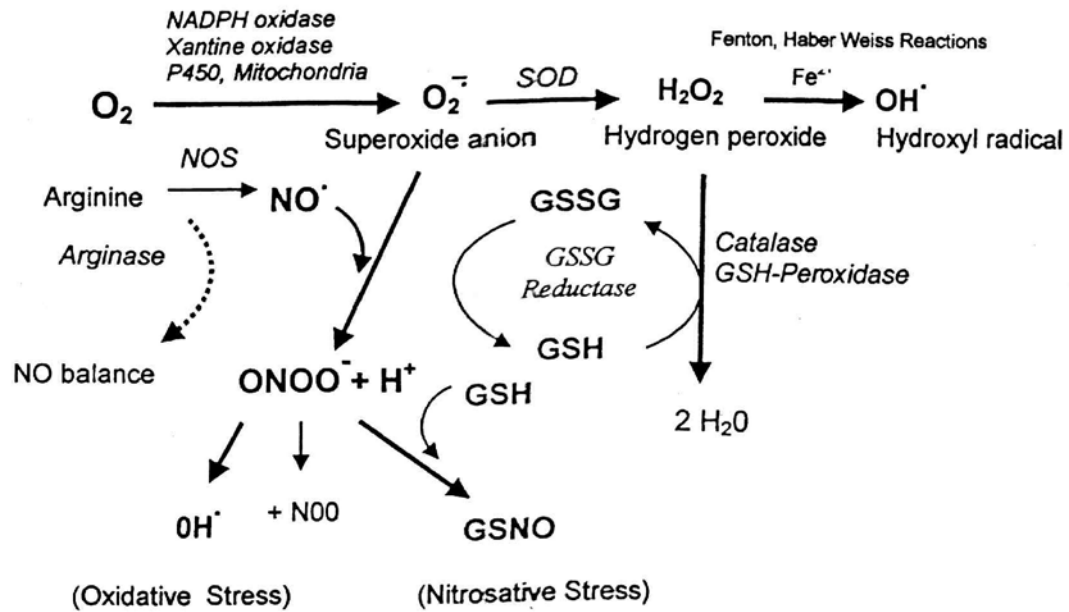
Fig.4.1: Major pathways for oxygen and nitrogen species. Reduction of oxygen leads to the formation of the highly reactive hydroxyl radical, via the superoxide anion and hydrogen peroxide. The hydroxyl radical is also formed by the decomposition of peryoxynitrite (ONOO⁻), which occurs by the reaction of nitric oxide with superoxide. An imbalance in the cellular concentration of antioxidant enzymes, such as superoxide dismutase (SOD), catalase and GSH peroxidase and of the glutathione redox system (GSH and GSSG reductase) results in oxidative stress. Peryoxynitrite reatcs with sulphydryl groups, such as in proteins and glutathione to cause nitrosative stress.

The reaction of NO with thiol groups modifies the activity of several enzymes intracellular content of thiols, which is a critical factor in determining the sensitivity of cells to nitrosative stress. Since brain mitochondria contain relatively large stores of glutathione, a depletion of these stores due to the action of NO or peroxynitrite may greatly affect chain respiratory activities and energy thresholds. A role for mitochondrial dysfunction in neurodegeneration is supported by decreased activities of cytochrome c oxidase (complex IV) in AD (Davis *et al.,* 1997) and of NADH dehydrogenase (complex I) in PD (Schapira, 2000).

The results obtained from this study confirm the notion that glycation / AGE formation on proteins is an important modification, which triggers the activation of immune-competent cells such as microglia and macrophages. This activation was evident by a significant increase in the production of NO, measured as nitrite in the cell medium, following incubation of J774A.1 macrophages and N-11 microglia with BSA-AGE (2 μM). A 17 fold- and 12 fold-increase in NO production was measured in of J774A.1 macrophages and N-11 microglia, respectively. This is consistent with the finding that

glycated albumin induces the production of NO in endothelial cells (Amore *et al.,* 1997). Amore et al. measured a 16- fold increase in NOS activity, using the ^{3}[H] citrulline assay, and an induction of mRNA iNOS in murine endothelial cells after incubation with Amadori adducts of human serum albumin (HSA, 35 mg/ml). Both BSA-AGE and LPS (50 µg/ml), a well-known mediator of oxidative stress in murine astrocytes (McNaught *et al.,* 2000), murine microglia (Possel *et al.,* 2000) and human monocytes (Cohen *et al.,* 2001), caused maximal production of NO in N-11 microglia.

4.3 Glycation precursors and oxidative stress

α-Oxoaldehydes react with lysine and arginine residues in proteins to form AGEs (Thornalley, 1998). Exposure of cells to high concentrations of α-oxoaldehydes (Kang *et al.,* 1996) or inhibition of detoxification with a specific inhibitor (Thornalley, 1996) results in growth arrest and toxicity. Elevated intracellular concentrations of the α-oxoaldehydes MG and 3-DG have been shown to contribute to oxidative stress in murine $P388D_1$ macrophages (Abordo *et al.,* 1999). However, in the present study, MG and 3-DG did not induce NO production in N-11 microglia, following a 24 h incubation. This lack of effect was not due to cytotoxicity of MG at concentrations between 0.4 - 10 µM, nor of 3-DG (0.4 - 250 µM), as determined by the MTT assay. MG and 3-DG have been shown to have neurotoxic effects on rat neurons, with lethal concentrations (LC_{50}) of 130 µM for MG and 209 µM for 3-DG (Kikuchi *et al.,* 1999). MG (10 µM) has been shown to induce the production of reactive oxygen species (ROS) in U937 human monocytes (Okado *et al.,* 1996) and rat aortic smooth muscle cells (Che *et al.,* 1997). Apoptosis of U937 monocytes was reported to occur at concentrations between 10 – 300 µM for MG and 10 – 1000 µM for 3-DG (Okado *et al.,* 1996). However, only minimal changes in the cellular concentration of glyoxalase, the enzyme responsible for the detoxification of MG, were measured.

HSA modified by MG (HSA-MG) has been reported to stimulate the synthesis and secretion of macrophage-colony stimulating factor (Abordo *et al.,* 1996) and TNF-α (Abordo *et al.,* 1997) in human THP-1 monocytes. In the present study, MG was modified with BSA (BSA-MG) to test whether it could cause an induction of NO compared with MG alone. However, there was no significant increase in the production of NO by N-11 microglia. The disrepancy in the results reported here with those of Abordo et al. could be accounted for by several factors. Abordo et al. used a human monocyte cell line, whereas a murine microglia cell line was used in this study. The THP-1 monocytes are also likely to

express different receptors for AGE than the N-11 microglia, resulting in differences in AGE-induced signal transduction. In addition, different cell types possess different protection mechanisms against oxidative stress and the cellular concentrations of glyoxalase play a crucial role in determining the ability of cells to cope with an increased oxidative stress.

4.4 Oxidative stress in AD – a glycation link?

The detection of AGEs within and around the senile plaques and neurofibrillary tangles in the AD brain is consistent with previous reports (Smith *et al.,* 1995; Dickson *et al.,* 1996; Ko *et al.,* 1999) and suggests that AGEs are involved in the pathogenesis of this disease. Modification of paired helical filament tau, the principal component of neurofibrillary tangles, promotes aggregation insolubility and protease resistance (Gonzalez *et al.,* 1998; Ledesma *et al.,* 1998). In addition, glycated recombinant tau is capable of inducing the generation of free radicals via NFkB in SK-N-SH neuroblastoma cells (Yan *et al.,* 1995). There is evidence showing a greater amount of protein carbonyls present in AD compared with age-matched control brains (Smith *et al.,* 1997) and a close correlation between carbonyl levels and NFT density (Hensley *et al.,* 1995). Aß, the major protein component of senile plaques, is also considered to play a crucial role in the pathogenesis of AD.

4.4.1 AGE-Aß, but not the unmodified peptide, induced NO production in N-11 microglia

In this study it was shown that AGE-modified ßA4 induced a more pronounced production of NO in N-11 microglia cells than ßA4 alone. The higher potency of ßA4-MG compared with ßA4-Glc in terms of NO production was most likely caused by a different product distribution in the AGE preparation. These results are similar to those of Abordo *et al,* where stimulation of TNF-α and synthesis of M-CSF in THP-1 monocytes was shown to be higher with HSA-MG compared with HSA-Glc (Abordo *et al.,* 1996). The higher NO production induced by ßA4-MG compared with ßA4-Glc might also be biochemically relevant as MG, despite its low concentration in the cell**,** has a much higher reactivity than glucose. Since MG is detoxified by the glutathione-dependent glyoxalase system, formation of α-oxoaldehydes - derived AGEs is accelerated under conditions where cellular concentrations of glutathione are low, such as oxidative stress or energy depletion (Thornalley, 1998). Both the accumulation of NO, evident from increased amounts of

nitro-tyrosine-modified proteins (Smith *et al.,* 1997*;* Hensley *et al.,* 1998) and AGEs are found in the AD brain. Numerous studies suggest a correlation between oxidative stress in the AD brain, caused by an overproduction of free radicals including NO, and the formation of AGEs (Markesbery, 1999; Akiyama *et al.,* 2000). The formation of AGEs is complex and requires oxidative conditions and, in the latter reactions, generates reactive oxygen species. Hence, oxidative stress conditions are both a prerequisite and a consequence of AGE accumulation.

4.4.2 AGE- ßA4 produced a more potent effect than unmodified, fibrillar ßA4

Results from this study suggest that modification of ßA4 by AGEs stimulates NO production in N-11 microglia more potently than the unmodified, fibrillar peptide. In this study, only minimal levels of NO were detected after incubation of microglia with ßA4 (1-40), compared with significant levels recorded by Goodwin *et al* (1995), Meda (1995), and Ii *et al* (1996). However, these effects were due to a synergistic action of the ßA4 peptide and IFN-γ or LPS. In addition, immunohistochemical data showing co-localisation of AGE and ßA4 but not iNOS and ßA4 in glia of AD brains suggests that AGEs may induce a more pronounced activatory effect than ßA4 alone.

Although a direct pro-inflammatory effect of ßA4 has been reported (Klegeris *et al*., 1997; Weldon *et al.,* 1998; Akama and Van Eldik, 2000), this idea is supported by analysis of the inflammatory processes in transgenic mice (Tg2576) expressing high levels of the Swedish double mutation of human amyloid precursor protein. These mice progressively develop typical (AGE free, unpublished observation) amyloid plaques in cortical brain regions including gliosis and astrocytosis. Only IL-1ß, but none of the other cytokines including IL-1α, IL-1 receptor antagonist, IL-6, IL-10, IL-12, IL-18, IFN-γ, and macrophage migration inhibitory factor mRNA were found to be induced (Mehlhorn *et al*., 2000). The notion that AGE-modified-ß-amyloid induces a much greater nitroxidative stress to surrounding cells than unmodified ß-amyloid provides an explanation for the minor neuronal losses and inflammatory changes and radical damage observed in transgenic mice overexpressing the human mutant amyloid precursor protein compared to the AD brain (Sturchler-Pierrat *et al.,* 1997; Holcomb *et al.,* 1999). From this study, it is proposed that an AGE-induced upregulation of iNOS expression could contribute to an increased level of oxidative stress, neuronal damage and functional loss in the AD brain. Although ßA4 activates some transduction factors such as NF-κB, it appears that AGEs are more potent inducers of an intricately regulated immunorelevant gene such as iNOS.

4.4.3 AGEs induce iNOS in N-11 microglia

The synthesis of NO occurs during the oxidation of the L-arginine to L-citrulline (Mayer and Hemmens, 1997) and is catalysed by the nitric oxide synthase (NOS) family of enzymes. Activation of NOS requires various factors and co-factors, including tetrahyropterin (BH4), NADPH, FAD, and FMN (Fig 4.2). In the present study it was shown that iNOS mRNA and enzyme activity could be induced by BSA-AGE in a time-dependent manner in N-11 microglia cells. Hence, AGEs induce the production of NO by upregulation of the expression of iNOS and thus cause a persistent increase in NO generation (nitroxidative stress). This could have possible detrimental effects on the energy production in mitochondria of adjacent neurons (Heales *et al.,* 1999). The relevance of AGE-induced iNOS expression can be explained on the transcriptional level, as the mouse macrophage iNOS gene promoter contains several binding sites for LPS-related and interferon (IFN)-related response elements. LPS-inducible factors include NF-κB, AP-1, IFN-γ - response element and Stat1 (Lowenstein, 1993; Gao *et al*., 1998). The identical transcription factors, NF-κB (Hattori *et al.,* 1999), AP-1 (Iwashima *et al.,* 2000) and Stat-1 (Huang *et al.,* 1999) are also upregulated by AGEs. In humans, the iNOS gene is regulated in a similar manner, here IFN-γ, IL-1β and TNF-α have been found to regulate two AP-1 sites and an upstream NF-κB site (Chu *et al.,* 1998).
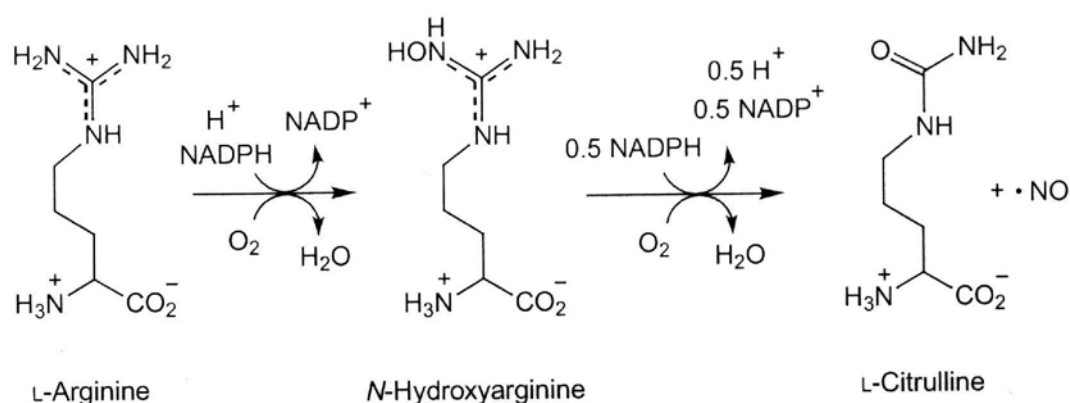

Fig 4.2: The reaction of nitric oxide synthases to form nitric oxide (NO).

4.4.4 AGEs are co-localised with iNOS in the AD brain

The finding of AGE accumulation in astrocytes, microglia and neurons in the AD brain is in agreement with previous reports (Dickson *et al.,* 1996; Takeda *et al.,* 1996; Takeda *et al.,* 1998). Furthermore, the detection of reactive microglia directly adjacent to AGE-positive neurons provides further evidence for a critical role of these cells in the degeneration of vulnerable neurons in AD. Hence AGE accumulated in neurons could be one source of AGE-induced activation of microglia, resulting in the generation of free radicals and cytokines (Iida *et al.,* 1994; Finch and Cohen, 1997; Thornalley, 1998,) and further neuronal damage. The presence of AGEs in neurons may not only cause injury via microglial activation, but also via a direct cytotoxic effect (Loske *et al.,* 1998). In addition, disturbances are seen in lysosomal protein degradation in human AD pyramidal neurons, where endosomal enlargement contributes to a larger total endosomal volume per neuron (Cataldo *et al.,* 1997), concomitantly with an increased AGE load in this cell type (Li *et al.,* 1994).

Co-localisation of AGE and iNOS in astrocytes and microglia cells not only supports a role for AGE in nitrooxidative stress in the AD brain (Finch and Cohen, 1997, Münch *et al.,* 1998a; Thornalley, 1998), but also a pathway for AGE-induced activation via the upregulation of iNOS. In the present study, AGEs were localised mainly in astrocyte processes, whereas iNOS-immunoreactivity was found in both the processes and soma of astrocytes. It is conceivable that AGEs in the processes cause oxidative stress, which is transduced to the soma to activate iNOS. Thus indicating the necessity of a mediator of AGE activation, which is most likely reactive oxygen species. This finding is in agreement with the notion that AGEs induce oxidative stress (Yan *et al.,* 1995; Bierhaus *et al.,* 1998, Li *et al.,* 1998, Thornalley, 1998; Mohamed *et al.,* 1999), which, as this study suggests, may involve the expression of iNOS. Accordingly, the importance of AGEs in nitrooxidative stress was confirmed by the lack of iNOS-positive staining astroglia in the absence of AGE reactivity.

4.4.5 Role of glial cells in producing NO in the AD brain

Microglia cells are derived from the mononuclear phagocytic system and comprise approximately 20 % of the total glial population in the CNS (Kreutzberg, 1996). They become highly activated during inflammation and although capable of phagocytosis, microglia principally respond by secreting free radicals and cytokines (Giulian *et al.,* 1999), thus destroying neighbouring neurons and their processes. Microglia have been

implicated to play an important role in the neuroinflammatory processes which accompany AD. For instance, in this study activated (AGE positive) glia were shown surrounding ß-amyloid (AGE-positive) plaques, in the AD brain. This is consistent with previous reports (Dickson *et al.,* 1996; Smith *et al.,* 1996). Moreover, the detection of ßA4 fibrils in the endoplasmic reticulum and in deep infoldings of the cell membranes of microglia associated with ß- amyloid plaques was demonstrated by Frackowiak *et al.,* (1992) suggests a role for microglia in the deposition of ßA4 in the AD brain. In addition, activated microglia are proposed to play a pivotal role in the transformation of diffuse (non-pathological) amyloid deposits into mature/neuritic plaques (Maal-Schiemann *et al.,* 1994; Sheng *et al.,* 1997). As well as microglia, astrocytes have been suggested to be a major source of NO in the human brain (Komori *et al*., 1998; Akama and Van Eldik, 2000).

From the results reported here, it is suggested that an upregulation in the expression of iNOS occurs in astrocytes and, to a lesser extent, in microglia in the AD brain. Astrocytes are derived from the neuroectoderm of the neural tube and constitute the most numerous cellular population of the central nervous system. A variety of functions have been assigned to astrocytes, including the guidance of neurons during development, the uptake metabolism and compartmentalisation of neurotransmitters, the control of blood-CNS exchanges, phagocytosis and the secretion of cytokines and neurotrophic factors (Rutka *et al.,* 1997). Furthermore, immunohistochemical data from this study shows that astrocytes immunoreactive for AGE and iNOS mainly appeared around mature but not diffuse β-amyloid plaques in the AD brain. This supports the notion that astrocytosis may be a secondary rather than a primary feature during plaque development (Wiegel *et al.,* 2000) in AD.

It is well established that astrocytes and microglia can be induced by various cytokines or (when stimulated) by β-amyloid to express iNOS *in vitro* (Meda *et al.,* 1995; Komori *et al*., 1998; Akama and Van Eldik, 2000). Although the production of NO via the activation of iNOS from astrocytes in the human brain is widely accepted (Morgen *et al.,* 2000; Sasaki *et al.,* 2000), the expression of iNOS in human microglia is controversial. Some authors claim that the expression of iNOS occurs in human astrocytes but not in reactive microglia (Liu *et al.,* 1996; Wallace *et al.,* 1997; Zhao *et al.,* 1998). Contrary to this view, the immunohistochemical results of this study as well as other studies support a role for microglia in producing NO in the human brain. For instance, *in vitro* induction of NO has been reported in the CHME-5 human microglial cell line (Edwards *et al.,* 2000).

Moreover, iNOS activity in microglia has been reported in cases of ischaemia (Love *et al.,* 1999), oedemia (Ludwig *et al.,* 2000), multiple sclerosis (De Groot *et al.,* 1997¸Hooper *et al.,* 1997) and in brains infected with the human immunodeficiency virus (HIV) (Rostasy *et al.,* 1999). Despite the functional differences for iNOS between mice and human, it is possible that human microglia can be induced to express iNOS and generate NO, particularly in light of their role in secreting free radicals and inflammatory cytokines.

We did not observe any iNOS-positive neurons in AD nor control temporal cortices. This is in agreement with Wallace *et al.* (1997) and Lüth *et al.* (2000), who demonstrated iNOS in astrocytes but not neurons in the AD brain. Vodovotz *et al.* (1996), however, reported the presence of iNOS in AD tangle-bearing neurons but not astrocytes.

The results from this study support the finding that an autodestructive process, involving both overactive microglia and astroglia producing high levels of free radicals occurs at the characteristic lesions in AD (Akiyama *et al.,* 2000). Since AGEs accumulate in astrocytes, microglia and on β-amyloid plaques in AD, they may increasingly contribute to oxidative stress, evident by the co-localisation of AGE and iNOS in these glial cells. Thus an interesting future task would be to systematically compare the capability of AGEs vs βA4 in inducing iNOS and cytokine expression in different cell types of different species.

Little is known about the mechanism of AGE-mediated activation of NO in microglia. However, several receptors for AGEs have been isolated, including AGE-R1 (80K-H/p90), AGE-R2 (OST/p48), AGE-R3 (galectin-3), macrophage scavenger-receptor (MSR), and a receptor for AGEs (RAGE) (Li *et al.,* 1998; Schmidt and Stern, 2000) (Fig. 4.3). The experiments in this study show that RAGE is expressed by N-11 microglia. This is supported by the immunodetection of RAGE in both glial cells and neurons in the AD brain (Yan *et al.,* 1996; Sasaki *et al.,* 2001). Furthermore, engagement of RAGE by Aβ is reported to induce oxidative stress in microglia (Yan *et al*., 1997). Taken together, the results reported here support an involvement of RAGE in the induction of oxidative stress in microglia. There is still some controversy whether RAGE is the specific receptor for both ßA4 and AGEs, causing activation of identical signaling pathways. This controversy is based on such findings that ßA4 is toxic in cells lacking RAGE (Liu *et al.,* 1997) and that antioxidants which block RAGE signalling are not necessarily protective against ßA4 toxicity (Pike *et al.,* 1997). It is also unclear whether other possible receptors participate in AGE-induced signalling in microglia. For instance, an AGE-induced enhancement of the MSR has been reported in THP-1 monocytes (Iwashima *et al.,* 2000).
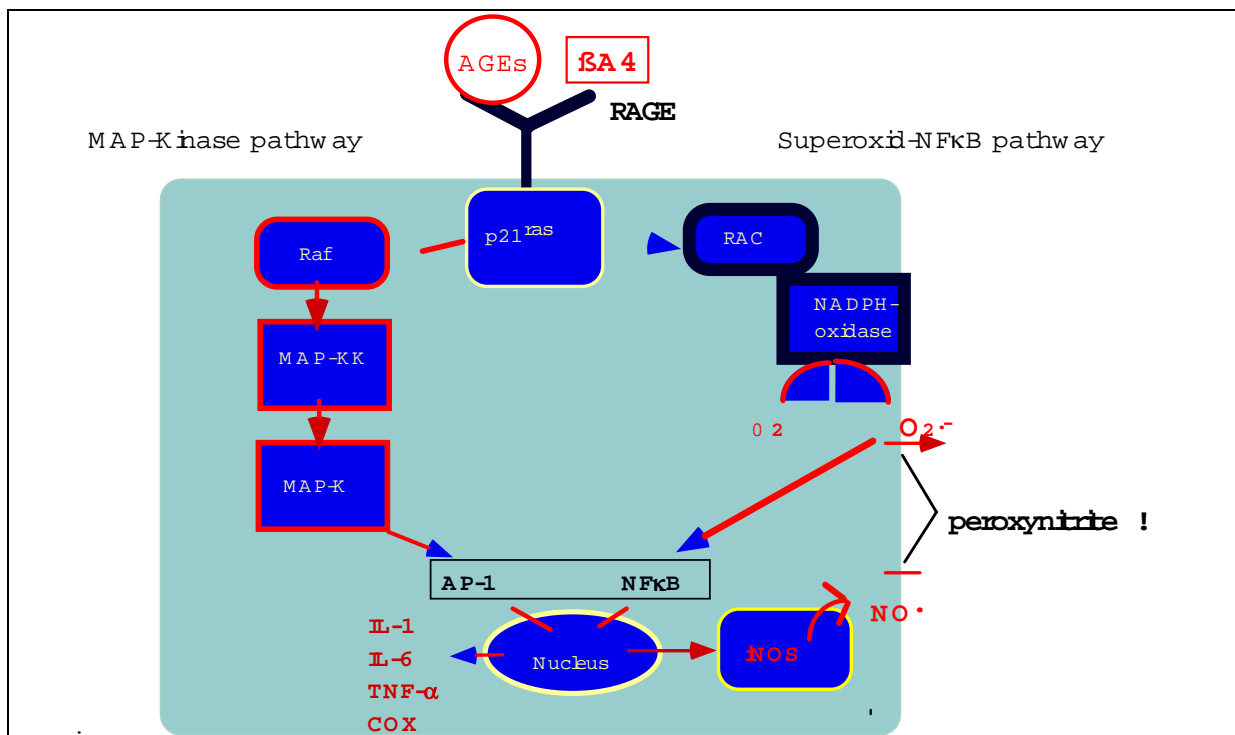
Fig. 4.3: Schematic sketch of the AGE/ßA4 signaling cascade

4.5 AGEs in PD

Recent findings indicate that AGEs are the major structural crosslinkers which cause the transformation of soluble cytoplasmic proteins to insoluble deposits, including the Lewy bodies in PD (Castellani *et al.,* 1996). Since AGE formation is accelerated by transition metals such as iron, and iron levels are increased in PD (Grunblatt *et al.,* 2000), AGE formation is likely to be increased under the conditions of oxidative stress found in the SN of PD patients. In this study, AGEs and α-synuclein were found co-localized in very early Lewy bodies in the brains of patients diagnosed with incidental Lewy body disease. These cases might be viewed as pre-PD, i.e. patients who presented with Lewy bodies without the development of clinical signs of PD. AGEs are both markers of transition metal induced oxidative stress as well as inducers of protein crosslinking and free radical formation by chemical and cellular processes. Thus it is likely that oxidative stress and AGEs participate in very early steps of Lewy body formation and resulting cell death in PD. This is supported by increased levels of the NF-κB-regulated gene products interleukin-6, and TNF-α in the PD brain (Bessler *et al.,* 1999). In addition, some AGE structures bind at least three times more transition metals such as iron and copper as the non-glycated proteins. Furthermore, the bound metal retains redox activity and participates in the catalytic oxidation of reactive sugars (Qian *et al.,* 1998). Reactions mediated by

these chelates may become involved in radical damage in PD, should similar "glycochelates'" form *in vivo* on Lewy bodies. An acute decrease in cellular glutathione, as occurs very early in PD, also leads to a decreased *in situ* activity of glyoxalase I, accumulation of β-oxoaldehydes and AGE-mediated crosslinking of cytoskeletal proteins (Thornalley, 1998). In summary, AGEs may be involved not only in the physical crosslinking of Lewy bodies, but also in the creation of intracellular oxidative stress as a disease-promoting factor. This is evident by the co-localisation of oxidative stress markers in Lewy bodies in the PD brain (Castellani *et al.,* 1996). Preventative treatment with antioxidants might thus become a promising therapy for the prevention of Lewy body formation and subsequent neurodegeneration.

4.6 Membrane permeable antioxidants as anti-inflammatory agents and inhibit radical amplification

In redox-active intracellular signal transduction, superoxide anions (or their conversion products, such as hydrogen peroxide and hydroxyl radicals) act as messengers to upregulate cytokine expression. Thus, membrane permeable antioxidants which inhibit the upregulation of cytokines or radical producing enzymes, could also be regarded as anti-inflammatory agents (Sano *et al.,* 1997; Roy and Packer, 1998; Behl *et al.,* 1999). This study shows that various members of this drug class are capable of inhibiting AGE-induced iNOS upregulation and NO synthesis.

4.6.1 Estrogen

The prevalence of AD is higher in women, even after taking their longer life span into account (Lautenschlager *et al.,* 1996). Although estrogen replacement therapy has been inversely correlated with prevalence and severity of AD (Henderson *et al.,* 2000), the exact mechanisms of estrogen-related neuroprotection are not known. In this study, nanomolar concentrations of 17ß-estradiol effectively blocked AGE-induced expression of iNOS in N-11 microglia. These results are consistent with previous reports showing 17ß-estradiol-induced decreases in the expression of iNOS in N9 microglia (Bruce-Keller *et al.,* 2000) and smooth muscle cells (Saito *et al.,* 1999). The potency of 17β-estradiol is most likely due to its small size, lack of charge and amphiphilic properties. Two types of estrogen receptors (ER) have been identified, an alpha (ERα) and a beta (ERβ) receptor. Both receptors are present in microglia (Mor *et al.,* 1999) and neurons (Nilsen *et al.,* 2000) and a MAPK pathway has been shown to mediate the anti-inflammatory effects of estrogen

in these cells (Singer *et al.,* 1999; Bruce-Keller *et al.,* 2000). However, the precise role of these receptors is unclear and although microglia express ERs, a receptor-independent action of estrogen in the human brain has been indicated (Behl *et al.,* 2000; Li *et al.,.* 2000; Bruce-Keller *et al.,* 2000).

4.6.2 *Gingko biloba* EGb 761

Extracts of the leaves of *Gingko biloba* (Egb) were introduced in Europe in 1965 for the treatment of peripheral arterial occlusive disease and dementia (De Veudis, 1991; Kleijnen and Knipschild, 1992). EGb is a complex containing 24 % flavonoid glycosides, 6 % terpene lactones, such as the ginkgolides A, B, C, J and bilobalide (De Veudis, 1991) In this study, a dose-dependent inhibition of an AGE-induced expression of iNOS in N-11 microglia was shown. The results with *Gingko biloba* extract EGb 761 provide one of the biochemical explanations to the clinical benefits of this drug, reported to improve cognitive functions of AD patients (Maurer *et al.*, 1997; Oben *et al.,* 1998). In particular, the terpene and flavone constituents of *Gingko biloba* are described as having antioxidative (Nathan *et al.*, 2000) and apoptotic qualities (Ahlemeyer *et al.,* 1999). The flavonoid glycosides have been shown to scavenge hydroxyl radicals, superoxide anions, whereas the terpene lactones preferentially scavenge superoxide anions (Nathan *et al.*, 2000). Moreover, ginkgolides B and J and bilobalide, but not ginkgolide A reacts with the superoxide anion (Scholtyssek *et al.,* 1997). Interestingly, the flavones bear close structural similarity to estradiol, which relies on the hydroxyl function on an intact phenolic A ring for its neuroprotective effects (Moosmann *et al.*, 1997).

4.6.3 Thioctic (α-lipoic) acid

R-(+)-thioctic acid is present as a cofactor in pyruvate and ketoglutarate dehydrogenase and has been detected in various natural sources including edible plant and animal products (Bustamante *et al.,* 1998). The reduced form of thioctic acid, dihydrolipoate, is a potent antioxidant, able to raise intracellular glutathione levels and attenuate redox-active signalling (Roy and Packer, 1998). N-acetylcysteine can also be absorbed from the diet and functions as an antioxidant by providing cysteine for glutathione synthesis (Holdiness *et al.,* 1991). The results in this study show that R-(+)-thioctic acid effectively inhibited ($IC_{50} = 500$ μM) an AGE-induced expression of iNOS and consequent production of NO in N-11 microglial cells. Furthermore, R-(+)-thioctic acid prevents AGE-mediated activation of NFkB in endothelial cells (Bierhaus *et al.,*

1997). The significant shift between the two curves for inhibition of NO and iNOS synthesis could be caused by a reaction of dihydrolipoate with NO, resulting in nitrosothiol formation. R-(+)-thioctic acid is capable of scavenging hydroxyl radicals, NO and peroxynitrite and dihydrolipoate additionally scavenges superoxide (Whiteman *et al.,* 1996). Dihydrolipoate is reported to have a low toxicity and is used in the treatment of patients with diabetic neuropathy (Androne *et al.,* 2000). The benefits of R-(+)-thioctic acid in improving some of the symptoms associated with AD are currently being tested (Henriettenstiftung, unpublished observations). Although N-acetylcysteine also inhibited sn AGE-induced production of NO, a much higher concentration (mM) was required for comparable effects. This has also been confirmed by other work (Merin *et al.,* 1996; Sen and Packer, 2000) and is mainly due to the ability of R-(+)-thioctic acid to utilise the activity of enzymes present in the human cell to continuously regenerate dihydrolipoate.

4.6.4 N-tert.-butyl-α-phenylnitrone (PBN)

PBN, a stable nitrone radical, has been described to inhibit free radical mediated events such as streptozotocin induced NF-κB activation and cytokine induced NO synthase expression in rats (Tabatabaie *et al*., 2000). Oxidative damage in the gerbil brain is reported to be reversed by chronic administration of PBN (Carney and Floyd, 1994). Since PBN reduced both AGE-induced iNOS expression and NO generation in N-11 microglia, spin traps could be used as modulators of redox-sensitive signal transduction. The mechanism of action of this spin trap does not appear to rely on its general free radical trapping ability *per se*, but rather in the suppression of genes induced by pro-inflammatory cytokines such as iNOS (Kotake *et al.,* 1998). However, as the inhibition detected in our study was only partial, more potent analogues need to be developed.

4.7 Combinatorial approaches to immunogenic AGE-structures. Characterization of anti-AGE antibodies with glycated peptide libraries on cellulose membranes (AGE-peptide spot libraries).

4.7.1 W540 versus APEG membranes

For the experiments with spot libraries, two types of solid-phase supports were used: conventional cellulose (W540) membranes and amino-polyethylene glycol (APEG) derivatized cellulose membranes. In comparison with the APEG membranes, the capacity and stability of peptides on W540 membranes was lower and extremely variable. The ßAla-ester bond is chemically unstable between pH 7.4 - 7.5, at increasing buffer concentrations (general acid-base catalysis) and at high temperatures. Hence, the ester bond to cellulose could be considered as one source of instability. The low yield of glycated peptides on W540B membranes was most probably caused by a loss of peptides from the membranes during glycation due to "high" pH (7.5) and high temperatures (50°C). For instance, Diem, Palm and Herderich found an increased labeling of tryptophan and histidine at pH > 5 (S. Diem, PhD thesis, Universität Würzburg, 2001).

Differences observed between W540 and APEG membranes could also arise from different proportions of the more stably glycated peptides compared to unchanged peptides. Results from the autoradiographs revealed more glycated peptides on APEG membranes. In addition to lysine and cysteine, other glycated amino acids detected on APEG membranes were arginine, asparagine, histidine and the aromatic amino acids. This could be due to the higher yield of peptide synthesis and peptide glycation on these membranes. However, despite the very low yields of glycated peptides on W540 membranes, undetected on autoradiographs, there were sufficient differences compared with unmodified peptides to allow immunodetection of the derivatized spots. In summary, although APEG membranes are more costly, the advantages in their reproducibility and stability outweigh the former. To maximise their use, an arrangement of two libraries consisting of 12 x 12 amino acids was produced on one APEG membrane. A further advantage of APEG over W540 membranes is that the conditions at which the APEG membranes can be applied (pH and temperature) are more physiological.

4.7.2 Relative reactivities of sugars with dipeptide library

The reactivities of the sugars with the peptide libraries displayed a pattern of symmetry, hence showing glycation of one amino acid, either at the C- or N- terminus. In

addition to glucose, the reducing sugar ribose was investigated for its reactivity with amino acid side chains. Glycation with ribose is a faster reaction (12 – 24 h) compared with glucose (weeks or months) and has been used in *in vitro* kinetic studies on the inhibition of AGE formation (Booth *et al.,* 1997; Khalifah *et al.,* 1999).   In the present work, "interrupted" glycation with ribose generally produced higher yields of stably glycated peptides than with glucose.

Both glucose and ribose bound to the amino acid side chains of cysteine, lysine and arginine on the peptide library. In addition, ribose reacted with the side chains of histidine and asparagine. The reactivity of side chains is largely determined by the availability of thiol groups (cysteine), primary amino groups (lysine), and, to a lesser degree, guanidino groups (arginine) or imidazolyl groups (histidine) and amides (asparagine). Amide groups in amino acid amides such as in asparagine are less nucleophilic than primary amino groups in lysine and react much slowlier. It was assumed that the indol residue in tryptophan is also subject to reactions with glucose. The formation of Amadori or Heyn's products from lysine and arginine is well understood and involves a common pathway. This is initiated by the reaction of a reducing sugar with the amino group of lysine to generate an Amadori product and, following dehydration, cross-linking intermediates. The guanidinium group of arginine then traps dicarbonyl moeities to produce a stable, covalent crosslink. For instance, the AGE precursors glyoxyl, MG and 3-DG are known to react preferentially with lysine and arginine residues. The reaction of glyoxyl with lysine residues forms CML and pentosidine (Wells-Knecht *et al.,* 1995). The reaction of MG with lysine and arginine residues results in the formation of CEL, MOLD and imidazolone derivatives (Ahmed *et al.,* 1997; Oya *et al.,* 1999). The reaction of 3-DG with arginine, then with lysine residues leads to the formation of pyrraline, pentosidine, CML and imidazolone (Niwa and Tsukushi, 2001). Pentosidine is also formed by the reaction of ribose first with a lysine residue on proteins to form an Amadori product, which then reacts with an arginine residue (Sell *et al.,* 1992).

Maillard-type modifications of histidine and cysteine have been analyzed in products from food technology (Hilmes and Fischer, 1997). It is likely that a reaction of these amino acids involves a nucleophilic attack of the thiol group of cysteine or the imidazolyl group of histidine to the carbonyl group of the respective sugar. The high reactivity of cysteine, which is known to yield the reversible hemi- or thioacetal adduct (Lo *et al.,* 1994), might suggest an important role of cysteine-containing peptides and proteins (e.g., glutathione) in the scavenging and detoxification of carbonyl compounds *in vivo*

(Haugaard, 2000). Another role for cysteine could be in the formation of intramolecular cross-linking of ribonuclease, which involves the sequence arginine-cysteine-lysine (Watkins *et al.,* 1985).

Altogether, the dipeptide library approach sensitively reflects the reciprocal reactivity of sugars with peptides. Solid-phase peptide libraries provide a standardized basis for comparison of the reactivities not only of sugars, but also of other molecules reacting with proteins.

4.7.3 Epitope mapping with anti-AGE antibodies

In the present study, the N-terminus of the tripeptides were blocked and the reactive sides chains exposed for glycation, thereby mimicking the physiological situation in a protein as close as possible. Experiments from this study showed that lysine and arginine were the most common immunogenic AGE epitopes. As expected, the monoclonal anti-CML antibody recognised both glucose- and ribose- modified lysine. CML has been described as the major AGE antigen detected in tissue proteins by polyclonal anti-AGE antibodies (Reddy *et al.,* 1995). Also, as expected, the monoclonal anti-imidazolone antibody showed affinity towards modified arginine. Imidazolones are the reaction products of arginine and 3-DG and are common epitopes of AGE-modified proteins *in vitro* (Niwa and Tsukushi, 2001). As the anti-imidazolone antibody showed strong reactivity for arginine residues modified by glucose but only very weak reactivity with arginine modified by ribose, it could be concluded that ribose does not react with arginine to form imidazolone. Also some reaction of ribose, but not glucose, with histidine and asparagine were apparent. Since similar differences using the anti-AGE antibodies were not observed, other unidentified AGEs could be formed by the reaction between the imidazolyl groups of histidine with ribose. The polylclonal anti-AGE antibodies recognised both lysine and arginine residues. In addition to lysine and arginine, the amino acid side chains of glutamine (at the C-terminus only) were recognised by the polyclonal anti-KLH-AGE antibody. The neutral but polar side chains of asparagine and glutamine can serve as donor residues and as such contribute to cross-linking by hydrogen bonds.

Control experiments to test the reactivities of the primary and second antibodies with the non-glycated peptide libraries were necessary in order to define the specificity of the antibodies. In summary, testing the relative reactivities of reducing sugars with a membrane-bound synthetic dipeptide library is an efficient way to overcome the inherent difficulties that accompany the analysis of products from reactions with complex substrates

like proteins. This approach offers insight into the specific activity of certain amino acid side chains for reaction with sugars or AGE-modified proteins under comparable conditions. It also has applications in testing the potency of AGE inhibitors on the level of individual amino acids.

4.8 Conclusions

The results obtained from this study confirm the notion that glycation of long-lived proteins to form AGEs is an important modification, which triggers oxidative stress in microglia. It is shown that AGE-modified BSA and AGE-modified ßA4, but not their unmodified proteins, induce NO production in N-11 murine microglia cells. This was due to upregulation of the iNOS could be mediated by the receptor for AGEs (RAGE). Furthermore, AGE-induced enzyme activation and NO production could be blocked by intracellular-acting antioxidants (the estrogen derivative, 17ß-estradiol, *Ginkgo biloba* special extract EGb 761, R-(+)-thioctic acid, and a nitrone-based free radical trap, N-tert.-butyl-α-phenylnitrone (PBN)), presumably through the scavenging of radical intermediates acting as second messengers.

A role for AGEs is implicated in the neurodegenerative disorders of AD and PD. Both amyloid plaques and NFTs are insoluble and resistant to proteolytic enzymes suggesting that glycation, disulphide bond formation, phosphorylation and/or formation of core fragments all contribute to extensive cross-linking between protein monomers. Furthermore, co-localisation of AGE and iNOS in astrocytes in AD temporal (Area 22) and entorhinal (Area 28, 34) cortices supports an AGE-induced oxidative stress in AD. A role for activated microglia in oxidative stress is also implicated, though to a lesser extent compared with astrocytes, evident by partial co-localisation with AGE and iNOS in the AD brain. A role for AGEs in contributing to AD pathology is suggested by the detection of astrocytes co-localised with AGE and iNOS as well as AGE and β-amyloid in the vicinity of mature but not diffuse β-amyloid plaques in the AD brain. In addition, the importance of AGEs in PD is supported by the co-localisation of AGEs with very early Lewy bodies in the substantia nigra of cases with incidental Lewy body disease.

In order to compare individual reactivities of amino acids for nonenzymatic modifications and identify the specific epitopes of anti-AGE antibodies, SPOT libraries were employed. The sugars, glucose and ribose, reacted preferentially with lysine, arginine, and cysteine. The anti-AGE-antibodies predominantly recognised lysine and arginine amino acid residues, which are the most common of the known AGE epitopes.

These results support an AGE-induced oxidative damage due to the action of free radicals, such as NO, occurring in the AD and PD brains. Furthermore, the involvement of astrocytes and microglia in this pathological process was confirmed immunohistochemically in the AD brain. It is suggested that oxidative stress and AGEs participate in the very early steps of Lewy body formation and resulting cell death in PD. Since the iNOS gene can be regulated by redox-sensitive transcription factors, the use of membrane permeable antioxidants could be a promising strategy for the treatment and prevention of chronic inflammation in neurodegenerative disorders. An increased understanding of the biochemical signaling pathways of AGEs will help in the identification of exact targets for pharmacological intervention with anti-inflammatory compounds, AGE-inhibitors and antioxidants.

References

Abordo EA, Westwood ME, Thornalley PJ. (1996) Synthesis and secretion of macrophage colony stimulating factor by mature human monocytes and human monocytic THP-1 cells induced by human serum albumin derivatives modified with methylglyoxal and glucose-derived advanced glycation endproducts. Immunol Lett. Oct;53(1):7-13.

Abordo EA, Minhas HS, Thornalley PJ. (1999) Accumulation of alpha-oxoaldehydes during oxidative stress: a role in cytotoxicity. Biochem Pharmacol. Aug 15;58(4):641-8.

Ahlemeyer B, Mowes A, Krieglstein J. Inhibition of serum deprivation- and staurosporine-induced neuronal apoptosis by Ginkgo biloba extract and some of its constituents. Eur J Pharmacol. 1999 Feb 19;367(2-3):423-30

Ahmed MU, Brinkmann Frye E, Degenhardt TP, Thorpe SR, Baynes JW. (1997) N-epsilon-(carboxyethyl)lysine, a product of the chemical modification of proteins by methylglyoxal, increases with age in human lens proteins. Biochem J. Jun 1;324 (Pt 2):565-70

Akama KT, Van Eldik LJ. (2000) Beta-amyloid stimulation of inducible nitric-oxide synthase in astrocytes is interleukin-1beta- and tumor necrosis factor-alpha (TNFalpha)-dependent, and involves a TNFalpha receptor-associated factor- and NFkappaB-inducing kinase-dependent signaling mechanism. J Biol Chem. Mar 17;275(11):7918-24

Akiyama H, Barger S, Barnum S, Bradt B, Bauer J, Cole GM, Cooper NR, Eikelenboom P, Emmerling M, Fiebich BL, Finch CE, Frautschy S, Griffin WS, Hampel H, Hull M, Landreth G, Lue L, Mrak R, Mackenzie IR, McGeer PL, O'Banion MK, Pachter J, Pasinetti G, Plata-Salaman C, Rogers J, Rydel R, Shen Y, Streit W, Strohmeyer R, Tooyoma I, Van Muiswinkel FL, Veerhuis R, Walker D, Webster S, Wegrzyniak B, Wenk G, Wyss-Coray T. (2000) Inflammation and Alzheimer's disease. Neurobiol Aging. May-Jun;21(3):383-421. Review.

American Pyschiatric Association: (1997) Practice guideline for the treatment of patients with Alzhiemer's disease and other dementias of late life. Am J Pyschiatry; 157 (Suppl):1-39

Amore, A., Cirina, P., Mitola, S., Peruzzi, L., Gianoglio, B., Rabbone, I., Sacchetti, C., Cerutti, F., Grillo, C. and Coppo, R. (1997) Nonenzymatically glycated albumin (Amadori adducts) enhances nitric oxide synthase activity and gene expression in endothelial cells. Kidney Int, 51, 27-35.

Androne L, Gavan NA, Veresiu IA, Orasan R. (2000) In vivo effect of lipoic acid on lipid peroxidation in patients with diabetic neuropathy. In Vivo. Mar-Apr;14(2):327-30.

Behl C. (1999) Alzheimer's disease and oxidative stress: implications for novel therapeutic approaches. Prog Neurobiol. Feb;57(3):301-23. Review.

Behl C, Moosmann B, Manthey D, Heck S. (2000) The female sex hormone oestrogen as neuroprotectant: activities at various levels. Novartis Found Symp.;230:221-34; discussion 234-8.

Bessler H, Djaldetti R, Salman H, Bergman M, Djaldetti M. (1999) IL-1 beta, IL-2, IL-6 and TNF-alpha production by peripheral blood mononuclear cells from patients with Parkinson's disease. Biomed Pharmacother. Apr;53(3):141-5.

Bierhaus A, Chevion S, Chevion M, Hofmann M, Quehenberger P, Illmer T, Luther T, Berentshtein E, Tritschler H, Müller M, Wahl P, Ziegler R, Nawroth PP (1997) Advanced glycation end product-induced activation of NfkB is suppressed by alpha-lipoic acid in cultured endothelial cells. Diabetes 46: 1481-1490

Bierhaus A, Hofmann MA, Ziegler R, Nawroth PP. (1998) AGEs and their interaction with AGE-receptors in vascular disease and diabetes mellitus. I. The AGE concept. Cardiovasc Res. Mar;37(3):586-600. Review.

Booth AA, Khalifah RG, Todd P, Hudson BG.In vitro kinetic studies of formation of antigenic advanced glycation end products (AGEs). Novel inhibition of post-Amadori glycation pathways. J Biol Chem. 1997 Feb 28;272(9):5430-7.

Braak, E.Braak, The human entorhinal cortex: normal morphology and lamina specific pathology in various diseases, Neurosci.Res. 15 (1992) 6-31.

Braak H, Braak E (1995) Staging of Alzheimers disease-related neurofibrillary changes. Neurobiology of Aging 16: 271-278

Braak H, Rub U, Sandmann-Keil D, Gai WP, de Vos RA, Jansen Steur EN, Arai K, Braak E. (2000) Parkinson's disease: affection of brain stem nuclei controlling premotor and motor neurons of the somatomotor system. Acta Neuropathol (Berl). May;99(5):489-95.

Bredt D.S. (1999) Endogenous nitric oxide synthesis: biological functions and pathophysiology. Free Radic Res, 6, 577- 596

Brownlee M (1995) Advanced protein glycosylation in diabetes and aging. Annual Review of Medicine 46: 223-234

Brownlee M. (2000) Negative consequences of glycation. Metabolism. Feb;49(2 Suppl 1):9-13. Review.

Bruce-Keller AJ, Keeling JL, Keller JN, Huang FF, Camondola S, Mattson MP. (2000) Antiinflammatory effects of estrogen on microglial activation Endocrinology. Oct;141(10):3646-56

Burney S, Niles JC, Dedon PC, Tannenbaum SR. (1999) DNA damage in deoxynucleosides and oligonucleotides treated with peroxynitrite. Chem Res Toxicol. Jun;12(6):513-20.

Bustamante J, Lodge JK, Marcocci L, Tritschler HJ, Packer L, Rihn BH. (1998) Alpha-lipoic acid in liver metabolism and disease. Free Radic Biol Med. Apr;24(6):1023-39. Review

Calabrese V, Bates TE, Stella AM. (2000) NO synthase and NO-dependent signal pathways in brain aging and neurodegenerative disorders: the role of oxidant/antioxidant balance Neurochem Res. Oct;25(9-10):1315-41

Carney JM, Floyd RA. (1994) Brain antioxidant activity of spin traps in Mongolian gerbils. Methods Enzymol.;234:523-6

Castellani, R., Smith, M. A., Richey, P. L., and Perry, G. (1996) Glycoxidation and oxidative stress in Parkinson disease and diffuse Lewy body disease. Brain Res. 737, 195-200.

Cataldo AM, Barnett JL, Pieroni C, Nixon RA (1997) Increased neuronal endocytosis and protease delivery to early endosomes in sporadic Alzheimers-disease - neuropathologic evidence for a mechanism of increased beta-amyloidogenesis. Journal of Neuroscience 17: 6142-6151

Chang RC, Hudson P, Wilson B, Haddon L, Hong JS. (2000) Influence of neurons on lipopolysaccharide-stimulated production of nitric oxide and tumor necrosis factor-alpha bycultured glia. Brain Res. Jan 24;853(2):236-44

Che W, Asahi M, Takahashi M, Kaneto H, Okado A, Higashiyama S, Taniguchi N. (1997) Selective induction of heparin-binding epidermal growth factor-like growth factor by methylglyoxal and 3-deoxyglucosone in rat aortic smooth muscle cells. The involvement of reactive oxygen species formation and a possible implication for atherogenesis in diabetes. J Biol Chem. Jul 18;272(29):18453-9.

Chu SC, Marks-Konczalik J, Wu HP, Banks TC, Moss J. (1998) Analysis of the cytokine-stimulated human inducible nitric oxide synthase (iNOS) gene: characterization of differences between human and mouse iNOS promoters. Biochem Biophys Res Commun. Jul 30;248(3):871-8.

Cohen ML, Douvdevani A, Chaimovitz C, Shany S. (2001) Regulation of TNF-alpha by 1alpha,25-dihydroxyvitamin D3 in human macrophages from CAPD patients Kidney Int. Jan;59(1):69-75

Corradin, S.B., Mauel, J., Donini, S.D., Quattrocchi, E. and Ricciardi-Castagnoli, P. (1993) Inducible nitric oxide synthase activity of cloned murine microglial cells. Glia, 7, 255-62.

Davis RE, Miller S, Herrnstadt C, Ghosh SS, Fahy E, Shinobu LA, Galasko D, Thal LJ, Beal MF, Howell N, Parker WD. (1997) Mutations in mitochondrial cytochrome c oxidase genes segregate with late-onset Alzheimer disease. Proc Natl Acad Sci U S A. Apr 29;94(9):4526-31

De Groot CJ, Ruuls SR, Theeuwes JW, Dijkstra CD, Van der Valk P. Immunocytochemical characterization of the expression of inducible and constitutive isoforms of nitric oxide synthase in demyelinating multiple sclerosis lesions. J Neuropathol Exp Neurol. 1997 Jan;56(1):10-20

De Veudis, F.V. (1991). *Ginkgo biloba* extract (EGb 761): Pharmacological Activities and Clinical Applications: pp1-187. Elsevier, Paris

Dickson DW, Sinicropi S, Yen SH, Ko LW, Mattiace LA, Bucala R, Vlassara H. (1996) Glycation and microglial reaction in lesions of Alzheimer's disease. Neurobiol Aging. Sep-Oct;17(5):733-43.

Dunn JA, McCance DR, Thorpe SR, Lyons TJ, Baynes JW. (1991) Age-dependent accumulation of N epsilon-(carboxymethyl)lysine and N epsilon-(carboxymethyl)hydroxylysine in human skin collagen. Biochemistry. Feb 5;30(5):1205-10.

Dyer DG, Blackledge JA, Thorpe SR, Baynes JW. (1991) Formation of pentosidine during nonenzymatic browning of proteins by glucose. Identification of glucose and other carbohydrates as possible precursors of pentosidine in vivo.J Biol Chem. Jun 25;266(18):11654-60.

Dyer DG, Dunn JA, Thorpe SR, Bailie KE, Lyons TJ, McCance DR, Baynes JW. (1993) Accumulation of Maillard reaction products in skin collagen in diabetes and aging J Clin Invest. Jun;91(6):2463-9

Edwards JA, Denis F, Talbot PJ. Activation of glial cells by human coronavirus OC43 infection. J Neuroimmunol. 2000 Aug 1;108(1-2):73-81.

Ehlerding G, Schaeffer J, Drommer W, Miyata T, Koch KM, Floege J. (1998) Alterations of synovial tissue and their potential role in the deposition of beta2-microglobulin-associated amyloid. Nephrol Dial Transplant. Jun;13(6):1465-75.

Finch CE, Cohen DM (1997) Aging, metabolism, and Alzheimer disease - review and hypotheses. Experimental Neurology 143: 82-102

Floege J, Ketteler M. (2001) beta2-Microglobulin-derived amyloidosis: An update.Kidney Int. Feb;59(Suppl 78):164-171.

Floyd, R.A. (1999) Antioxidants, oxidative stress, and degenerative neurological disorders. Proc Soc Exp Biol Med, , 222, 236 –245

Forno S. Pathology of Parkinson's disease. In: Marsden C.D., Fahn S., eds. Movement disorders, neurology 2. London: Butterworth Scientific, 1981: 21-40

Frackowiak J, Wisniewski HM, Wegiel J, Merz GS, Iqbal K, Wang KC. Ultrastructure of the microglia that phagocytose amyloid and the microglia that produce beta-amyloid fibrils. Acta Neuropathol (Berl). 1992;84(3):225-33.

Frank, R. (1992) SPOT synthesis: an easy technique for the positionally addressable, parallel chemical synthesis on a membrane support. Tetrahedron 48, 9217–9232.

Frank, R. (1995) Simultaneous and combinatorial chemical synthesis techniques for the generation and screening of molecular diversity. J. Biotechnol. 41, 259–272.

Frank, R. & Overwin, H. (1996) SPOT synthesis. Epitope analysis with arrays of synthetic peptides prepared on cellulose membranes. Methods Mol. Biol. 66, 149–169).

Gao, J.J., Filla, M.B., Fultz, M.J., Vogel, S.N., Russell, S.W. and Murphy, W.J. (1998) Autocrine/Paracrine IFN-ab mediates the lipopolysaccharide-induced activation of transcription factor stat1a in mouse macrophages: pivotal role of stat1a in induction of the inducible nitric oxide synthase gene. J. Immunology, 161, 4803-4810.

Garlind A, Brauner A, Hojeberg B, Basun H, Schultzberg M. (1999) Soluble interleukin-1 receptor type II levels are elevated in cerebrospinal fluid in Alzheimer's disease patients. Brain Res. Apr 24;826(1):112-6.

Giulian D. (1999) Microglia and the immune pathology of Alzheimer disease. Am J Hum Genet. Jul;65(1):13-8. Review.

Glomb MA, Monnier VM. (1995) Mechanism of protein modification by glyoxal and glycolaldehyde, reactive intermediates of the Maillard reaction. J Biol Chem. Apr 28;270(17):10017-26.

Gomez-Tortosa, E., Newell, K., Irizarry, M. C., Sanders, J. L., and Hyman, B. T. (2000) alpha-Synuclein immunoreactivity in dementia with Lewy bodies: morphological staging and comparison with ubiquitin immunostaining. Acta Neuropathol. (Berl). 99, 352-7.

Gonzalez C, Farias G, Maccioni RB. (1998) Modification of tau to an Alzheimer's type protein interferes with its interaction with microtubules. Cell Mol Biol (Noisy-le-grand). Nov;44(7):1117-27.

Goodwin JL, Uemura E, Cunnick JE. Microglial release of nitric oxide by the synergistic action of beta-amyloid and IFN-gamma. Brain Res. 1995 Sep 18;692(1-2):207-14.

Grandhee SK, Monnier VM. (1991) Mechanism of formation of the Maillard protein cross-link pentosidine. Glucose, fructose, and ascorbate as pentosidine precursors. J Biol Chem. Jun 25;266(18):11649-53.

Greene DA, Stevens MJ, Obrosova I, Feldman EL. (1999) Glucose-induced oxidative stress and programmed cell death in diabetic neuropathy. Eur J Pharmacol. Jun 30;375(1-3):217-23. Review.

Grunblatt E, Mandel S, Youdim MB. (2000) Neuroprotective strategies in Parkinson's disease using the models of 6-hydroxydopamine and MPTP. Ann N Y Acad Sci.;899:262-73. Review

Guntern R, Bouras C, Hof PR, Vallet PG. (1992) An improved thioflavine S method for staining neurofibrillary tangles and senile plaques in Alzheimer's disease. Experientia. Jan 15;48(1):8-10.

Guo ZH, Mattson MP. (2000) Neurotrophic factors protect cortical synaptic terminals against amyloid and oxidative stress-induced impairment of glucose transport, glutamate transport and mitochondrial function. Cereb Cortex. Jan;10(1):50-7

Han B, DuBois DC, Boje KM, Free SJ, Almon RR. (1999) Quantification of iNOS mRNA with reverse transcription polymerase chain reaction directly from cell lysates. Nitric Oxide. Aug;3(4):281-91.

Hattori Y, Banba N, Gross SS, Kasai K. (1999) Glycated serum albumin-induced nitric oxide production in vascular smooth muscle cells by nuclear factor kappaB-dependent transcriptional activation of inducible nitric oxide synthase. Biochem Biophys Res Commun. May 27;259(1):128-32.

Haugaard N. (2000) Reflections on the role of the thiol group in biology. Ann N Y Acad Sci.;899:148-58. Review

Hayase F, Nagaraj RH, Miyata S, Njoroge FG, Monnier VM. (1989) Aging of proteins: immunological detection of a glucose-derived pyrrole formed during maillard reaction in vivo. J Biol Chem. Mar 5;264(7):3758-64.

Hayashi T, Yamada K, Esaki T, Muto E, Chaudhuri G, Iguchi A. (1998) Physiological concentrations of 17beta-estradiol inhibit the synthesis of nitric oxide synthase in macrophages via a receptor-mediated system. J Cardiovasc Pharmacol. Feb;31(2):292-8.

Heales SJ, Bolanos JP, Stewart VC, Brookes PS, Land JM, Clark JB. (1999) Nitric oxide, mitochondria and neurological disease. Biochim Biophys Acta. Feb 9;1410(2):215-28. Review.

Henderson VW, Paganini-Hill A, Miller BL, Elble RJ, Reyes PF, Shoupe D, McCleary CA, Klein RA, Hake AM, Farlow MR. (2000) Estrogen for Alzheimer's disease in women: randomized, double-blind, placebo-controlled trial. Neurology. Jan 25;54(2):295-301

Hensley K, Hall N, Subramaniam R, Cole P, Harris M, Aksenov M, Aksenova M, Gabbita SP, Wu JF, Carney JM, et al. (1995) Brain regional correspondence between Alzheimer's disease histopathology and biomarkers of protein oxidation. J Neurochem. Nov;65(5):2146-56.

Hensley, K., Maidt, M.L., Yu, Z.Q., Sang, H., Markesbery, W.R. and Floyd, R.A. (1998) Electrochemical Analysis Of Protein Nitrotyrosine and Dityrosine In the Alzheimer Brain Indicates Region-Specific Accumulation. J. Neurosci., 18, 8126-8132.

Hensley K, Robinson KA, Gabbita SP, Salsman S, Floyd RA. (2000) Reactive oxygen species, cell signaling, and cell injury. Free Radic Biol Med. May 15;28(10):1456-62. Review

Hilmes, C. & Fischer, A. (1997) Inhibitory effect of sulfur-containing amino acids on burnt off-flavours in canned liver sausages. Meat Sci. 46, 199–210.

Holcomb LA, Gordon MN, Jantzen P, Hsiao K, Duff K, Morgan D. (1999) Behavioral changes in transgenic mice expressing both amyloid precursor protein and presenilin-1 mutations: lack of association with amyloid deposits. Behav Genet. May;29(3):177-85.

Holdiness MR. Clinical pharmacokinetics of N-acetylcysteine. Clin Pharmacokinet. 1991 Feb;20(2):123-34. Review.

Hooper DC, Bagasra O, Marini JC, Zborek A, Ohnishi ST, Kean R, Champion JM, Sarker AB, Bobroski L, Farber JL, Akaike T, Maeda H, Koprowski H. (1997) Prevention of experimental allergic encephalomyelitis by targeting nitric oxide and peroxynitrite: implications for the treatment of multiple sclerosis. Proc Natl Acad Sci U S A. Mar 18;94(6):2528-33.

Hoyer S. (1998) Is sporadic Alzheimer disease the brain type of non-insulin dependent diabetes mellitus? A challenging hypothesis. J Neural Transm.;105(4-5):415-22

Huang JS, Guh JY, Hung WC, Yang ML, Lai YH, Chen HC, Chuang LY. (1999) Role of the Janus kinase (JAK)/signal transducters and activators of transcription (STAT) cascade in advanced glycation end-product-induced cellular mitogenesis in NRK-49F cells. Biochem J. Aug 15;342 (Pt 1):231-8.

Huttunen HJ, Kuja-Panula J, Sorci G, Agneletti AL, Donato R, Rauvala H. (2000) Coregulation of neurite outgrowth and cell survival by amphoterin and S100 proteins through receptor for advanced glycation end products (RAGE) activation J Biol Chem. Dec 22;275(51):40096-105.

Ii M, Sunamoto M, Ohnishi K, Ichimori Y. (1996) beta-Amyloid protein-dependent nitric oxide production from microglial cells and neurotoxicity. Brain Res. May 13;720(1-2):93-100.

Iida Y, Miyata T, Inagi R, Sugiyama S, Maeda K (1994) Beta(2)-microglobulin modified with advanced glycation end products induces interleukin-6 from human macrophages - role in the pathogenesis of hemodialysis-associated amyloidosis. Biochemical & Biophysical Research Communications 201: 1235-1241

Ikeda K, Nagai R, Sakamoto T, Sano H, Araki T, Sakata N, Nakayama H, Yoshida M, Ueda S, Horiuchi S. Immunochemical approaches to AGE-structures: characterization of anti-AGE antibodies. J Immunol Methods. 1998 Jun 1;215(1-2):95-104.

Iwashima Y, Eto M, Hata A, Kaku K, Horiuchi S, Ushikubi F, Sano H. (2000) Advanced glycation end products-induced gene expression of scavenger receptors in cultured human monocyte-derived macrophages. Biochem Biophys Res Commun. Oct 22;277(2):368-80.

Jenner, P., and Olanow, C. W. (1998) Understanding cell death in Parkinson's disease. Ann. Neurol. 44, S72-84

Kang Y, Edwards LG, Thornalley PJ. (1996) Effect of methylglyoxal on human leukaemia 60 cell growth: modification of DNA G1 growth arrest and induction of apoptosis. Leuk Res. May;20(5):397-405.

Kato H, van Chuyen N, Utsunomiya N, Okitani A. (1986) Changes of amino acids composition and relative digestibility of lysozyme in the reaction with alpha-dicarbonyl compounds in aqueous system. J Nutr Sci Vitaminol (Tokyo). Feb;32(1):55-65.

Keller JN, Pang Z, Geddes JW, Begley JG, Germeyer A, Waeg G, Mattson MP. (1997) Impairment of glucose and glutamate transport and induction of mitochondrial oxidative stress and dysfunction in synaptosomes by amyloid beta-peptide: role of the lipid peroxidation product 4-hydroxynonenal. J Neurochem. Jul;69(1):273-84.

Khalifah, R. G., Baynes, J. W., and Hudson, B. G. (1999) Amadorins: novel post-Amadori inhibitors of advanced glycation reactions. Biochem. Biophys. Res. Commun. 257, 251-8.

Khatchaturian Z.S. Diagnosis of Alzheimer's disease. Archives of Neurology 42 (1985) 1097 - 1105.

Kiemer AK, Vollmar AM. (1997) Effects of different natriuretic peptides on nitric oxide synthesis in macrophages. Endocrinology. Oct;138(10):4282-90.

Kikuchi S, Shinpo K, Moriwaka F, Makita Z, Miyata T, Tashiro K. (1999) Neurotoxicity of methylglyoxal and 3-deoxyglucosone on cultured cortical neurons: synergism between glycation and oxidative stress, possibly involved in neurodegenerative diseases. J Neurosci Res. Jul 15;57(2):280-9.

Kikumori, T., Kambe, F., Nagaya, T., Imai, T., Funahashi, H. and Seo, H. (1998) Activation of transcriptionally active nuclear factor-kappaB by tumor necrosis factor-alpha and its inhibition by antioxidants in rat thyroid FRTL-5 cells. Endocrinology, 139, 1715-22.

Kimura T, Takamatsu J, Miyata T, Miyakawa T, Horiuchi S. (1998) Localization of identified advanced glycation end-product structures, N epsilon(carboxymethyl)lysine and pentosidine, in age-related inclusions in human brains. Pathol Int. Aug; 48(8):575-9.

Kislinger T, Fu C, Huber B, Qu W, Taguchi A, Du Yan S, Hofmann M, Yan SF, Pischetsrieder M, Stern D, Schmidt AM. N(epsilon)-(carboxymethyl)lysine adducts of proteins are ligands for receptor for advanced glycation end products that activate cell signaling pathways and modulate gene expression. J Biol Chem. 1999 Oct 29;274(44):31740-9.

Klegeris A, Walker DG, McGeer PL. (1997) Interaction of Alzheimer beta-amyloid peptide with the human monocytic cell line THP-1 results in a protein kinase C-dependent secretion of tumor necrosis factor-alpha. Brain Res. Jan 30;747(1):114-21.

Klegeris A, McGeer EG, McGeer PL. (2000) Inhibitory action of 1-(2-chlorophenyl)-N-methyl-N-(1-methylpropyl)-3-isoquinolinecarboxamide (PK 11195) on some mononuclear phagocyte functions. Biochem Pharmacol. May 15;59(10):1305-14

Kleijnen J, Knipschild P. Ginkgo biloba for cerebral insufficiency. Br J Clin Pharmacol. 1992 Oct;34(4):352-8. Review.

Knowles, R.G. (1997) Nitric oxide biochemistry. Biochem. Soc. Trans., 25, 895-901.

Ko LW, Ko EC, Nacharaju P, Liu WK, Chang E, Kenessey A, Yen SH. (1999) An immunochemical study on tau glycation in paired helical filaments. Brain Res. Jun 5;830(2):301-13

Kotake Y, Sang H, Miyajima T, Wallis GL. (1998) Inhibition of NF-kappaB, iNOS mRNA, COX2 mRNA, and COX catalytic activity by phenyl-N-tert-butylnitrone (PBN). Biochim Biophys Acta. Nov 19;1448(1):77-84.

Kreutzberg GW. (1996) Microglia: a sensor for pathological events in the CNS. Trends Neurosci. Aug;19(8):312-8. Review.

Lamas, S, Perez-Sala, D, Moncada, S. (1998) Nitric oxide: from discovery to the clinic Trends Pharmacol Sci, 19, 436 –438

Laemmli UK. (1970) Cleavage of structural proteins during the assembly of the head of bacteriophage Nature. Aug 15;227(259):680-5.

Lander HM, Tauras JM, Ogiste JS, Hori O, Moss RA, Schmidt AM. Activation of the receptor for advanced glycation end products triggers a p21(ras)-dependent mitogen-activated protein kinase pathway regulated by oxidant stress. J Biol Chem. 1997 Jul 11;272(28):17810-4

Lautenschlager NT, Cupples LA, Rao VS, Auerbach SA, Becker R, Burke J, Chui H, Duara R, Foley EJ, Glatt SL, Green RC, Jones R, Karlinsky H, Kukull WA, Kurz A, Larson EB, Martelli K, Sadovnick AD, Volicer L, Waring SC, Growdon JH, Farrer LA. Risk of dementia among relatives of Alzheimer's disease patients in the MIRAGE study: What is in store for the oldest old? Neurology. 1996 Mar;46(3):641-50.

Ledesma MD, Bonay P, Avila J (1995) Tau protein from Alzheimers disease patients is glycated at its tubulin-binding domain. Journal of Neurochemistry 65: 1658-1664

Ledesma MD, Perez M, Colaco C, Avila J. Tau glycation is involved in aggregation of the protein but not in the formation of filaments. Cell Mol Biol (Noisy-le-grand). 1998 Nov;44(7):1111-6

Leibson CL, Rocca WA, Hanson VA, Cha R, Kokmen E, OBrien PC, Palumbo PJ (1997) Risk of dementia among persons with diabetes mellitus - a population-based cohort study. Am J Epidemiol: 301-308

Li JJ, Voisin D, Quiquerez AL, Bouras C (1994) Differential expression of advanced glycosylation end-products in neurons of different species. Brain Research 641: 285-288

Li YM, Dickson DW. (1997) Enhanced binding of advanced glycation endproducts (AGE) by the ApoE4 isoform links the mechanism of plaque deposition in Alzheimer's disease. Neurosci Lett. May 2;226(3):155-8.

Li JJ, Dickson D, Hof PR, Vlassara H. (1998) Receptors for advanced glycosylation endproducts in human brain: role in brain homeostasis. Mol Med. Jan;4(1):46-60.

Li R, Shen Y, Yang LB, Lue LF, Finch C, Rogers J. (2000) Estrogen enhances uptake of amyloid beta-protein by microglia derived from the human cortex. J Neurochem. Oct;75(4):1447-54.

Ling X, Sakashita N, Takeya M, Nagai R, Horiuchi S, Takahashi K. (1998) Immunohistochemical distribution and subcellular localization of three distinct specific molecular structures of advanced glycation end products in human tissues. Lab Invest. Dec;78(12):1591-606.

Liu J, Zhao ML, Brosnan CF, Lee SC. (1996) Expression of type II nitric oxide synthase in primary human astrocytes and microglia: role of IL-1beta and IL-1 receptor antagonist. J Immunol. Oct 15;157(8):3569-76.

Liu SX, Chen Y, Zhou M, Wan J. (1998) Oxidized cholesterol in oxidized low density lipoprotein may be responsible for the inhibition of LPS-induced nitric oxide production in macrophages. Atherosclerosis. Jan;136(1):43-9.

Liu Y, Dargusch R, Schubert D (1997) Beta amyloid toxicity does not require RAGE protein. Biochemical & Biophysical Research Communications 237: 37-40

Lo, T.W.C., Westwood, M.E., McLellan, A.C., Selwood, T. & Thornalley, P.J. (1994) Binding and modification of proteins by methylglyoxal under physiological conditions—a kinetic and mechanistic study with N-alpha-acetylarginine, N-alpha-acetylcysteine, and N-alpha-acetyllysine, and bovine serum albumin. J. Biol. Chem. 269, 32299–32305

Loidl-Stahlhofen A, Spiteller G. (1994) alpha-Hydroxyaldehydes, products of lipid peroxidation. Biochim Biophys Acta. Mar 3;1211(2):156-60.

Loske C, Neumann A, Cunningham AM, Nichol K, Schinzel R, Riederer P, Munch G. (1998) Cytotoxicity of advanced glycation endproducts is mediated by oxidative stress. J Neural Transm.;105(8-9):1005-15.

Love S. (1999) Oxidative stress in brain ischemia. Brain Pathol. Jan;9(1):119-31. Review.

Lowenstein, C.J., Alley, E.V., Raval, P., Snowman, A.M., Snyder, S.H., Russell, S.W., Murphy, W.J. (1993) Macrophage nitric oxide synthase gene: Two upstream regions mediate induction by interferon γ and lipopolysaccharide. Proc. Natl. Acad. Sci. USA, 90, 9730-9734.

Ludwig HC, Ahkavan-Shigari R, Rausch S, Schallock K, Quentin C, Ziegler D, Bockermann V, Markakis E. (2000) Oedema extension in cerebral metastasis and correlation with the expression of nitric oxide synthase isozymes (NOS I-III). Anticancer Res. Jan-Feb;20(1A):305-10.

Luterman JD, Haroutunian V, Yemul S, Ho L, Purohit D, Aisen PS, Mohs R, Pasinetti GM. (2000) Cytokine gene expression as a function of the clinical progression of Alzheimer disease dementia. Arch Neurol. Aug;57(8):1153-60.

Lüth HJ, Holzer M, Gertz HJ, Arendt Th (2000) Aberrant expression of nNOS in pyramidal neurons in Alzheimer's disease is highly co-localized with p21 ras and p16INK4a. Brain Res 852: 45 –55

Ma Z, Westermark P, Westermark GT. (2000) Amyloid in human islets of Langerhans: immunologic evidence that islet amyloid polypeptide is modified in amyloidogenesis. Pancreas. Aug;21(2):212-8

Maat-Schieman ML, Rozemuller AJ, van Duinen SG, Haan J, Eikelenboom P, Roos RA. (1994) Microglia in diffuse plaques in hereditary cerebral hemorrhage with amyloidosis (Dutch). An immunohistochemical study. J Neuropathol Exp Neurol. Sep;53(5):483-91.

Mandelkow E, Song YH, Schweers O, Marx A, Mandelkow EM (1995) On the structure of microtubules, tau, and paired helical filaments. Neurobiology of Aging 16: 347-354

Mark RJ, Keller JN, Kruman I, Mattson MP (1997) Basic fgf attenuates amyloid beta-peptide-induced oxidative stress, mitochondrial dysfunction, and impairment of Na+/K+-ATPase activity in hippocampal neurons. Brain Research 756: 205-214

Markesbery WR, Carney JM. Oxidative alterations in Alzheimer's disease. Brain Pathol. 1999 Jan;9(1):133-46. Review.

Mattson MP, Culmsee C, Yu Z, Camandola S. Roles of nuclear factor kappaB in neuronal survival and plasticity. J Neurochem. 2000 Feb;74(2):443-56. Review.

Maurer K, Ihl R, Dierks T, Frolich L. (1997) Clinical efficacy of Ginkgo biloba special extract EGb 761 in dementia of the Alzheimer type. J Psychiatr Res. Nov-Dec;31(6):645-55.

Mayer B, Hemmens B. Biosynthesis and action of nitric oxide in mammalian cells. Trends Biochem Sci. 1997 Dec;22(12):477-81. Review.

McGeer PL, Schulzer M, McGeer EG. (1996) Arthritis and anti-inflammatory agents as possible protective factors for Alzheimer's disease: a review of 17 epidemiologic studies. Neurology. Aug;47(2):425-32.

McKhann G., Drachmann D., Folstein M., Katzman R., Price D., Stadlan E.M. (1984) Clinical diagnosis of Alzheimer's disease: report of the NINCDS-ADRDA work group under the auspices of Department of Health and Human Services Task Force on Alzheimer's disease, Neurology, 34 934 -944.

McNaught KS, Jenner P. (2000) Extracellular accumulation of nitric oxide, hydrogen peroxide, and glutamate in astrocytic cultures following glutathione depletion, complex I inhibition, and/or lipopolysaccharide-induced activation. Biochem Pharmacol. Oct 1;60(7):979-88.

Mecocci P, Beal MF, Cecchetti R, Polidori MC, Cherubini A, Chionne F, Avellini L, Romano G, Senin U. (1997) Mitochondrial membrane fluidity and oxidative damage to mitochondrial DNA in aged and AD human brain. Mol Chem Neuropathol. May;31(1):53-64.

Meda L, Cassatella MA, Szendrei GI, Otvos L, Baron P, Villalba M, Ferrari D, Rossi F. (1995) Activation of microglial cells by beta-amyloid protein and interferon-gamma. Nature. Apr 13;374(6523):647-50.

Mehlhorn G, Hollborn M, Schliebs R. (2000) Induction of cytokines in glial cells surrounding cortical beta-amyloid plaques in transgenic Tg2576 mice with Alzheimer pathology. Int J Dev Neurosci. Jul-Aug;18(4-5):423-31

Merin JP, Matsuyama M, Kira T, Baba M, Okamoto T. (1996) Alpha-lipoic acid blocks HIV-1 LTR-dependent expression of hygromycin resistance in THP-1 stable FEBS Lett. Sep 23;394(1):9-13.

Miranda KM, Espey MG, Wink DA. (2000) A discussion of the chemistry of oxidative and nitrosative stress in cytotoxicity. J Inorg Biochem. Apr;79(1-4):237-40.

Miyata T, Inagi R, Iida Y, Sato M, Yamada N, Oda O, Maeda K, Seo H. (1994) Involvement of beta 2-microglobulin modified with advanced glycation end products in the pathogenesis of hemodialysis-associated amyloidosis. Induction of human monocyte chemotaxis and macrophage secretion of tumor necrosis factor-alpha and interleukin-1. J Clin Invest. Feb;93(2):521-8.

Mohamed AK, Bierhaus A, Schiekofer S, Tritschler H, Ziegler R, Nawroth PP. The role of oxidative stress and NF-kappaB activation in late diabetic complications. Biofactors. 1999;10(2-3):157-67. Review

Monford J.C., Javoy-Agid F., Hauw J., Dubois B., Agid Y. (1985) Brain glutamate decorboxylase in Parkinson's disease with particular reference to premortem severity index, Brain 108 301 - 313.

Moosmann, B., Uhr, M. and Behl, C. (1997) Neuroprotective potential of aromatic alcohols against oxidative cell death. FEBS Lett., 413, 467-472.

Mor G, Nilsen J, Horvath T, Bechmann I, Brown S, Garcia-Segura LM, Naftolin F. Estrogen and microglia: A regulatory system that affects the brain. J Neurobiol. 1999 Sep 15;40(4):484-96. Review

Morgan AC, Chang HY, Liu JS, Hua LL, Lee SC. High extracellular potassium modulates nitric oxide synthase expression in human astrocytes. J Neurochem. 2000 May;74(5):1903-12

Morohoshi M, Fujisawa K, Uchimura I, Numano F. The effect of glucose and advanced glycosylation end products on IL-6 production by human monocytes. Ann N Y Acad Sci. 1995 Jan 17;748:562-70.

Münch G, Mayer S, Michaelis J, Hipkiss AR, Riederer P, Muller R, Neumann A, Schinzel R, Cunningham AM. (1997) Influence of advanced glycation end-products and AGE-inhibitors on nucleation-dependent polymerization of beta-amyloid peptide. Biochim Biophys Acta. Feb 27;1360(1):17-29.

Münch G, Schinzel R, Loske C, Wong A, Durany N, Li JJ, Vlassara H, Smith MA, Perry G, Riederer P (1998a) Alzheimer's disease - synergistic effects of glucose deficit, oxidative stress and advanced glycation endproducts. Journal of Neural Transmission 105 (4-5): 439-61. Review.

Münch, G., Riederer, P., Cunningham, A., and Braak, E. (1998b). Advanced glycation endproducts are associated with Hirano bodies in Alzheimer's disease. Brain Res. 796, 307-310.

Nagai R, Matsumoto K, Ling X, Suzuki H, Araki T, Horiuchi S. Glycolaldehyde, a reactive intermediate for advanced glycation end products, plays an important role in the generation of an active ligand for the macrophage scavenger receptor. Diabetes. 2000 Oct;49(10):1714-23

Nagaraj RH, Monnier VM. (1992) Isolation and characterization of a blue fluorophore from human eye lens crystallins: in vitro formation from Maillard reaction with ascorbate and ribose. Biochim Biophys Acta. Mar 5;1116(1):34-42

Nagaraj RH, Shipanova IN, Faust FM. (1996) Protein cross-linking by the Maillard reaction. Isolation, characterization, and in vivo detection of a lysine-lysine cross-link derived from methylglyoxal. J Biol Chem. Aug 9;271(32):19338-45

Nakamura K, Nakazawa Y, Ienaga K. (1997) Acid-stable fluorescent advanced glycation end products: vesperlysines A, B, and C are formed as crosslinked products in the Maillard reaction between lysine or proteins with glucose. Biochem Biophys Res Commun. Mar 6;232(1):227-30.

Nathan P. (2000) Can the cognitive enhancing effects of ginkgo biloba be explained by its pharmacology? Med Hypotheses. Dec;55(6):491-97

Nilsen J, Mor G, Naftolin F. (2000) Estrogen-regulated developmental neuronal apoptosis is determined by estrogen receptor subtype and the Fas/Fas ligand system. J Neurobiol. Apr;43(1):64-78

Niwa T, Katsuzaki T, Miyazaki S, Miyazaki T, Ishizaki Y, Hayase F, Tatemichi N, Takei Y. (1997) Immunohistochemical detection of imidazolone, a novel advanced glycation end product, in kidneys and aortas of diabetic patients. J Clin Invest. Mar 15;99(6):1272-80.

Niwa T. (1999) 3-Deoxyglucosone: metabolism, analysis, biological activity, and clinical implication. J Chromatogr B Biomed Sci Appl. Aug 6;731(1):23-36. Review.

Niwa T, Tsukushi S. (2001) 3-Deoxyglucosone and AGEs in uremic complications: Inactivation of glutathione peroxidase by 3-deoxyglucosone. Kidney Int. Feb;59(Suppl 78):37-41.

Okado A, Kawasaki Y, Hasuike Y, Takahashi M, Teshima T, Fujii J, Taniguchi N. Induction of apoptotic cell death by methylglyoxal and 3-deoxyglucosone in macrophage-derived cell lines. Biochem Biophys Res Commun. 1996 Aug 5;225(1):219-24.

Oken BS, Storzbach DM, Kaye JA. The efficacy of Ginkgo biloba on cognitive function in Alzheimer disease. Arch Neurol. 1998 Nov;55(11):1409-15. Review.

Ott A, Breteler MMB, Vanharskamp F, Stijnen T, Hofman A (1998) Incidence and risk of dementia - the Rotterdam study. American Journal of Epidemiology 147: 574-580

Oya T, Hattori N, Mizuno Y, Miyata S, Maeda S, Osawa T, Uchida K. Methylglyoxal modification of protein. Chemical and immunochemical characterization of methylglyoxal-arginine adducts. J Biol Chem. 1999 Jun 25;274(26):18492-502.

Paul RG, Bailey AJ. The effect of advanced glycation end-product formation upon cell-matrix interactions. Int J Biochem Cell Biol. 1999 Jun;31(6):653-60

Pike CJ, Ramezanarab N, Cotman CW (1997) Beta-amyloid neurotoxicity in vitro - evidence of oxidative stress but not protection by antioxidants. Journal of Neurochemistry 69: 1601-1611

Possel H, Noack H, Putzke J, Wolf G, Sies H.Selective upregulation of inducible nitric oxide synthase (iNOS) by lipopolysaccharide (LPS) and cytokines in microglia: In vitro and in vivo studies Glia. 2000 Oct;32(1):51-9.

Qian, M. W., Liu, M., and Eaton, J. W. (1998). Transition metals bind to glycated proteins forming redox active glycochelates - implications for the pathogenesis of certain diabetic complications. Biochem. Biophys. Res. Commun. 250, 385-389.

Raj DS, Choudhury D, Welbourne TC, Levi M. (2000) Advanced glycation end products: a Nephrologist's perspective. Am J Kidney Dis. Mar;35(3):365-80. Review.

Reddy S, Bichler J, Wells-Knecht KJ, Thorpe SR, Baynes JW. (1995) N epsilon-(carboxymethyl)lysine is a dominant advanced glycation end product (AGE) antigen in tissue proteins. Biochemistry. Aug 29;34(34):10872-8.

Roses AD, Gilbert J, Xu PT, Sullivan P, Popko B, Burkhart DS, Rothrook TC, Saunders AM, Maeda N, Schmechel DF (1997) ApoE and Alzheimer disease - human susceptibility genes and appropriate transgenic models. Brain Pathology 7: 1033-1036

Roy, S. and Packer, L. (1998) Redox regulation of cell functions by alpha-lipoate: biochemical and molecular aspects. Biofactors, 8, 17-21.

Rubbo H, Radi R, Trujillo M, Telleri R, Kalyanaraman B, Barnes S, Kirk M, Freeman BA. Nitric oxide regulation of superoxide and peroxynitrite-dependent lipid peroxidation. Formation of novel nitrogen-containing oxidized lipid derivatives. J Biol Chem. 1994 Oct 21;269(42):26066-75.

Rutka JT, Murakami M, Dirks PB, Hubbard SL, Becker LE, Fukuyama K, Jung S, Tsugu A, Matsuzawa K. (1997) Role of glial filaments in cells and tumors of glial origin: a review. J Neurosurg. Sep;87(3):420-30. Review

Saito S, Aras RS, Lou H, Ramwell PW, Foegh ML. (1999) Effects of estrogen on nitric oxide synthase expression in rat aorta allograft and smooth muscle cells. J Heart Lung Transplant. Oct;18(10):937-45.

Samson FE, Nelson SR. The aging brain, metals and oxygen free radicals Cell Mol Biol (Noisy-le-grand). 2000 Jun;46(4):699-707

Sano M, Ernesto C, Thomas RG, Klauber MR, Schafer K, Grundman M, Woodbury P, Growdon J, Cotman CW, Pfeiffer E, Schneider LS, Thal LJ. A controlled trial of selegiline, alpha-tocopherol, or both as treatment for Alzheimer's disease. The Alzheimer's Disease Cooperative Study. N Engl J Med. 1997 Apr 24;336(17):1216-22.

Sasaki S, Shibata N, Komori T, Iwata M. (2000) iNOS and nitrotyrosine immunoreactivity in amyotrophic lateral sclerosis Neurosci Lett. Sep 8;291(1):44-8

Sasaki N, Toki S, Chowei H, Saito T, Nakano N, Hayashi Y, Takeuchi M, Makita Z. (2001) Immunohistochemical distribution of the receptor for advanced glycation end products in neurons and astrocytes in Alzheimer's disease. Brain Res. Jan 12;888(2):256-262.

Sayre LM, Perry G, Atwood CS, Smith MA. (2000) The role of metals in neurodegenerative diseases Cell Mol Biol (Noisy-le-grand). Jun;46(4):731-41

Schapira AH. (2000) Mitochondrial disorders. Curr Opin Neurol. Oct;13(5):527-32

Schicktanz D. (2000) Synthetische Peptidbibliotheken (kombinatorische Bibliotheken) in der Analytik alters - und krankheitsbedingter Veränderungen durch

Schmidt AM, Stern DM. (2000) RAGE: A New Target for the Prevention and Treatment of the Vascular and Inflammatory Complications of Diabetes. Trends Endocrinol Metab. Nov 1;11(9):368-375.

Scholtyssek H, Damerau W, Wessel R, Schimke I. (1997) Antioxidative activity of ginkgolides against superoxide in an aprotic environment. Chem Biol Interact. Oct 24;106(3):183-90.

Schulz JB, Lindenau J, Seyfried J, Dichgans J. (2000) Glutathione, oxidative stress and neurodegeneration. Eur J Biochem. Aug;267(16):4904-11. Review.

Sell DR, Lapolla A, Odetti P, Fogarty J, Monnier VM. (1992) Pentosidine formation in skin correlates with severity of complications in individuals with long-standing IDDM. Diabetes. Oct;41(10):1286-92.

Sen CK, Packer L. (2000) Thiol homeostasis and supplements in physical exercise. Am J Clin Nutr. Aug;72(2 Suppl):653S-69S. Review.

Shea TB. (1997) Phospholipids alter tau conformation, phosphorylation, proteolysis, and association with microtubules: implication for tau function under normal and degenerative conditions. J Neurosci Res. Oct 1;50(1):114-22.

Sheng JG, Mrak RE, Griffin WS. (1997) Neuritic plaque evolution in Alzheimer's disease is accompanied by transition of activated microglia from primed to enlarged to phagocytic forms. Acta Neuropathol (Berl). Jul;94(1):1-5.

Shinpo K, Kikuchi S, Sasaki H, Ogata A, Moriwaka F, Tashiro K. (2000) Selective vulnerability of spinal motor neurons to reactive dicarbonyl compounds, intermediate products of glycation, in vitro: implication of inefficient glutathione system in spinal motor neurons. Brain Res. Apr 7;861(1):151-9.

Sian, J., Gerlach, M., Youdim, M. B., and Riederer, P. (1999) Parkinson's disease: a major hypokinetic basal ganglia disorder. J. Neural Transm. 106, 443-76.

Singer CA, Figueroa-Masot XA, Batchelor RH, Dorsa DM. The mitogen-activated protein kinase pathway mediates estrogen neuroprotection after glutamate toxicity in primary cortical neurons. J Neurosci. 1999 Apr 1;19(7):2455-63.

Smith MA, Taneda S, Richey PL, Miyata S, Yan SD, Stern D, Sayre LM, Monnier VM, Perry G. (1994) Advanced Maillard reaction end products are associated with Alzheimer disease pathology. Proc Natl Acad Sci U S A. Jun 7;91(12):5710-4.

Smith, M.A., Sayre, L.M., Monnier, V.M. and Ferry, G. (1996) Oxidative posttranslational modifications in Alzheimer's disease - a possible pathogenic role in the formation of senile plaques and neurofibrillary tangles. Mol. Chem. Neuropathol., 28, 41-48.

Smith MA, Harris PLR, Sayre LM, Perry G (1997) Iron accumulation in Alzheimer disease is a source of redox-generated free radicals. Proceedings of the National Academy of Sciences of the United States of America 94: 9866-9868

Smith, M.A., Harris, P.L.R., Sayre, L.M., Beckman, J.S. and Perry, G. (1997) Widespread peroxynitrite-mediated damage in Alzheimer's disease. J. Neurosci., 17, 2653-2657.

Smith MA, Rottkamp CA, Nunomura A, Raina AK, Perry G. (2000) Oxidative stress in Alzheimer's disease. Biochim Biophys Acta. Jul 26;1502(1):139-44. Review

Souza JM, Daikhin E, Yudkoff M, Raman CS, Ischiropoulos H. Factors determining the selectivity of protein tyrosine nitration. Arch Biochem Biophys. 1999 Nov 15;371(2):169-78

Spillantini, M. G., Crowther, R. A., Jakes, R., Hasegawa, M., and Goedert, M. (1998) Alpha-synuclein in filamentous inclusions of lewy bodies from Parkinson's disease and dementia with Lewy bodies. Proc. Natl. Acad. Sci. USA. 95, 6469-6473.

Tabatabaie, T., Graham, K.L., Vasquez, A.M., Floyd, R.A. and Kotake, Y. (2000) Inhibition of the cytokine-mediated inducible nitric oxide synthase expression in rat insulinoma cells by phenyl N-tert-butylnitrone. Nitric Oxide, 4, 157-67.

Takeda A, Yasuda T, Miyata T, Goto Y, Wakai M, Watanabe M, Yasuda Y, Horie K, Inagaki T, Doyu M, Maeda K, Sobue G. Advanced glycation end products co-localized with astrocytes and microglial cells in Alzheimer's disease brain. Acta Neuropathol (Berl). 1998 Jun;95(6):555-8.

Takedo A, Yasuda T, Miyata T, Mizuno K, Li M, Yoneyama S, Horie K, Maeda K, Sobue G. Immunohistochemical study of advanced glycation end products in aging and Alzheimer's disease brain. Neurosci Lett. 1996 Dec 27;221(1):17-20.

Thornalley PJ, Edwards LG, Kang Y, Wyatt C, Davies N, Ladan MJ, Double J. (1996) Antitumour activity of S-p-bromobenzylglutathione cyclopentyl diester in vitro and in vivo. Inhibition of glyoxalase I and induction of apoptosis. Biochem Pharmacol. May 17;51(10):1365-72.

Thornalley PJ. (1998) Glutathione-dependent detoxification of alpha-oxoaldehydes by the glyoxalase system: involvement in disease mechanisms and antiproliferative activity of glyoxalase I inhibitors. Chem Biol Interact. Apr 24;111-112:137-51. Review

Vitek, M.P., Bhattacharya, K., Glendening, J.M., Stopa, E., Vlassara, H., Bucala, R., Manogue, K. and Cerami, A. (1994) Advanced glycation end products contribute to amyloidosis in Alzheimer disease. Proc. Natl. Acad. Sci. USA, 91, 4766-4770.

Vodovotz Y., Lucia M.S., Flanders K.C., Chesler L., Xie Qu., Smith T.W., Weidner F., Mumford R., Webber R., Nathan C., Roberts A.B., Lippa C.F., and Sporn M.B. (1996) Inducible nitric oxide synthase in tangle-bearing neurons of patients with Alheimer's disease, J. Exp. Medicine 184 1425 – 1433

Wallace M.N., Geddes J.G., Farquhar D.A., and Masson M.R. (1997)   Nitric oxide synthase in reactive astrocytes adjacent to ß-amyloid plaques, Exp. Neurol. 144 266 -272.

Watkins NG, Thorpe SR, Baynes JW. (1985) Glycation of amino groups in protein. Studies on the specificity of modification of RNase by glucose. J Biol Chem. Sep 5;260(19):10629-36.

Weber, K., Schmahl, W., and Münch, G. (1998) Distribution of advanced glycation end products in the cerebellar neurons of dogs. Brain Res. 791, 11-7.

Wegiel J, Wang KC, Tarnawski M, Lach B. Microglia cells are the driving force in fibrillar plaque formation, whereas astrocytes are a leading factor in plague degradation. Acta Neuropathol (Berl). 2000 Oct;100(4):356-64.

Weiss MF, Erhard P, Kader-Attia FA, Wu YC, Deoreo PB, Araki A, Glomb MA, Monnier VM. (2000) Mechanisms for the formation of glycoxidation products in end-stage renal disease. Kidney Int. Jun;57(6):2571-85.

Weldon DT, Rogers SD, Ghilardi JR, Finke MP, Cleary JP, O'Hare E, Esler WP, Maggio JE, Mantyh PW. (1998) Fibrillar beta-amyloid induces microglial phagocytosis, expression of inducible nitric oxide synthase, and loss of a select population of neurons in the rat CNS in vivo. J Neurosci. Mar 15;18(6):2161-73. Review

Wells-Knecht KJ, Zyzak DV, Litchfield JE, Thorpe SR, Baynes JW. (1995) Mechanism of autoxidative glycosylation: identification of glyoxal and arabinose as intermediates in the autoxidative modification of proteins by glucose. Biochemistry. Mar 21;34(11):3702-9.

Westwood ME, Thornalley PJ. (1995) Molecular characteristics of methylglyoxal-modified bovine and human serum albumins. Comparison with glucose-derived advanced glycation endproduct-modified serum albumins. J Protein Chem. Jul;14(5):359-72.

Whiteman M, Tritschler H, Halliwell B. (1996) Protection against peroxynitrite-dependent tyrosine nitration and alpha 1-antiproteinase inactivation by oxidized and reduced lipoic acid. FEBS Lett. Jan 22;379(1):74-6.

Yan SD, Yan SF, Chen X, Fu J, Chen M, Kuppusamy P, Smith MA, Perry G, Godman GC, Nawroth P, Zweiter JL, Stern D (1995) Non-enzymatically glycated tau in Alzheimers disease induces neuronal oxidant stress resulting in cytokine gene expression and release of amyloid beta-peptide. Nature Medicine 1: 693-699

Yan SD, Chen X, Fu J, Chen M, Zhu H, Roher A, Slattery T, Zhao L, Nagashima M, Morser J, Migheli A, Nawroth P, Stern D, Schmidt AM. (1996) RAGE and amyloid-beta peptide neurotoxicity in Alzheimer's disease. Nature. Aug 22;382(6593):685-91

Yan SD, Zhu HJ, Fu J, Yan SF, Roher A, Tourtellotte WW, Rajavashisth T, Chen X, Godman GC, Stern D, Schmidt AM (1997) Amyloid-beta peptide-receptor for advanced glycation endproduct interaction elicits neuronal expression of macrophage-colony stimulating factor - a proinflammatory pathway in Alzheimer-disease. Proceedings of the National Academy of Sciences of the United States of America 94: 5296-5301

Youdim, M. B. H., and Riederer, P. (1997) Understanding Parkinson's disease. Scientific American. 276, 52-59

Zhao ML, Liu JS, He D, Dickson DW, Lee SC. (1998) Inducible nitric oxide synthase expression is selectively induced in astrocytes isolated from adult human brain. Brain Res. Dec 7;813(2):402-5

Abbreviations

βA4	beta-amyloid peptide
μ	micro
AD	Alzheimer's disease
AGE	advanced glycation endproducts
ADRDA	Alzheimer's Disease and Related Disorders Association
AP-1	activating protein-1
APEG	amine derivatised polyethylene glycol
ApoE4	apolipoprotein E
BSA	bovine serum albumin
CEA	chicken egg albumin
CEL	N^ε-(Carboxyethyl)lysine
CML	N^ε-(Carboxymethyl)lysine
CNS	central nervous system
CSF	cerebrospinal fluid
DCM	dichloromethane
DEPC	diethylpyrucarbonate
3-DG	3-deoxyglucosone
DIC	N,N'-diisopropylcarbodiimide
DMF	dimethylformamide
DMEM	Dulbecco's modified Eagle's medium
DMSO	dimethylsulfoxide
DNA	deoxyribonucleic acid
DSM	Diagnostic and Statistical Manual of Mental Disorders
ECL	enhanced chemiluminescence
ELISA	enzyme-linked immunosorbent assay
ERK	extracellular signal-regulated kinase
FCS	fetal calf serum
FPLC	fluid pressure liquid chromatography
g	gram
GSH	reduced glutathioneg
GSSG	oxidised glutathioneg
h	hour
H & E	Haematoxylin and Eosin
Hb	haemoglobin
HOBT	1-hydroxybenzotriazole
HPLC	high-performance liquid chromatography
IFN-γ	interferon gamma
IL	interleukin
iNOS	inducible nitric oxide synthase
kDa	kilo Dalton
KLH	keyhole limpet hemocyanine
l	litre
LAL	Limulus Amebocyte Lysate
LPS	lipopolysaccharide
MALDI-TOF	matrix-assisted laser desorption/ionization time-of-flight mass spectrometry
MAP	microtubuli associated protein
MAPK	mitogen-activated protein kinase
mg	milligram
MG	methylglyoxal

min	minute
ml	millilitre
mol	moles
MOLD	methyglyoxal – lysine – dimer
MSR	macrophage scavenger-receptor
MTT	3-(4,5-dimethylthiazol-2-yl)2,5-diphenyl tetrazolium bromide
NBB	Netherland Brain Bank
NF-κB	nuclear factor-kappa B
NINCDS	National Institute of Neurologic and Communicative Disorders and Stroke
NO	nitric oxide
nmol	nanomole
NMI	*N*-methylimidazole
PBN	N-tert.-butyl-α-phenylnitrone
PBS	phosphate-buffered saline
PD	Parkinson's disease
PHF	paired helical filaments
PMSI	Premortem Severity Index
RAGE	receptor for advanced glycation endproducts
RNA	ribonucleic acid
RNAse	ribonuclease
RT-PCR	reverse transcriptase polymerase chain reaction
SDS-PAGE	sodium dodecyl sulfate – polacrylamide gel electrophoresis
SN	Substantia Nigra
TBS	Tris-buffered saline
TFA	trifluoroacetic acid
TNF- α	tumour necrosis factor - alpha
W540	Whatman 540

<div align="center">

LEBENSLAUF

Amanda Wong
</div>

1. Persönliche Daten

- geb. am 22.11.1973

- ledig

- Australien

2. Schulbildung

1979 - 1985	Besuch der Grundschule in Oatley
1986 - 1991	Besuch der Penshurst Girls' High School
Nov. 1991	Abschlussprüfung (Higher School Certificate, HSC)

3. Studium

1992 - 1993	Zahnmedizin an der Universität Sydney
1994-1996	Studium der Biowissenschaften (Bachelor of Science, BSc. (Honours); Hauptfächer: Anatomie, Physiologie) und Studium der Geisteswissenschaften (Bachelor of Arts, BA; Hauptfach: Deutsch) an der Universität New South Wales, Sydney

4. Berufsausbildung

Mai - Juli 1996	Wissenschaftliche Mitarbeiterin in Psychologie an der Universität Sydney.
Juni - Nov. 1996	Wissenschaftliche Mitarbeiterin in "Cerebral Malaria in Mice Models" Projekt an der Universität Sydney.
Jan. - Aug. 1997	Mitarbeiterin in Kardiologie/Medizin an der Universität Sydney und in Psychologie am Cumberland College of Health Sciences, Sydney.
Okt. - Dez. 1999	DAAD Doktorandin in Biochemie an der Universität Würzburg.
Jan. 2000 - Feb. 2001	Fortführung der Doktorarbeit an der Universität Leipzig

5. Auszeichnungen

      1. Zahnmedizin - Zertifikat für besondere Leistungen in Anatomie und Präparat

        - Sommer Forschungsstipendium

      (vom Dez. 1992 bis Feb. 1993)

      2. Biowissenschaft - 1995 "Honours" Stipendium

      3. Penshurst Girls' High School - 1991 Erster Platz in Englisch, Mathematik, Geschichte, Physik

6. Zusätzliche Erfahrungen in der Forschung

Dez. 1992 – Feb. 1993	Forschungsprojekt in der Zahnmedizin – „A scanning electron microscopic investigation of the human cavernous sinus"
1994	Projekt in Neuroanatomie – "Vascular Dementia"
1995	"Honours" Forschung in Anatomie (First Class Honours) – „Chronic alcohol consumption does not cause hippocampal neuron loss in humans"

7. Nebenberufliche Tätigkeiten

Okt. 1997 – Dez. 1999	Betreung von Studenten (Medizin und Zahnmedizin) im Biochemie Praktikum an der Universität Würzburg

8. Computer Kenntnisse

IBM und Macintosh Microsoft Office – Adobe Photoshop D1 3.0, Canvas 3.5.4, Corel Draw 8.0, Corel Paint 8.0, Endnote Plus 2.0.2, Excel 7.0, Magellan Word 7.0, NIH Image, Power Point 7.0, Pro-image Plus, Statview 4.5, XRS 2.2 (Jena, Germany).

Publications

Refereed journal articles

[1] A.Wong, R.Arnold, G.A. Doran (1994) A scanning electron microscopic investigation of the human cavernous sinus. Australian Dental Journal 39:4

[2] A.J. Harding, A.Wong, M. Svoboda, J.J. Kril and G.M. Halliday (1997) Chronic alcohol consumption does not cause hippocampal neuron loss in humans. Hippocampus 7:1, 78-87

[3] G. Münch, M. Gerlach, J. Sian, A.Wong, P. Riederer (1998) Advanced glycation endproducts in Neurodegeneration - more than early markers of oxidative stress. Ann Neurol 44 : 85-88

[4] G Munch, R Schinzel, C Loske, A Wong, N Durany, JJ Li, H Vlassara, MA Smith, G Perry, P Riederer. (1998) Alzheimer's disease--synergistic effects of glucose deficit, oxidative stress and advanced glycation endproducts. J Neural Transm.;105(4-5):439-61. Review.

[5] G. Münch, H.J. Lüth, A.Wong, Th. Arendt, (2000) Advanced glycation endproducts and α -synuclein co-localise with inducible nitric oxide in Alzheimer's disease. J. Chem. Neuroanat. 20; 253-257

[6] A.Wong, R.Schinzel, A. Simm, G. Münch (2000) Advanced glycation endproducts induce nitric oxide production in microglia by redox-sensitive signal transduction (submitted to Eur. J. Biochem.)

[7] A.Wong, H.J. Lüth, Th. Arendt, G. Münch (2000) Advanced glycation endproducts co-localise with inducible nitric oxide in Alzheimer's disease (submitted to Br. Res.)

[8] C. Loske, R. Schinzel, A.Wong, P. Riederer and G. Münch (2001) Advanced glycation endproducts change glucose utilization and cause ATP depletion in SH-SY5Y neuroblastoma cells J. Neurochem. (submitted to J. Neurochem)

[9] A.Wong[1], S. Dukic-Stefanovic[1], D. Schicktanz[1], D. Palm, P. Riederer, T. Niwa, R. Schinzel and G. Münch.(2001) Combinatorial approaches to immunogenic AGE-structures - characterisation of AGE antibodies with an AGE dipeptide spot library (in preparation)

[1] equal first author

Published Abstracts

[1] A.J. Harding, <u>A.Wong</u>, M. Svoboda, J.J. Kril and G.M. Halliday (1996) Is the hippocampus affected in alcoholics with memory loss? Proc. Austr. Neuroscience Society, Vol. 7 (poster) abstr. 172

[2] <u>A.Wong,</u> M. Svoboda, J.J. Kril and G.M. Halliday (1996) Do similar hippocampal changes occur in Alzheimer's disease and old age? Proc. Austr. Neuroscience Society Vol. 7 (poster) abstr. 174

[3] <u>A.Wong</u>, R.Schinzel, G. Münch (1998) Novel intracellular-acting antioxidants inhibit nitric oxide synthase expression by advanced glycation endproducts in microglia. (poster and lecture) DAAD conference, Bayreuth.

[4] <u>A.Wong</u>, R.Schinzel, G. Münch (1999) Novel intracellular-acting antioxidants inhibit nitric oxide synthase expression by advanced glycation endproducts in microglia. Proc. Austr. Neuroscience Society (poster) Vol. 12 abstr. 153

[5] <u>A.Wong</u>, R.Schinzel, G. Münch (1999) Intracellular-acting antioxidants attenuate nitric oxide production by advanced glycation endproducts.- neuroprotective stategies in Alzheimer's disease Joint meeting of the International Society for Neurochemistry and the European Society for Neurochemistry Vol. 7 abstr. (poster) 115

[6] <u>A.Wong</u>, H.J.Lüth, G. Münch, Th. Arendt (2000) Accumulation of advanced glycation endproducts in brain tissue in Alzheimer's disease. Symposium "advanced glycation endproducts", Jena (poster) abstr.

Statement

I hereby declare that this thesis is my own work and that, to the best of my belief, it contains no material previously published or written by another person nor material which to a substantial extent has been accepted for the award of any other degree or diploma of a university or other institute of higher learning, except where due acknowledgement is made in the text of the thesis.

A.Wong

On the eighteenth day of February, 2001

<u>Acknowledgements</u>